ABSTRACT

YIN, LANJUN. Evaluation of Skin-Nonwoven Interaction for Skin Physiology and Sensation of Absorbent Hygiene Products (Under the direction of Dr. Eunkyoung Shim and Dr. Emiel DenHartog).

The emergence of absorbent hygiene products has dramatically improved the quality of life and has become essential for modern life. However, the use of absorbent hygiene products still causes concerns about skin health problems like irritant contact dermatitis as they interact with the skin through intimate contact. A good skin health status and pleasant tactile sensation are demanded. A study of the interaction between the skin and the topsheet nonwoven fabrics of absorbent hygiene products can help to understand the effects on skin physiology and sensation. In this study, a benchmark of commercial topsheet nonwoven fabrics in contact with the skin was carried out and the typical properties like fiber diameter, fabric thickness, surface roughness, etc. were characterized. Both an in vitro and in vivo friction measurement approach was developed to evaluate the interaction between fabric and skin. The transepidermal water loss (TEWL) and skin redness were measured before and after the friction test in vivo to evaluate the skin physiology status. Ordinal scales for the pleasantness sensation, localized skin sensation, texture sensation, wetness sensation, and stickiness sensation were developed for the tactile sensation evaluation. The skin simulants used in the in vitro test showed that the coefficient of friction was more determined by the surface properties while the contribution of bulk deformation was reflected in the stick-slip motion. The in vivo friction test showed a higher friction force tended to cause a larger influence on skin physiology and sensation in a dry and neutral environment (22°C, ~50%RH). However, this relationship was not held in a warm environment (35°C, ~50%RH). Both smooth and rough fabrics caused a high friction force in the warm environment but the smooth fabric had less effects on skin physiology and sensation. This implies the adhesion friction might

have less influence on skin status than deformation friction. In this case, the friction coefficient may not be an efficient parameter to indicate the effects of fabric-skin interaction on skin physiology and sensation. The deformation friction could be a more direct indicator for the effects on skin and the dynamic stick-slip behavior observed in the in vitro friction measurement should be studied. The approach for TEWL and skin color measurement provided a way to quantitatively evaluate the effects of friction on skin physiological properties. It showed wetness and high temperature both caused a significant increase in TEWL and the wetness also caused a significant increase in skin redness. Additionally, the skin sensation was less pleasant in wet or warm environments. This suggests wetness and high temperature were unfavorable for skin barrier function and skin sensation. The spunbond, thermal calender bonded fabric with a small bond area was perceived as more pleasant than that with a big bond area because of a smoother sensation. Nevertheless, the surface roughness of fabrics measured by the Kawabata Evaluation System did not indicate the texture sensation of these topsheet nonwoven fabrics. This discrepancy suggests considering the spatial variation of these fabrics for the roughness sensation rather than the arithmetic mean height only.

© Copyright 2020 by Lanjun Yin

All Rights Reserved

Evaluation of Skin-Nonwoven Interaction for Skin Physiology and Sensation of Absorbent Hygiene Products

by
Lanjun Yin

A dissertation submitted to the Graduate Faculty of
North Carolina State University
in partial fulfillment of the
requirements for the degree of
Doctor of Philosophy

Fiber and Polymer Science

Raleigh, North Carolina
2020

APPROVED BY:

_____	_____
Dr.Eunkyoung Shim Co-Chair of Advisory Committee	Dr. Emiel DenHartog Co-Chair of Advisory Committee
_____	_____
Dr. Behnam Pourdeyhimi	Dr. Joel J. Pawlak

BIOGRAPHY

Lanjun Yin was born in Jinan, China, in 1994. She obtained her bachelor's degree in Textiles Engineering from Jiangnan University, China, in 2016. She started to study at North Carolina State University from August 2015 and earned a master's degree in Textile Engineering in 2017 under the direction of Dr. Jesse Jur. Her thesis topic was "Design of Screen-Printed Electrodes on Infant Garment for Electrocardiogram Measurement". After graduating, she started a doctoral program under the direction of Dr. Eunkyoung Shim and Dr. Emiel DenHartog to study the influence of skin-fabric interaction on skin comfort. Through her studies, she realized how important textiles can be for the improvement of healthcare and people's well-being. She hopes she can keep learning and growing in this field and use what she learned to add value to society. More importantly, she hopes to keep curiosity and creativity by experiencing and enjoying life.

ACKNOWLEDGMENTS

I would first like to thank my advisors, Dr. Eunkyoung Shim, and Dr. Emiel DenHartog, for their support, mentorship, and guidance throughout my research. I appreciate their contributions of time, ideas, and funding to help me complete my doctoral degree. They are very experienced researchers and great scientists. I appreciate that I can work with them as their students and got to learn a lot from them. I also thank my committee members Dr. Behnam Pourdeyhimi and Dr. Joel Pawlak for their scientific advice and knowledge, as well as insightful discussions and suggestions. Thanks to the Nonwoven Institute for providing projects and funding to me and all the other graduate students who need opportunities to do research.

I would like to thank all the people who assisted in my research: my industrial advisors, lab managers, lab mates, and group members. I would like to thank all my friends for their support and help over the past years. It is their love that makes this journey more joyful.

Last but certainly not least, I must express my profound gratitude to my parents for their love and support. I would not have made it this far without them.

TABLE OF CONTENTS

LIST OF TABLES

LIST OF FIGURES

CHAPTER 1 Introduction

Hygiene products are an important application field for nonwovens. There is a high demand for hygiene products such as baby diapers, feminine hygiene, wet wipes as these are life necessities. The motivation for innovating these products is not only the increased demand but more importantly, the higher requirement for product quality. Since these nonwoven products are used for personal hygiene or even in a medical setting, there can be a high requirement for their performance mainly including good absorbency and quick dispersal, no liquid leakage, good retention of moisture, soft to the skin, thin and light, as well as providing no safety risks. The functional performance of hygiene products has dramatically improved over the past 40 years. The current customer demand is more about the improvement of skin comfort than functional performance because skin health and comfort is a challenge that receives increasing attention. The concerns around skin health are related to skin irritation, dermatitis, skin lesion, and infections, especially for the hygiene products used for very sensitive skin. In addition to the skin health issues, any uncomfortable sensations like itch, hardness, roughness, can largely affect individuals' preference [1][2].

To illustrate the role of nonwoven materials in hygiene products, diapers can be taken as an example. The main components of a diaper include the topsheet, acquisition/distribution layer, absorbent core, and backsheet. All of them can be nonwovens (Figure 1.1). Firstly, the topsheet works as a cover next to the skin. It plays an important role as the first step to draw the liquid into the absorbent core and works as a barrier to keep the skin dry. Under the top layer, there is the acquisition or distribution layer that can be made of through-air bonded nonwovens to move the liquid away from the topsheet and distribute it evenly. The absorbent core can be cellulose blended with superabsorbent polymer (SAP) granules encapsulated by a nonwoven sheet or thermal-

bonded air-laid nonwovens loaded with SAP. This is the layer that can lock and store fluids. The backsheet is water-impermeable to avoid liquid leakage with good flexibility and high strength [1][3][4][5]. With layers of nonwoven construction, diapers can absorb fluids, spread and diffuse it evenly into the absorbent core, and work as a barrier to keep the skin dry. Other hygiene products have a similar structure and material application to get similar performance. The nonwoven material can provide diverse performance to satisfy the functional requirements and also can be produced at the large scale with low cost. This makes nonwoven materials preferred and practical. However, the user experience for nonwoven fabrics in absorbent hygiene products still needs improvement. The intimate contact with the skin under high pressure in a warm. humid, and occlusive environment can cause skin health issues and discomfort. Wetness and chafing were reported as the main factors that cause rashes [6][7]. The products are expected to be comfortable to the skin without safety or health risks during the time in use. The topsheet nonwoven fabric has been focused the most in terms of skin comfort because it is the layer that contacts the sensitive skin region. However, the evaluation and engineering of it in terms of skin comfort remains a challenge. There are no definite standards for skin comfort since this usually is a subjective evaluation that can vary from person to person [8][9][10][11].

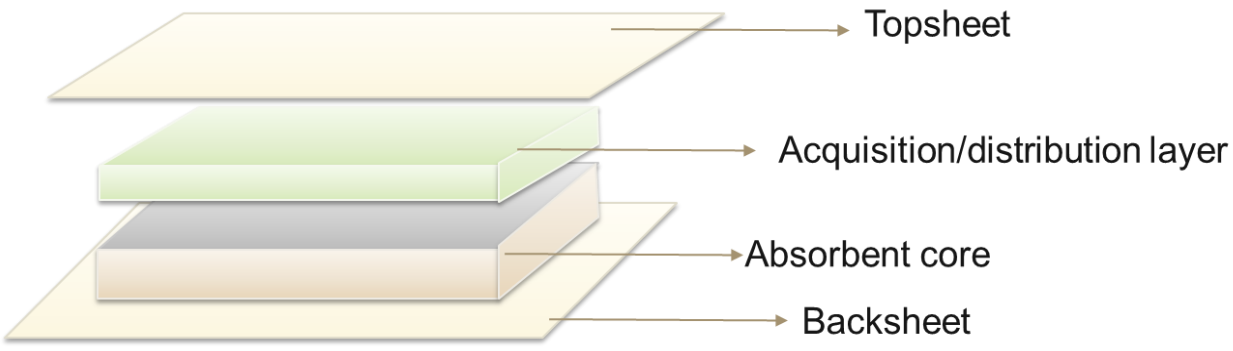

Figure 1.1. Basic layer construction of a disposable diaper.

To understand the interaction between human skin and topsheet nonwoven fabric, and explore the relationship between nonwoven characteristics and skin physiology, sensation, this study aims to investigate the effects of nonwoven material/structure parameters on tactile properties through friction under different environmental conditions. Chapter 2 is a review of the relevant literature. Chapter 3 is the evaluation of commercial topsheet nonwoven fabrics and conventional measurement methods for fabric hand related mechanical properties. All the commercial fabrics had a narrow range of properties and the friction coefficient measured by conventional methods was not significantly different. In Chapter 4, a friction measurement setup with skin simulants is developed and compared to the conventional friction measurement on a metal plate. Chapters 5 is a human subject study to explore the relationship between friction and skin physiology, sensation in neutral and warm environments. Chapter 6 discusses the effects of fabric material and bond area on skin physiology and sensation in dry and wet conditions. Chapter 7 provides an overall conclusion and recommendations for future studies.

CHAPTER 2 Literature Review

2.1 Skin Physiology

2.1.1 Skin Structure

The skin is the largest organ and covers the human body with an area of 1.7 m^2 to 2 m^2 on average. It is the outmost layer of the body and contacts the external environment directly, and it is the first barrier of the body to provide protection. Thus, the skin plays an important role in perceiving the outside environment and interacting with it. The skin can be divided into two types. One is the hairy (non-glabrous) skin which covers most of the body, and the other is the glabrous skin having no hair. Both of them have many sweat glands with a dense distribution between 200 glands/cm^2 to 600 glands/cm^2 [12]. Generally, the skin consists of three major tissue layers from the outside to the inside: epidermis, dermis, and hypodermis (Figure 2.1). Each of the major layers can be further divided into sublayers. The total thickness of the skin generally ranges from 1.5 mm to 4 mm, but it is very thin in the eyelid (0.2mm) while it is thick on the sole of the foot (6mm). The thickness of the epidermis is about 0.05 to 0.15 mm in hairy skin and twice in glabrous skin (0.1 mm to 0.3 mm). The epidermis is nonvascular, and 80% to 85% of epidermis cells are keratinocytes. The dermis has a thickness of 1 to 4 mm. It contains a fibrous matrix composed of a very dense fiber network and complex vascular apparatus and nerve fibers [13][14][15][16]. The hypodermis is fat tissue between the dermis and the muscles work as insulation and protective layer. The outmost layer of the skin is stratum corneum (SC), which is the outer layer of the epidermis. SC is the primary structure to provide the skin barrier function. It prevents the loss of body fluids like water, electrolytes, and also prevents the penetration of external substances or irritants by controlling the permeability of the skin [17][18]. The thickness of the SC is around 0.01 to 0.025 mm. The structure of SC is usually called a “brick and mortar” structure. The “brick”

are the corneocytes and the “mortar” is a lipidic intercellular matrix [19][16]. There is an amorphous lipid film on the outmost layer of the stratum corneum because of the sebum secreted by sebaceous glands. The thickness of this lipid film is usually less than 0.5 μm or negligible while it can be thicker than 4 μm in sebum rich area. Generally, the sebum secretion is the highest on central areas of the face like forehead and lowest on limbs [20]. The amount of sebum on the skin surface can change the surface free energy. The skin has a lower surface free energy and is more hydrophobic for low sebum sites while it has a higher surface free energy and is less hydrophobic for sebum rich area [21]. In addition, the surface lipid film may give the skin an adhesive behavior because of the hydrolipidic property[22][23][24]. However, there is no significant influence of the surface lipid film on the skin friction because of the very limited amount of it for most skin sites measured [25][26].

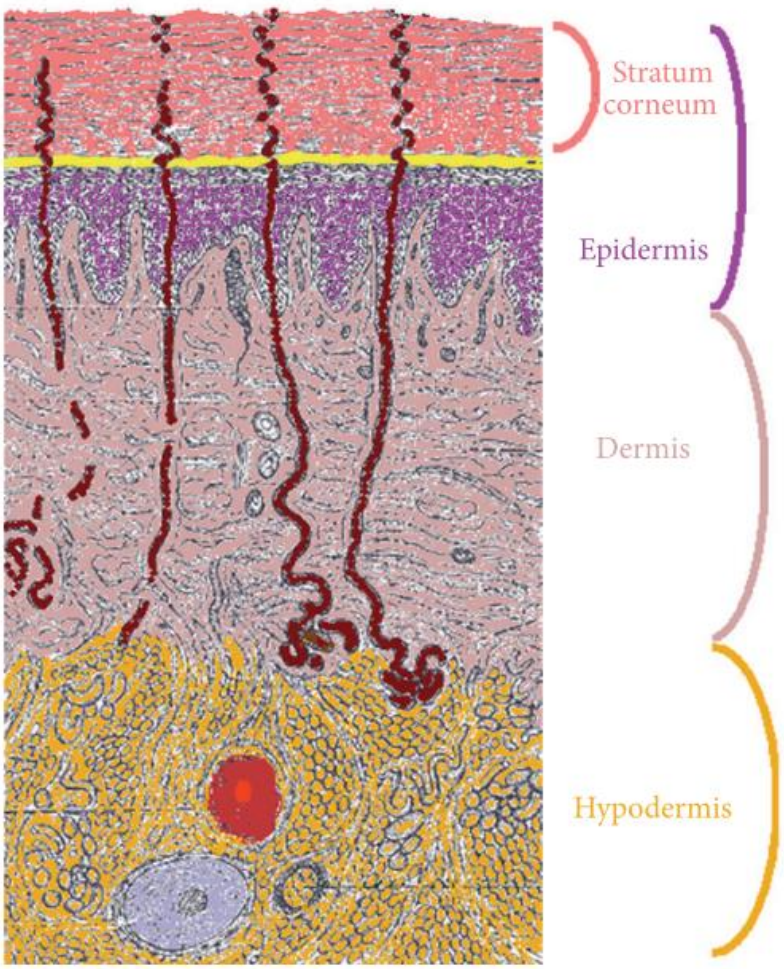

Figure 2.1. Schematic diagram of human skin showing three main layers: epidermis, dermis, hypodermis. Stratum corneum is the top layer of the epidermis [16].

2.1.2 Mechanical and Physical Properties

Skin is a nonlinear, non-homogenous, viscoelastic and anisotropic material in terms of its mechanical properties [14][15]. Young's modulus is one of the commonly used parameters to demonstrate skin mechanical properties. It is measured as a ratio of the stress over the strain in the skin deformation. Young's modulus of the skin is not constant and it depends on many factors. The main factors include the skin site of testing, measurement orientation with respect to Langer's lines which are the skin tension lines indicate the orientation of the underlying collagen fibers, the skin

hydration condition, skin thickness, testing methods and conditions [22][27][15]. The conventional methods to characterize Young's modulus are tensile, indentation, torsion, and suction measurements. The tensile stretching and indentation measurements are the most commonly used for the characterization of the modulus of in-plane and the normal direction respectively. Although both methods can have a broad range because of the measured skin sites, testing speed, the indentation depth and the measurement scale (nanoscopic to macroscopic level), the typical Young's modulus in the normal direction (lower than 0.1 MPa) is usually lower than it in the in-plane direction (1-100MPa). This means the skin can be more deformable in the normal direction than the in-plane direction under the same stress [28][29][30][31]. The tensile testing is usually done in vitro by testing excised skin while the indentation testing is more applicable to do in vivo [32]. Therefore, the indentation test has been used more to study the in vivo skin mechanical properties and the skin deformation in normal direction is commonly studied with friction since it can affect the frictional properties of skin. Kuilenburg et al. summarized the modulus of each skin layer in Table 2. 1 based on several references. All the values were measured by indentation testing. Based on this overview, the stiffness order is SC> epidermis> muscle> dermis> hypodermis. A broad range in these references can be caused by different test protocols, species, body sites and age of the subjects. Furthermore, the direct measurements for separate layers were done in vitro that can have altered mechanical properties compared to in vivo. According to the stiffness of different skin layers, a typical skin mode can have one stiff thin layer on the top of a soft layer and a rigid substrate [33][34]. Although the single layer of skin like the SC can have a very high Young's modulus, the measured Young's modulus of the whole skin in vivo can be low. There are several studies that measured Young's modulus in vivo on the volar forearm by the indentation test. Pailler-Mattei et al. did the measurement for 10 men about 30 years old. The penetration depth was

lower than 4.4 mm and the measured Young's modulus was between 10 kPa to 20 kPa [33]. Nachman and Franklin did it on a 29 years old woman and measured Young's modulus was around 10 kPa with a penetration depth lower than 1.2 mm [34]. Zahouani et al. measured Young's modulus of 8.3±2.1 kPa on 20 female subjects aged from 55 to 70 years old with a penetration depth of 1 mm [35]. According to these studies, the typical skin modulus in the normal direction can be lower than 20 kPa while the skin can have a higher modulus at higher indentation depth because of the influence of the subcutaneous tissue like muscle, which has a higher stiffness than the skin [32][36][33].

Table 2.1. Average values and ranges (in parentheses) of effective elastic modulus and thickness for each skin layer [37].

Skin layer, tissue		Elastic modulus E_i^* (MPa)	Thickness t_i (mm)
Stratum corneum	dry	500 (3.5–1000)	0.025 (0.01–0.04)
	wet	30 (10–50)	
Viable epidermis		1.5	0.095 (0.04–0.15)
Dermis		0.02 ($8–35\times10^{-3}$)	1.4 (0.8–2)
Hypodermis		2×10^{-3}	0.8
Muscle		0.25 (0.1–0.4)	

One of the most studied skin physical properties is skin topography. The commonly used technologies include ultrasound, confocal laser scanning microscopy, optical coherence tomography, and nuclear magnetic resonance [32][38]. The skin topography includes many surface features and one of the most used features is surface roughness [39]. By using scanning microscopy, a general range for surface roughness of the skin on the face and volar forearm was obtained, which is from 10 μm to 30 μm, and it has been shown that the surface roughness of human skin can increase with age [40][41].

2.1.3 Skin Simulant

It is a challenge to obtain reproducible results from the skin because of the complex and

variable physical and mechanical properties, and the difficulty to perform in vivo studies on human skin. Thus, materials to simulate the physical and mechanical properties of the skin have had a big interest in research related to human skin mechanical performance. The most commonly used materials to simulate skin mechanical properties are gelatinous substances and elastomers. The typical materials in the gelatinous substances include gelatin, agar, and agarose, etc. Elastomers such as silicone and polyurethane are widely used because of their viscoelastic properties and feasibility to customize the mechanical properties. There are other material options to simulate other skin properties such as thermal, optical, and surface properties [42]. Silicone rubber is the most used material in skin substitutes in terms of mechanical performance under compression [14]. In the study of tribology of human skin and tactile sensation, Lorica® Soft has been used widely, which is a synthetic leather made of polyurethane coated polyamide fleece [43][44][45][46]. It has been reported this material has a friction coefficient value similar to the human skin under dry conditions [44]. To approach the more comprehensive and complicated performance of human skin, multiple layers with various compositions have been used to further stimulate the skin mechanical behavior [34]. However, all the materials in research have been tested in a few situations only and have material limitations such as only being tested in dry condition or under one normal load, time-consuming to make, thus they haven't been fully accepted.

2.2 Skin Irritation and Dermatitis

Common symptoms of skin disorders, caused by using hygiene products like diapers and sanitary pads, are dryness, skin reddening, swelling or eroding, papules. This can be called diaper rash or dermatitis. At the early stage of dermatitis, the redness of the skin is the most obvious observation. The area of redness will increase with an increase in severity. In moderate and severe situations, there can be pustules, desquamation and/or edema. When a diaper rash lasts more than 72 hours, fungal infection such as candida infection is more likely to occur [47][48][49].

2.2.1 Causes

This study is focused on nonwoven hygiene products. Diaper dermatitis (DD) and incontinence-associated dermatitis (IAD) are the two most common issues related to the usage of hygiene products. A high skin humidity with shear forces between the fabric and the skin is the primary cause of skin irritation, and then, if there is a long duration of skin contact with urine and feces, there is a higher risk for the skin to be exposed to micro-organisms and bacteria that leads to dermatitis and skin infection [6][11][50][51][52]. The primary factors and principles leading to skin irritation are described below.

Wetness

Excessive wetness is considered the primary reason for skin irritation because it can irreversibly degrade the "brick and mortar" structure of the stratum corneum. With the changed structure, the skin barrier function is impaired. The skin becomes more permeable for irritants, and there is a higher risk for mechanical damage because of the increased surface coefficient of friction under wet conditions [53][54]. In addition, the wet microclimate around the skin benefits the growth and activity of microorganisms, and the penetration to the skin becomes easier at high humidity and higher temperature [10][11].

Mechanical factors

Friction can cause mechanical damages. Zimmerer et al. did experiments for skin abrasion using diaper patches and it reported skin loss(stratum corneum flakes) after rubbing. More skin loss was observed when the patch was loaded with liquid and when a higher friction coefficient was measured under this wet condition compared to dry patches[55]. The abrasion effects on the skin were also reported by Derler et al when they measured friction between fingers and abrasive papers [56]. Recent studies showed the convex skin surfaces in the diapered area which has a larger

contact area with the fabric than the folds, is more susceptible to the rash. The mechanical interaction between the skin and fabric can facilitate the damage of skin barrier and may directly cause skin injuries [50][54].

Urine and feces

Urine is the main reason for the increased pH values of the environment because of the presence of ammonia. Feces contain a lot of irritants and enzymes that can break down the proteins and fat in the skin, and thus impair the skin barrier and cause skin irritation [57][50].

pH

The common pH value of the skin surface is approximately between 4 and 6, which is acidic and beneficial to the enzymes that help to maintain the barrier function of the skin. However, a relatively high pH, which indicates an alkaline environment, inhibits the activity of the beneficial enzymes while it increases the activity of enzymes that degrade the skin barrier lipids. In addition, the pathogenic bacteria prefer a higher pH value for the skin. Therefore, an acidic situation of the skin surface is preferred to maintain skin health, and a neutral or alkaline environment can increase the sensitivity of skin irritants and reduce the antibacterial properties of skin [2]. The skin area covered by diapers normally shows a higher pH value. For example, the typical pH value at the baby diaper region is 6.2 to 6.8, when the outside region is 5.2 to 5.5. The higher pH results from the decomposition of urea, and it leads to an easier penetration for irritants to the skin and causes skin irritation in the diapered area [10].

Skin conditions

Since hygiene products can be used for people with very sensitive or fragile skin, the risk of skin irritation can be higher. For example, infants have much thinner skin than adults. The immune system hasn’t fully established. Thus, the skin is more fragile to be damaged or attacked,

especially for premature infants who do not have the fully functional skin as a protective barrier. Aging skin is more likely to undergo a functional degeneration. The flattening of the dermal-epidermal junction reduces the resistance to a shearing force which is the main cause of skin chafing. The reduction of collagen and elastin networks cause less stretchable, less resilient and more wrinkling skin. It also doesn't recover as quickly as younger skin. Therefore, it is more difficult to resist any harmful effects caused by external forces [10][58][57].

It is a remaining challenge to quantify all the factors and demonstrate the boundary between an at-risk situation and a good situation to ensure skin health. The dynamic use environment from a dry to a wet condition can not only affect the skin condition but also influence the properties of the fabric. It is necessary to make sure that the skin-fabric interaction does not lead to skin discomfort and skin injuries both under dry and wet conditions.

2.2.2 Parameters for Skin Condition Evaluation

The commonly used parameters to evaluate the skin condition are transepidermal water loss (TEWL), hydration of the Stratum Corneum (SC), pH, skin color, blood flow, and SC thickness [59][60][61][62]. To assess the barrier function of skin, TEWL is typically used. TEWL is the passive flux of water from dermis and epidermis to the surface of the SC [63]. The water loss is a result of the increased permeability of the stratum corneum, so a higher TEWL value indicates the skin is more permeable, and the increased TEWL is commonly used to indicate the higher sensitivity level of the skin [64][17]. Skin hydration is the water content of the SC[17]. The evaluation of skin hydration is usually evaluated by skin conductance or resistance measurement. It is known that skin hydration can progressively increase skin permeation thus reduce the barrier efficiency, while too low hydration leading to dry skin is also an issue [61][18][62]. Decreased hydration can be found in diseased skin [65] while the dermatitis area usually has high hydration

[66]. Skin pH is another parameter commonly used to represent the integrity of the skin barrier function as an acidic skin surface helps to ensure the barrier function under normal conditions [63][65]. Skin color can be measured by reflectance meter or digital analysis of images to assess skin redness or erythema [18][66][67]. These parameters can be used to explore the effects of friction between skin and nonwoven fabrics on the skin health condition.

2.2.3 How Friction Affects Skin Health

As mentioned in section 2.2.1, there are many factors that contribute to diaper dermatitis. Friction combined with the excessive wet condition is the biggest factor that can impair the skin barrier function and it relates to the performance of the topsheet fabric. The overhydration of the skin creates the environment for an easy break-in while friction is the key to break the protective barrier and thus cause injuries. Other factors like the presence of urine and feces can bring microorganisms and lead to some undesired enzyme-catalyzed reactions to further break the skin construction [52][54][50].

There are a few studies that have investigated the influence of friction on skin physiology by in vivo experiments. In 1955, Naylor conducted an in vivo experiment to investigate friction blisters by rubbing an area of skin over a polyethylene surface. During the experiments, the skin became red and stratum corneum began flaking, and then blisters occurred or the epidermis would rupture depending on the friction force and duration time. Naylor's work demonstrated that the friction force and the number of rubs or repeated times significantly affect the occurrence of blisters. He proposed that the skin can be protected by lowering the friction force, because the friction force determines the amount of work applied to the skin and the work the epidermis can withstand [68]. In 2015, Derler et al. have demonstrated the skin damage caused by friction by the observation of micro-scratches and a large number of abraded skin particles. However, the

correlation between the coefficient of friction and the amount of abraded skin particles was uncertain [56]. There are other studies that have reported friction was the primary reason for the superficial skin lesions, and friction can cause shear for deeper tissue leading to more serious skin damage combined with pressure [69][70].

In a word, friction applied to the skin can lead to skin structure change (e.g. skin becomes thicker under repeated small friction force [68]), skin lesion by abrasion of the skin surface and distortion of deeper tissue and body fluids.

2.3 Tactile Perception

2.3.1 Mechanism

The tactile perception is a term to describe the sensation perceived by the skin, which is how individuals feel when they touch an object. Okamoto defined it as " the perception of qualities and properties of the material surface by touch"[71]. The current understanding for the mechanism of tactile perception is the receptors located in the skin sense the object and transmit the information by an electrical signal through nerve fibers to the brain. Although the basic construction of the skin is the same for all body regions, there are two skin types that have some different properties. The two skin types are the glabrous skin and hairy (non-glabrous) skin. Most body regions are covered by the hairy skin, while a few regions are glabrous and these are mainly the skin sites on the hands and feet. The glabrous skin sites on hands, specifically the finger pad, and the palm, have been studied the most. Based on those studies, the glabrous skin receptors can be classified into three groups: mechanoreceptors, thermoreceptors, and nociceptors. The thermoreceptors and nociceptors are receptors that respond to the thermal and various harmful stimuli. The mechanoreceptors sense the mechanical deformation such as touch, pressure, vibration.

For the mechanoreceptors, there are low-threshold and high threshold mechanoreceptors that react to innocuous and harmful mechanical stimuli, respectively. The low-threshold mechanoreceptors are responsible for the gentle touch and other slight physical interactions between the skin and an object. They are commonly classified as four types and each type responds to certain stimuli based on the range of frequency. The Merkel's cell-neurite complex or Merkel's disc (SAI) and Ruffini corpuscle subcutaneous (SAII) are receptors with a slow-adaptation rate that react to sustained deformation. The corresponding frequency range for them is 5 to 15 Hz, and 15 to 400 Hz respectively. The rapid adaptation receptors that evoked by temporal changes in skin deformation are Meissner corpuscle (RAI or FAI) and Pacinian corpuscle (RAII or FAII). The corresponding frequency range is 20 to 50 Hz, and 60 to 400 Hz respectively [72][73]. A schematic view of the location and shape of the mechanoreceptors is shown in Figure 2. 2.

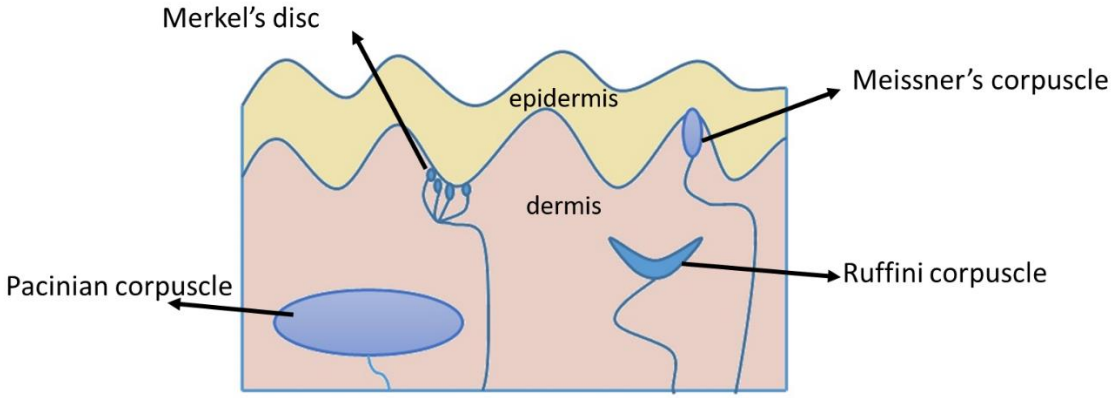

Figure 2.2. Schematic diagram of mechanoreceptors.

The perception that each receptor type can evoke is different, and the perception of one stimulus usually involves several responses from different receptors through. SAI can lead to sensations about object shape, pressure, two-dimensional texture, which would give the spatial

image of the touched object. SAII is believed to respond to skin stretch. RAI evokes the sensation about the horizontal movement that is produced by contact and velocity during the lateral movement. RAII also responds to movement but with much higher sensitivity compared to RAI [73][74][75][76].

The sensation of hairy skin is more complex and comprehensive because of the hair follicles. Merkel cell-axon complex (SAI), Ruffini corpuscle (SAII), and Pacinian corpuscle (RAII) also exist in the hairy skin regions. In addition, a C-type fiber or C-fiber was proposed for the hairy skin that responds to slow motion (the best range from 1 to 10 cm/s) with a remaining effect after the stimulus is removed. It is suggested the C-fiber is associated with the pleasantness perception of touch, the gentle stroking. Pawling et al. measured the facial electromyography and heart rate combined with subjective self-report when doing stroking touch. A positive correlation between subjective pleasantness and C-fiber activation was found [75][77].

According to the mechanism of tactile perception, the skin senses the mechanical stimuli by the skin deformation and vibration signal induced by the interaction with external objects. The different frequency and power generated by the interaction can trigger different receptors and cause various sensations. The tactile perception of fabrics is generated from the interaction between fabric and skin and friction is usually studied to characterize this interaction. The fabric surface properties are recognized as main effects that can influence the skin-fabric interaction and thus the tactile perception [74][78].

2.3.2 Evaluation Methods of Skin Comfort of Fabrics

Skin comfort is a subjective perception based on physical, physiological and psychological factors. Psychological and physiological factors are dynamic factors such as the state of being, mood, feelings, physical fitness, etc.. Physical factors include the factors like fabric properties,

environmental temperature, and humidity, and so on, which are relatively steady and measurable compared to psychological and physiological factors [79]. The skin comfort of fabric can be a transient sensation when the fabric is touched or handled, or be a tactile sensation that occurred during a period of time or after the skin-fabric contact [80].

Although skin comfort evaluation is essentially subjective, objective or quantitative evaluation is desired for engineering analysis. Since 1930s Dr. Pierce presented the idea of translating the subjective hand evaluation to a measurable quantity of fabrics, there are few methods developed to characterize the mechanical properties of fabrics and correlate them to fabric hand. The Kawabata evaluation system (KES) is the most famous and well-developed system that is applied to the evaluation of fabric hand currently. In this system, the complete testing methodology is achieved by four testing machines: tensile and shear testing, surface testing, compression testing, and bending testing. Besides KES, there are many variants of it such as SiroFAST, FAMOUS, CHES-FY, QIHES-F [81][80][82]. Although the KES measurement system is well-developed, drawbacks still exist. The biggest problem is the complexity of the system, the data interpretation, the acceptance of the methods for different applications, and the cost.

In addition to evaluation systems, there are standards and methods existing as individual testing and analytic method to measure one mechanical parameter or several parameters that reflect the stiffness, bulk compression or surface properties. There are a series of ASTM standards for the measurement of fabric properties such as stiffness (D1388-18, D4032-08, D6828-02). EDANA and INDA have produced Nonwovens Standard Procedures (NWSP, previous WSP standards). The standardized measurement method for nonwoven properties can be found there, such as cantilever bending (NWSP 90.1), Cusick drape (NWSP 90.4), Handle-O-Meter stiffness tester (NWSP 90.3) [83]. In addition, there are some new methods have been developed based on new technologies.

The electroencephalogram (EEG) has been reported as a potential method to study fabric softness because the Alpha rhythm of brainwave showed a positive correlation with the KES test results and subjective assessment[84].

Currently, it is still necessary to do a subjective evaluation for the comfort of fabrics. There are several steps to consider before doing the subjective evaluation. The first and the most important step would be defining the fabric based on the specific end-use. From this point of view, the use condition and situation, the state of users, and how the fabric contacts the skin has to be assessed, which includes the information of physical (e.g. environment temperature and humidity), physiological (e.g. heart rate change during workout) and psychological (e.g. softness is preferred for baby products) factors. Evaluators and the descriptive adjectives should then be selected based on the demand of the end-use of the fabric. The judgment can be associated with but not limited to, whether the evaluators come from the user group, or if they are experts in manufacturing this kind of product, but also gender, and age. The descriptive adjectives used should be easy to understand, as definite as possible and closely related to the end-user. A good reference can be the guidelines for the subjective evaluation of fabric hand-produced by AATCC (American Association of Textile Chemists and Colorists) [85].

Since most of the methods and studies are based on the understanding of glabrous skin sensation and were designed for fabric hand, it remains unclear whether the methods can be applied to other skin regions. The non-glabrous skin might have different interactions with fabrics leading to different sensations. For the application of absorbent hygiene products, buttocks are where the skin-fabric interaction occurs during the use so the sensation and physiology of the non-glabrous skin needs to be studied.

2.3.3 How Friction Affects Tactile Perception

As mentioned in section 2.3.1, the mechanoreceptors are excited by mechanical stimuli which can be generated by skin-object interaction. Friction is believed to be one of the major formats of the mechanical stimuli and it occurs whenever there is contact between the skin and the external object.

Most of the experiments exploring the effects of friction on tactile perception measured the friction between a finger and a surface, which can be various textiles, paper, or other materials. The fingertip or finger pad is a glabrous skin site that can have different sensation from the hairy skin sites. Nevertheless, the finger should be one of the most sensitive skin sites because there is a large number of receptors (more than 250 sensors/cm^2)[78][86]. Klöcker et al. used 48 different materials to build a Pleasant Touch Scale and gave the reference for different sensation of pleasant by finger-touch. It reported a negative correlation between the coefficient of friction and pleasantness sensation of surfaces[87][88]. Kim et al also reported a significant influence of friction coefficients on personal preference for automobile leather. A lower friction coefficient is more preferred. In addition, it mentioned a positive relationship between friction and stickiness sensation [89]. Chen and Ge showed the friction force and the friction-induced vibration can evoke brain response. The coefficient of friction has a negative impact on the comfort sensation of surface texture [90].

2.4 Friction

2.4.1 Concepts for Skin Friction Theories

Amonton's law is the classical theory about friction. It states the friction force is proportional to the normal load and independent of the contact area. Therefore, the ratio of the friction force to the normal load is constant, which is named the coefficient of friction. However,

it may not fit the skin friction. There are some experimental studies that have shown the coefficient of friction would change when the normal force changes. The reason for the inapplicability of Amonton's law is that the skin can exhibit viscoelastic properties and the contact area can be non-proportional to the normal load, thus the friction force would depend on the contact area [91][92]. In this case, the coefficient of friction is not a constant value anymore as a feature of the material. To better understand the friction force between the skin and a counter surface, a two-term model consists of adhesion and deformation components of friction (equation(1)) is commonly used [93][94][95] : $F_{friction} = F_{ad} + F_{def}$ (1)

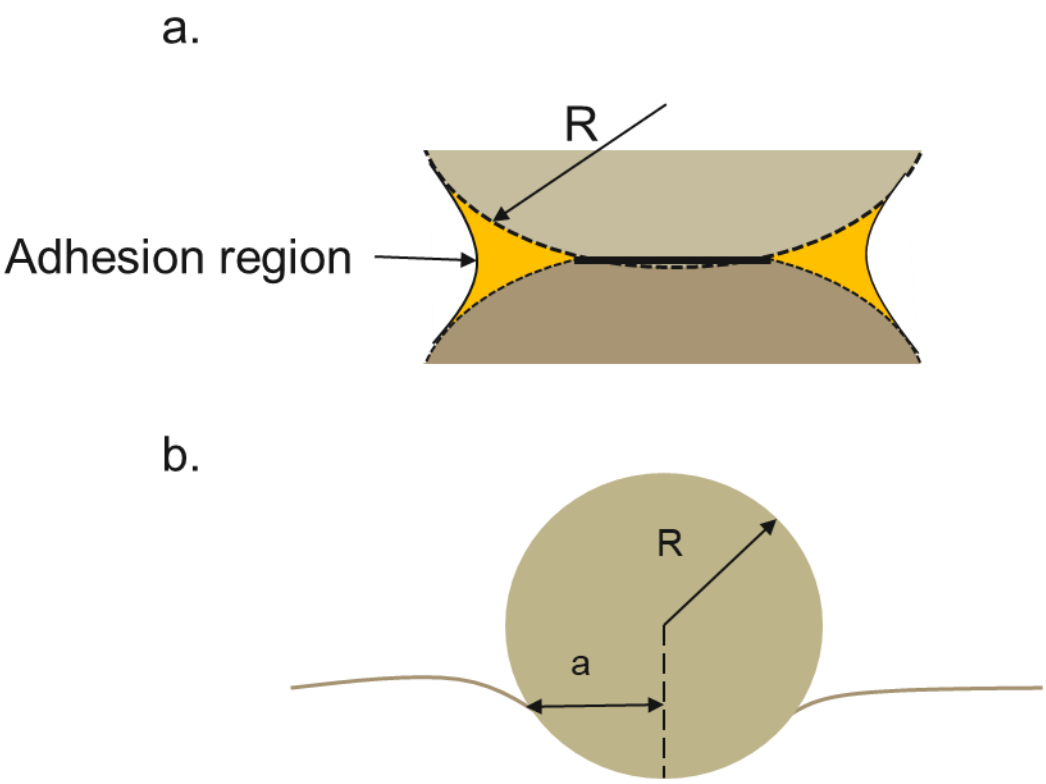

Figure 2.3. Schematic illustration of basic contact mechanic models. a: adhesion contact model; b: deformation contact model. R is the radius of the sphere. a is the radius of the circle of the contact area formed under a normal load.

Based on the contact model proposed by Johnson, Kendall, and Roberts (JKR) [96] (Figure 2.3, a.), the adhesion component is calculated using equation (2) where the R is the radius of curvature and the ω is the work of adhesion which can be estimated by the surface energy of the contact materials (γ_1, γ_2, the surface energy of two contact surfaces) (equation (3)) [95].

$$F_{ad} = \frac{3}{2}\pi R\omega \qquad (2)$$

$$\omega \approx 2\sqrt{\gamma_1\gamma_2} \qquad (3)$$

The deformation model is first proposed by Greenwood and Tabor [97] (Figure 2.3, b.). The force is expressed in equation (4) where the β is the viscoelastic loss fraction, a is the radius of the contact area circle, R is the radius of the curvature, and the N is the applied normal force.

$$F_{def} = \frac{3}{16}\beta\frac{a}{R}N \qquad (4)$$

Although the two-term friction model was created based on two elastic solids, it can help to understand the contact mechanism between skin and fabrics (viscoelastic materials). If considering the contacts between asperities on the fabric surface and the skin (skin as the substrate), the R in the equation, the radius of curvature, relates to the surface roughness of the fabric. By considering the equations above, the adhesion component of friction can be affected by the surface roughness and surface energy of fabrics, the surface energy of skin, and the contact area that depends on the normal load and elastic modulus of both skin and fabrics. The deformation component involves the energy loss of viscoelastic hysteresis of skin, the surface roughness of fabric, the contact area, and the normal force. In the literature, the adhesion force is considered the primary component of the friction of human skin and the deformation component is generally neglected [98]. However, the contribution of deformation can change depending on the contact

material, lubrication state, and the normal load. It is suggested to take the deformation into account when the skin is sliding against a rough surface under wet conditions, especially when the normal load is high [99][100]. The two-term friction model is usually used to understand the frictional behavior of the skin and in experimental studies. Another way to characterize friction is an extension of Amonton's law that can describe the relationship between the normal load and the friction force (equation (5)). The exponent depends on the contact condition thus it can carry the information about the contribution of the adhesion and deformation components. It is reported the typical value of the exponent for the friction of human skin is between 0.6 and 1.1 [46].

$$F_{friction} = \mu \times N^{m} \approx F_{ad} + F_{def} \qquad (5)$$

2.4.2 Impact Factors of Skin Friction

2.4.2.1 Normal Load/Contact Pressure

The normal load is a common factor that has been investigated for its influence on friction coefficients. The contact pressure is related to the normal load but carries more information than it, as it takes the contact area into account. Thus, the contact pressure can better demonstrate the conditions of skin friction, because the skin is a soft, viscoelastic material and the contact area can change considerably under different normal loads. Nevertheless, the measurement of the real contact area between fabric and skin is a challenge, so the apparent contact area is usually used to estimate the contact pressure (Figure 2.4). In the majority of the literature, the increase of normal force can decrease the coefficient of friction while the size of this decrease can vary based on the range of the normal force [101][102][103][104]. The same trend for contact pressure and friction coefficients was reported [105]. The explanation is that the contact surface is flattened and becomes smoother under higher compression so the friction reduces. In Derler and Gerhardt's review, the decrease of the coefficient of friction with the increase of pressure is more pronounced

under wet conditions than dry conditions. This is because of a larger increase in contact area under wet conditions caused by the hydration and softening of the skin [106][107][108].

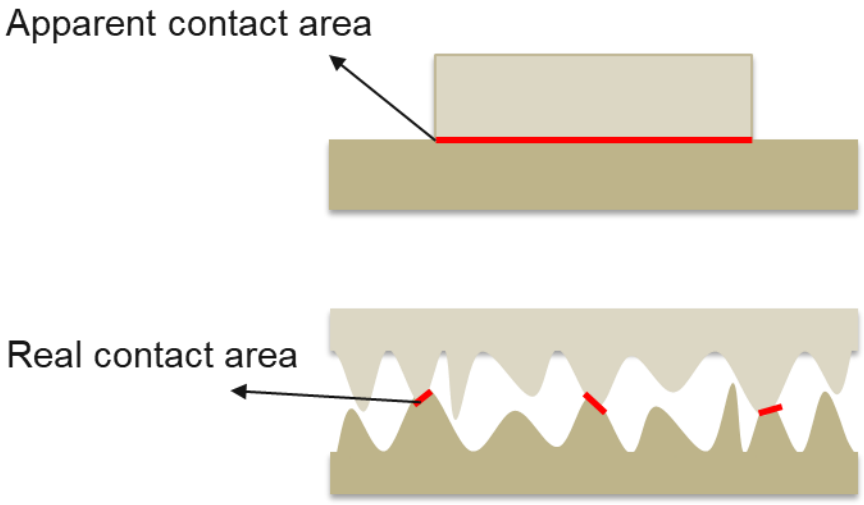

Figure 2.4. The apparent contact area and the real contact area in the contact of two surfaces.

2.4.2.2 Skin Wetness, Temperature, and Humidity

A bell-curve was proposed to demonstrate the relationship between the coefficient of friction and the amount of water (Figure 2.5) based on studies of friction between fingers and glass. It indicated that the friction coefficient reached the highest value for the damp skin compared to the dry and very wet skin [109][110]. However, whether this relationship is appropriate for skin-fabric interaction is unknown. In experimental studies for skin-fabric interaction, the results all suggest the liquid on the skin-fabric interface can increase friction compared to dry skin [111][112][113][114]. The decrease of friction coefficient has not been reported for wet conditions. One possible reason is the liquid amount applied to these experiments is not high enough to form a water film that lubricates the interface and reduces the friction. Another reason can be the material difference because fabrics can absorb a certain amount of liquid. In addition, the relationship may be affected by the normal load. André et al. showed the bell-shaped relationship

between the coefficient of friction and skin hydration for the low normal load (<3.5N) but the relationship attenuates under higher normal load [115]. This indicates the impact of wetness on friction under high normal force may get lower.

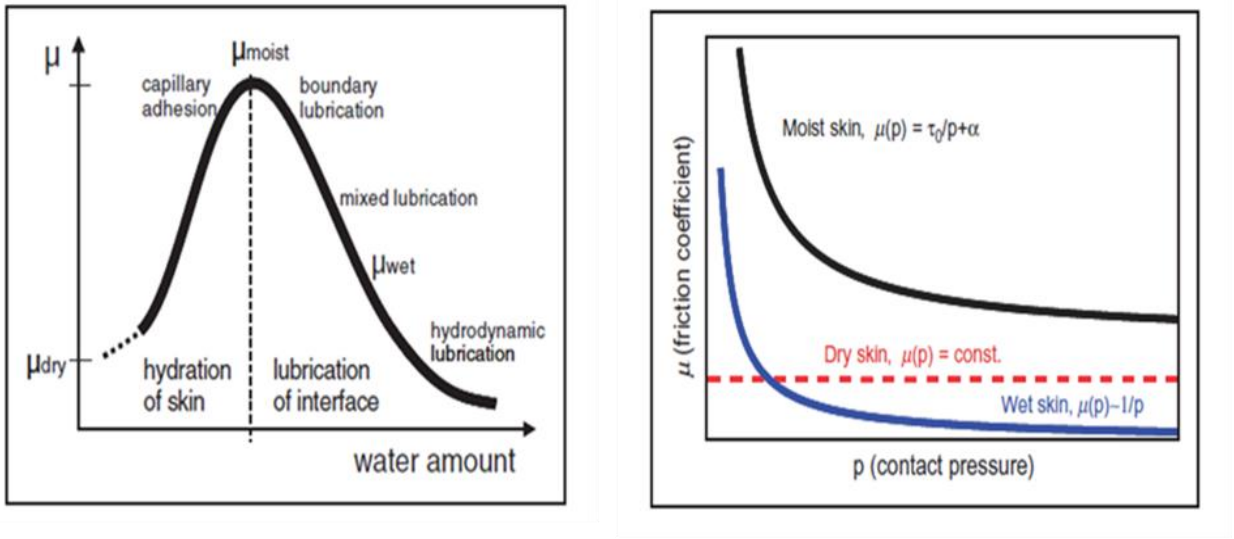

Figure 2.5. Derler et al. proposed a bell-curved relationship between the coefficient of friction and the water amount on the skin (left graph). The right graph is the coefficient of friction for dry, moist and wet skin as a function of contact pressure (right graph) [110].

In studies of friction between fabric and volar forearm, an increase of friction has been reported with the increase of the ambient temperature and relative humidity, which indicates the vital impact of the microclimate to skin-fabric interactions. It showed the biggest influence occurred when the temperature and humidity both changed. The increase of humidity had more impact on friction than temperature, especially at a relatively dry and cool climate condition. The main reasons for the influence of temperature and humidity are the change of the interface by the production and evaporation of sweat, and the decrease of stiffness caused by the increase of skin hydration under higher temperature and humidity [116][112].

2.4.2.3 Surface Texture

Smoothness and friction are reported as the most useful indicator for the fabric hand [117][118]. It is believed that the frictional behavior of skin can be largely affected by the surface texture of the contact surface because the counter surface texture can affect the deformation of the skin and thus change the contact area. The most commonly used property to characterize surface texture is surface roughness. The arithmetic mean height Ra is typically used to characterize the surface roughness, which is the arithmetic mean of the surface heights from the mean line in the evaluation length (Figure 2.6). The mean line is where the deviation of the height distribution is zero. The mathematical expression of Ra is [119][100]:

$$Ra = \frac{|Z_1| + |Z_2| + \ldots + |Z_n|}{n}$$

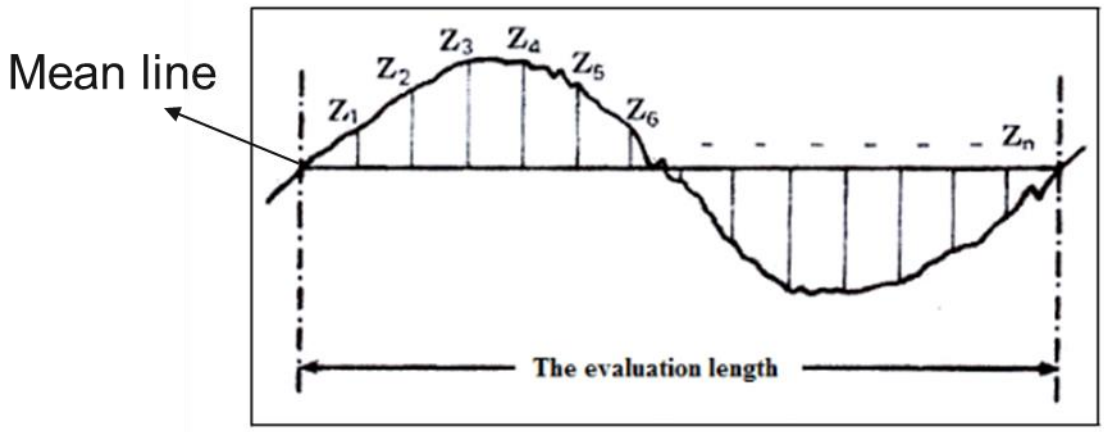

Figure 2.6. Mathematical evaluation of Ra [119].

The relationship between surface roughness and friction can be different depending on the situation. Li et al. did friction measurements by sliding the fingertip on sandpaper. There were four sandpaper samples tested with a surface roughness between 2 to 60 μm. It showed a proportional

relationship between the friction coefficient and surface roughness. The friction coefficient and the perception of roughness increased with the increase of surface roughness of the sandpaper. The explanation for this relationship is the plowing interaction that the skin embeds into the gap between high amplitude particles on the sandpaper surface, which increases the frictional resistance force [120]. Nevertheless, Klaassen and his colleagues measured friction between silicone and a skin simulant (Lorica Soft). They found a U-shaped relationship between the surface roughness and friction for this soft material. They reported the friction was the lowest when the surface roughness was about 4 μm and the investigated surface roughness was in the range from 0.5 μm to 7.8 μm, which meant the lowest friction appeared at the medium roughness surface [41]. The different relationships may be caused by the different contact materials (hard or soft), and the surface roughness range. It is hypothesized that there are two stages based on the contribution of deformation and interlocking of two surfaces. The first stage is when the surface has a low roughness and there is slight skin deformation so the plowing or interlocking effects are small. At this stage, the surface with lower roughness is smoother and has bigger contact area while a surface with higher roughness and not be fully compressed can have a reduced real contact area. Therefore, the friction can decrease with the increased surface roughness because of the reduced contact area. The second stage is when the roughness is higher and asperities of the surface protrude to the skin. This can lead to bigger contact area and induce the effects of mechanical interlocking of two surfaces so the friction can increase with the increased surface roughness because of the increased effects of ploughing [41][121][100].

Although Ra is commonly used to study the surface roughness-friction correlation, it does not involve the information about the profile shapes of the asperities, and the density or the spacing between asperities. The studies of whether and how that information can affect the friction are

lacking but it was proposed that small spacing between asperities might prevent the skin from filling the valleys and reduce the contact area [122][121].

2.4.2.4 Other factors

There are limited studies on other factors that affect skin friction. Some studies showed the effects of factors related to skin performance such as anatomical locations, gender, and age [123][124][111][102]. Therefore, it is essential to define the contact condition when comparing the friction measured on human skin.

2.5 Topsheet Nonwoven Fabrics for Hygiene Products

2.5.1 Materials and Technologies

Nonwoven fabrics have been selected to use for hygiene products because of the low cost, disposability, and feasibility to be engineered for various purposes. Both natural and synthetic fibers have been used but synthetic fiber/resins such as polypropylene (PP), PP/polyethylene (PE) and poly(ethylene terephthalate) (PET) /PE bicomponent fibers are dominant materials used for topsheet fabrics. Hydrophilic rayon was used for topsheet materials before but, recently, it was changed to hydrophobic fibers such as PP and PE to maintain a dry interface between skin and topsheet [7][125]. The three dominant materials used for topsheet nonwoven fabrics are PP, PE, and PET. All of them are versatile by tailoring the molecular weight and molecular weight distribution to fit a broad range of applications. PP is the most used material in nonwovens, especially in hygiene applications. The melting temperature of PP is from 160℃ to 170℃. The density is in the range of 0.88 to 0.91 g/cm^3 so it is very light. [126][127]. The typical density of PET is 1.38 g/ cm^3. The melting temperature is from 260℃ to 270℃. It can have good resistance to moisture, good resistance to abrasion, and good elastic recovery [127]. The low molecular weight PE that has a typical density of 0.9 g/cm^3 is usually used to produce bicomponent fibers.

The melting point is around 120 ℃, which is lower than PP and PET so it usually is used as the sheath material while PP or PET is the core in a bicomponent fiber and makes thermal bonding easier [127][128][129].

The frictional behavior of the topsheet fabrics can be affected by the surface energy and elastic modulus of the materials. According to the adhesion term of friction force, higher surface energy can increase the adhesion force. This corresponds to what is reported in several studies of the relationship between friction and surface energy [130][131][132][133]. PP and PE are the commonly used surface materials of topsheet nonwoven fabrics. Although the surface energy of PP and PE can be similar, it may also be different enough to distinguish the friction force depending on the crystallinity of the specific polymer used because the crystalline regions have higher surface energy than amorphous regions [133][134][135]. In addition to the surface energy, the elastic modulus by indentation can also influence the adhesion force because a higher contact radius is expected when the material has a lower elastic modulus and easier to deform. The higher contact radius can increase the adhesion force. The elastic modulus is related to the crystallinity as well. A higher crystallinity can lead to a higher elastic modulus, a harder surface and reduce the friction force [136][137].

The main applied technologies for topsheet nonwoven fabrics are spunbond, thermal calender bonding, and carding, through-air bonding. The spunbond technology is the most universal method used for disposable products and hygiene products [138]. The achievement of low basis weight nonwovens is one of the biggest advantages of the spunbond process [1][9]. The thermal calender bonding is a typically used bonding technology combined with spunbond because it is suitable to be used for fabrics with low thickness. In addition, it can give a well-designed texture for the fabric surface by adjusting the pattern on the roll surface [139][140]. Another

common way for topsheet production is carding for web formation in conjunction with through-air bonding. Generally, the carding process can make high bulk and low rigidity webs. The through-air bonding can retain the web loft which can ideally combine the low rigidity carded webs to give the fabric a softer property [141][139].

2.5.2 Friction between Skin and Topsheet Nonwoven Fabrics

There are limited studies on how nonwoven fabric material or structure parameters can influence on skin-fabric friction. Fiber size, bond area, and basis weight are the parameters that have been reported. Falloon et al. measured the friction between nonwoven fabrics and volar forearm. The investigated spunbond, thermal calender bonded fabrics showed the one with finer fiber size(3.6 dtex) had a lower coefficient of friction than the one with higher fiber size (6.5 dtex) when the material, basis weight, and bonding area are the same [142]. Falloon and Cottenden also measured the friction between nonwoven fabrics and skin simulant (artificial leather). The results showed the spunbond nonwoven fabric with a lower bond area (11%) had higher coefficient of friction than the fabric with higher bond area (18%). The fabric with lower basis weight (13g/m^2) showed lower coefficient of friction than the fabric with higher basis weight (18g/m^2, 25g/m^2) [143]. The impact on friction from these parameters is likely caused by the influence on surface topography. While the fiber size can change the contact radius on the fiber scale, the bond area can play a role on a fabric scale. Since the bond area has a lower amplitude than the unbonded area, it can affect the surface roughness. The basis weight of a fabric can alter the thickness and density. It may affect the surface roughness combined with the bond pattern on a macroscopic level or affect the surface roughness on a microscopic level (fiber scale). However, the nonwoven fabrics used in the reported studies are very limited to two or three samples and the explanation lacks evidence to support it. Further work is needed to investigate the effects of fabric

material/structure parameters on skin-fabric friction and their effects on the fabric surface properties.

2.6 References

[1] H. Fuchs and W. Kittelmann, “Characteristics and application of nonwovens,” in *Nonwoven Fabrics: Raw Materials, Manufacture, Applicaion, Characteristics, Testing Processes*, 2003.

[2] J. K. Bender, J. Faergemann, and M. Sköld, “Skin Health Connected to the Use of Absorbent Hygiene Products: A Review,” *Dermatol. Ther. (Heidelb).*, vol. 7, no. 3, pp. 319–330, Sep. 2017.

[3] J. Bae, H. Kwon, and J. Kim, “Safety evaluation of absorbent hygiene pads: A review on assessment framework and test methods,” *Sustainability (Switzerland)*, vol. 10, no. 11. MDPI AG, 11-Nov-2018.

[4] J. R. Ajmeri and C. J. Ajmeri, “Nonwoven personal hygiene materials and products,” in *Applications of Nonwovens in Technical Textiles*, Woodhead Publishing, 2010, pp. 85–102.

[5] M. T. Gillies, *Nonwoven materials : recent developments*. Park Ridge, N.J. : Noyes Data Corp, 1979.

[6] K. H. Hong, S. C. Kim, T. J. Kang, and K. W. Oh, “Effect of Abrasion and Absorbed Water on the Handle of Nonwovens for Disposable Diapers,” *Text. Res. J.*, vol. 75, no. 7, pp. 544–550, Jul. 2005.

[7] D. Das and B. Pourdeyhimi, *Composite nonwoven materials : structure, properties and applications*. Elsevier Science, 2014.

[8] “INDA | Hygiene.” [Online]. Available: http://www.inda.org/about-nonwovens/nonwoven-markets/hygiene/. [Accessed: 18-Sep-2017].

[9] J. R. A J M E R I and C. J. A J M E R I, J. R. Ajmeri, and C. J. Ajmeri, “Nonwoven personal hygiene materials and products,” in *Applications of Nonwovens in Technical Textiles*, Woodhead Publishing, 2010, pp. 85–102.

[10] B. Runeman, “Skin interaction with absorbent hygiene products,” *Clin. Dermatol.*, vol. 26, no. 1, pp. 45–51, Jan. 2008.

[11] M. Odio and L. Thaman, “Diapering, Diaper Technology, and Diaper Area Skin Health,” *Pediatr. Dermatol.*, vol. 31, no. s1, pp. 9–14, Nov. 2014.

[12] A. Abdouni, M. Djaghloul, C. Thieulin, R. Vargiolu, C. Pailler-Mattei, and H. Zahouani, “Biophysical properties of the human finger for touch comprehension: influences of ageing and gender.,” *R. Soc. open Sci.*, vol. 4, no. 8, p. 170321, Aug. 2017.

[13] V. B. Mountcastle, “The Evolution and Structure of the Hand,” in *The sensory hand: Neural mechanisms of somatic sensation.*, Harvard University Press., 2005, pp. 41–50.

[14] M. Azmi, Nurul Nadiah; Azhar, Ilya Izyan Shahrul; Jamaluddin, “A Brief Review and Framework towards Synthesising Silicone-Hydrogel Materials that Mimic Skin Deformation Behaviour,” *Appl. Mech. Mater.*, vol. 680, pp. 70–73, 2014.

[15] A. Kalra and A. Lowe, “An Overview of Factors Affecting the Skins Youngs Modulus,” *J. Aging Sci.*, vol. 4, no. 2, pp. 1–5, Aug. 2016.

[16] M. A. Abellan, H. Zahouani, and J. M. Bergheau, “Contribution to the determination of in vivo mechanical characteristics of human skin by indentation test,” *Comput. Math. Methods Med.*, vol. 2013, p. 814025, 2013.

[17] J. du Plessis *et al.*, “International guidelines for the *in vivo* assessment of skin properties in non-clinical settings: Part 2. transepidermal water loss and skin hydration,” *Ski. Res. Technol.*, vol. 19, no. 3, pp. 265–278, Aug. 2013.

[18] H. Zhai and H. I. Maibach, “Occlusion vs. skin barrier function,” *Ski. Res. Technol.*, vol. 8, no. 1, pp. 1–6, Feb. 2002.

[19] C. Pailler-Mattei, S. Pavan, R. Vargiolu, F. Pirot, F. Falson, and H. Zahouani, “Contribution of stratum corneum in determining bio-tribological properties of the human skin,” *Wear*, vol. 263, no. 7–12, pp. 1038–1043, Sep. 2007.

[20] A. Firooz *et al.*, “Variation of biophysical parameters of the skin with age, gender, and body region,” *Sci. World J.*, vol. 2012, 2012.

[21] A. Elkhyat, F. Fanian, A. Abdou, H. Amarouch, and P. Humbert, “Influence of the sebum and the hydrolipidic layer in skin wettability and friction,” in *Agache’s Measuring the Skin: Non-invasive Investigations, Physiology, Normal Constants: Second Edition*, Springer International Publishing, 2017, pp. 191–202.

[22] C. Pailler-Mattéi and H. Zahouani, “Analysis of adhesive behaviour of human skin in vivo by an indentation test,” *Tribol. Int.*, vol. 39, no. 1, pp. 12–21, Jan. 2006.

[23] P.-H. Cornuault, L. Carpentier, M.-A. Bueno, J.-M. Cote, and G. Monteil, “Influence of physico-chemical, mechanical and morphological fingerpad properties on the frictional distinction of sticky/slippery surfaces.,” *J. R. Soc. Interface*, vol. 12, no. 110, p. 0495, Sep. 2015.

[24] C. Pailler-Mattéi and H. Zahouani, “Study of adhesion forces and mechanical properties of human skin in vivo,” *J. Adhes. Sci. Technol.*, vol. 18, no. 15–16, pp. 1739–1758, Jan. 2004.

[25] S. Kondo, “The Frictional Properties Between Fabrics and the Human Skin,” *J. Japan Res. Assoc. Text. End-Uses*, vol. 43, no. 264, pp. 264–275, 2002.

[26] A. B. Cua, K.-P. Wilhelm, and H. I. Maibach, “Skin Surface Lipid and Skin Friction: Relation to Age, Sex and Anatomical Region,” *Skin Pharmacol. Physiol.*, vol. 8, no. 5, pp. 246–251, 1995.

[27] K. A. Newell, “Wound Closure,” in *Essential Clinical Procedures*, Elsevier Inc., 2007, pp. 313–341.

[28] K. A and L. A, “Mechanical Behaviour of Skin: A Review,” *J. Mater. Sci. Eng.*, vol. 5, no. 4, pp. 1–7, May 2016.

[29] A. Ní Annaidh, K. Bruyère, M. Destrade, M. D. Gilchrist, and M. Otténio, "Characterization of the anisotropic mechanical properties of excised human skin," *J. Mech. Behav. Biomed. Mater.*, vol. 5, no. 1, pp. 139–148, Jan. 2012.

[30] F. Khatyr, C. Imberdis, P. Vescovo, D. Varchon, and J. M. Lagarde, "Model of the viscoelastic behaviour of skin in vivo and study of anisotropy," *Ski. Res. Technol.*, vol. 10, no. 2, pp. 96–103, May 2004.

[31] C. T. McKee, J. A. Last, P. Russell, and C. J. Murphy, "Indentation versus tensile measurements of young's modulus for soft biological tissues," *Tissue Eng. - Part B Rev.*, vol. 17, no. 3, pp. 155–164, Jun. 2011.

[32] K. A and L. A, "Mechanical Behaviour of Skin: A Review," *J. Mater. Sci. Eng.*, vol. 5, no. 4, pp. 1–7, May 2016.

[33] C. Pailler-Mattei, S. Bec, and H. Zahouani, "In vivo measurements of the elastic mechanical properties of human skin by indentation tests," *Med. Eng. Phys.*, vol. 30, no. 5, pp. 599–606, Jun. 2008.

[34] M. Nachman and S. E. E. Franklin, "Artificial Skin Model simulating dry and moist in vivo human skin friction and deformation behaviour," *Tribol. Int.*, vol. 97, pp. 431–439, May 2016.

[35] H. Zahouani, C. Pailler-Mattei, B. Sohm, R. Vargiolu, V. Cenizo, and R. Debret, "Characterization of the mechanical properties of a dermal equivalent compared with human skin in vivo by indentation and static friction tests," *Ski. Res. Technol.*, vol. 15, no. 1, pp. 68–76, 2009.

[36] H. Joodaki and M. B. Panzer, "Skin mechanical properties and modeling: A review," *J Eng. Med.*, vol. 232, no. 4, pp. 323–343, Apr. 2018.

[37] J. Van Kuilenburg, M. A. Masen, and E. Van Der Heide, "Contact modelling of human skin: What value to use for the modulus of elasticity?," *Proc. Inst. Mech. Eng. Part J J. Eng. Tribol.*, vol. 227, no. 4, pp. 349–361, 2013.

[38] F. M. Hendriks, D. Brokken, J. T. W. M. van Eemeren, C. W. J. Oomens, F. P. T. Baaijens, and J. B. A. M. Horsten, "A numerical-experimental method to characterize the non-linear mechanical behaviour of human skin," *Ski. Res. Technol.*, vol. 9, no. 3, pp. 274–283, Aug. 2003.

[39] C. Trojahn, G. Dobos, M. Schario, L. Ludriksone, U. Blume-Peytavi, and J. Kottner, "Relation between skin micro-topography, roughness, and skin age," *Ski. Res. Technol.*, vol. 21, no. 1, pp. 69–75, Feb. 2015.

[40] Y. Masuda, M. Oguri, T. Morinaga, and T. Hirao, "Three-dimensional morphological characterization of the skin surface micro-topography using a skin replica and changes with age," *Ski. Res. Technol.*, vol. 20, no. 3, pp. 299–306, Aug. 2014.

[41] M. Klaassen, E. G. de Vries, and M. A. Masen, "Friction in the contact between skin and a soft counter material: effects of hardness and surface finish," *J. Mech. Behav. Biomed. Mater.*, Jan. 2019.

[42] A. K. Dąbrowska *et al.*, “Materials used to simulate physical properties of human skin,” *Ski. Res. Technol.*, vol. 22, no. 1, pp. 3–14, Feb. 2016.

[43] A. M. Cottenden, David J. Cottenden, “A study of friction mechanisms between a surrogate skin (Lorica soft) and nonwoven fabrics,” *J. Mech. Behav. Biomed. Mater.*, vol. 28, pp. 410–426, Dec. 2013.

[44] S. Derler, U. Schrade, and L.-C. Gerhardt, “Tribology of human skin and mechanical skin equivalents in contact with textiles,” *Wear*, vol. 263, no. 7, pp. 1112–1116, Sep. 2007.

[45] S. S. Falloon and A. Cottenden, “Friction between a surrogate skin (Lorica Soft) and nonwoven fabrics used in hygiene products,” *Surf. Topogr. Metrol. Prop.*, vol. 4, no. 3, p. 034010, Sep. 2016.

[46] M. M. Hurtado, M. Peppelman, X. Zeng, P. E. J. van Erp, and E. Van Der Heide, “Tribological behaviour of skin equivalents and ex-vivo human skin against the material components of artificial turf in sliding contact,” *Tribol. Int.*, vol. 102, pp. 103–113, Oct. 2016.

[47] S. Borkowski, “Diaper Rash Care and Management,” *Pediatr. Nurs.*, vol. 30, no. 6, pp. 467–70, 2004.

[48] P. Stamatas, Georgios N, “Diaper Rash,” *Pediatr. Parents*, vol. 29, no. 9/10, p. 29, 2013.

[49] S. Bağlam and B. Engin, “Diaper (napkin) dermatitis: A fold (intertriginous) dermatosis,” *Clin. Dermatol.*, vol. 33, no. 4, pp. 477–482, Jul. 2015.

[50] D. J. Atherton, “Understanding irritant napkin dermatitis,” *Int. J. Dermatol.*, vol. 55, pp. 7–9, Jul. 2016.

[51] U. Blume-Peytavi, M. Hauser, L. Lünnemann, G. N. Stamatas, J. Kottner, and N. Garcia Bartels, “Prevention of Diaper Dermatitis in Infants-a Literature Review,” *Pediatr. Dermatol.*, vol. 31, no. 4, pp. 413–429, Jul. 2014.

[52] G. N. Stamatas and N. K. Tierney, “Diaper Dermatitis: Etiology, Manifestations, Prevention, and Management,” *Pediatr. Dermatol.*, vol. 31, no. 1, pp. 1–7, Jan. 2014.

[53] M. Saadatmand *et al.*, “Skin hydration analysis by experiment and computer simulations and its implications for diapered skin,” *Ski. Res. Technol.*, vol. 23, no. 4, pp. 500–513, Nov. 2017.

[54] U. Blume-Peytavi and V. Kanti, “Prevention and treatment of diaper dermatitis,” *Pediatr. Dermatol.*, vol. 35, pp. s19–s23, Mar. 2018.

[55] R. E. Zimmerer, K. D. Lawson, and C. J. Calvert, “The Effects of Wearing Diapers on skin,” *Pediatr. Dermatol.*, vol. 3, pp. 95–101, 1986.

[56] S. Derler, M. Preiswerk, G.-M. Rotaru, J.-P. Kaiser, and R. M. Rossi, “Friction mechanisms and abrasion of the human finger pad in contact with rough surfaces,” *Tribol. Int.*, vol. 89, pp. 119–127, Sep. 2015.

[57] H. Beele *et al.*, “Incontinence-Associated Dermatitis: Pathogenesis, Contributing Factors, Prevention and Management Options,” *Drugs Aging*, vol. 35, no. 1, pp. 1–10, Jan. 2018.

[58] R. M. Lavker, P. S. Zheng, and G. Dong, “Morphology of aged skin.,” *Clin. Geriatr. Med.*, vol. 5, no. 1, pp. 53–67, Feb. 1989.

[59] F. Giusti, A. Martella, L. Bertoni, and S. Seidenari, “Skin Barrier, Hydration, and pH of the Skin of Infants Under 2 Years of Age,” *Pediatr. Dermatol.*, vol. 18, no. 2, pp. 93–96, Mar. 2001.

[60] J. W. Fluhr, R. Darlenski, I. Angelova-Fischer, N. Tsankov, and D. Basketter, “Skin Irritation and Sensitization: Mechanisms and New Approaches for Risk Assessment 1. Skin Irritation,” *Ski. Pharmacol Physiol*, vol. 21, pp. 124–135, 2008.

[61] Q. Zhang, M. Murawsky, T. LaCount, G. B. Kasting, and S. K. Li, “Transepidermal water loss and skin conductance as barrier integrity tests,” *Toxicol. Vitr.*, vol. 51, pp. 129–135, Sep. 2018.

[62] J. M. Crowther *et al.*, “Measuring the effects of topical moisturizers on changes in stratum corneum thickness, water gradients and hydration in vivo,” *Br. J. Dermatol.*, vol. 159, no. 3, pp. 567–577, Jun. 2008.

[63] L. Ludriksone, N. Garcia Bartels, V. Kanti, U. Blume-Peytavi, and J. Kottner, “Skin barrier function in infancy: a systematic review,” *Arch. Dermatol. Res.*, vol. 306, no. 7, pp. 591–599, Sep. 2014.

[64] V. Rogiers, “EEMCO Guidance for the Assessment of Transepidermal Water Loss in Cosmetic Sciences,” *Skin Pharmacol. Appl. Skin Physiol.*, vol. 14, no. 2, pp. 117–128, 2001.

[65] M. M. Young, A. Franken, and J. L. du Plessis, “Transepidermal water loss, stratum corneum hydration, and skin surface pH of female African and Caucasian nursing students,” *Ski. Res. Technol.*, vol. 25, no. 1, pp. 88–95, Jan. 2019.

[66] G. N. Stamatas, C. Zerweck, G. Grove, and K. M. Martin, “Documentation of Impaired Epidermal Barrier in Mild and Moderate Diaper Dermatitis In Vivo Using Noninvasive Methods,” *Pediatr. Dermatol.*, vol. 28, no. 2, pp. 99–107, Mar. 2011.

[67] A. R. Matias, M. Ferreira, P. Costa, and P. Neto, “Skin colour, skin redness and melanin biometric measurements: comparison study between Antera ® 3D, Mexameter ® and Colorimeter ®,” *Ski. Res. Technol.*, vol. 21, no. 3, pp. 346–362, Aug. 2015.

[68] N. P and P. F. D. NAYLOR, “EXPERIMENTAL FRICTION BLISTERS,” *Br. J. Dermatol.*, vol. 67, no. March, p. 2015, Oct. 1955.

[69] N. A. Lahmann and J. Kottner, “Relation between pressure, friction and pressure ulcer categories: A secondary data analysis of hospital patients using CHAID methods,” *Int. J. Nurs. Stud.*, vol. 48, no. 12, pp. 1487–1494, Dec. 2011.

[70] X. Mao, Y. Yamada, Y. Akiyama, and S. Okamoto, “Characteristics of Dummy Skin Contact Mechanics During Developing Process of Skin Abrasion Trauma,” *Tribol. Lett.*, vol. 65, no. 4, p. 133, Dec. 2017.

[71] S. Okamoto, H. Nagano, and Y. Yamada, “Psychophysical Dimensions of Tactile Perception of Textures,” *IEEE Trans. Haptics*, vol. 6, no. 1, pp. 81–93, 2013.

[72] X. Xie *et al.*, “A Review of Smart Materials in Tactile Actuators for Information Delivery,” *J. Carbon Res.*, vol. 3, no. 4, p. 38, Dec. 2017.

[73] X. Zhou *et al.*, “Correlation between tactile perception and tribological and dynamical properties for human finger under different sliding speeds,” *Tribol. Int.*, vol. 123, pp. 286–295, 2018.

[74] S. Chen, S. Ge, W. Tang, J. Zhang, and N. Chen, “Tactile perception of fabrics with an artificial finger compared to human sensing,” *Text. Res. J.*, vol. 85, no. 20, pp. 2177–2187, 2015.

[75] V. E. Abraira and D. D. Ginty, “The Sensory Neurons of Touch,” *Neuron*, vol. 79, pp. 618–639, 2013.

[76] E. Asaga, K. Takemura, T. Maeno, A. Ban, and M. Toriumi, “Tactile evaluation based on human tactile perception mechanism,” *Sensors Actuators, A Phys.*, vol. 203, pp. 69–75, 2013.

[77] R. Pawling, P. R. Cannon, F. P. Mcglone, and S. C. Walker, “C-tactile afferent stimulating touch carries a positive affective value,” 2017.

[78] S. Bensaid, J. F. Osselin, L. Schacher, and D. Adolphe, “The effect of pattern construction on the tactile feeling evaluated through sensory analysis,” *J. Text. Inst.*, vol. 97, no. 2, pp. 137–145, 2006.

[79] G. J. Pontrelli, “Comfort by Design,” *Text. Asia*, no. 21, pp. 52–61, 1990.

[80] I. L. Ciesielska-Wróbel and L. Van Langenhove, “The hand of textiles – definitions, achievements, perspectives – a review,” *Text. Res. J.*, vol. 82, no. 14, pp. 1457–1468, Sep. 2012.

[81] F. T. Peirce, “The ‘Handle’ of Cloth As A Measurable Quantity,” *J. Text. Inst.*, pp. T377–T416, 1930.

[82] Y. Sun, M. Zhang, G. Liu, and Z. Du, “Measurement of fabric handle characteristics based on the Quick-Intelligent Handle Evaluation System for Fabrics (QIHES-F),” *Text. Res. J.*, vol. 0, no. 00, pp. 1–13, 2018.

[83] N. Mao, “Methods for characterisation of nonwoven structure, property, and performance,” in *Advances in Technical Nonwovens*, Woodhead Publishing, 2016, pp. 155–211.

[84] X. Zhang, J. Yue, J. Jia, and G. Wang, “An electroencephalogram study on softness cognition of silk fabric hand,” *J. Text. Inst.*, vol. 107, no. 12, pp. 1601–1606, Dec. 2016.

[85] F. Sun, R. Gao, X. Hu, Z. Du, and W. Yu, “Experimental study on an effective method for the friction property of fabrics by the comprehensive handle evaluation system for fabrics and yarns system,” *Text. Res. J.*, vol. 88, no. 8, pp. 882–891, Feb. 2018.

[86] E. Classen, “Comfort testing of textiles,” *Adv. Charact. Test. Text.*, pp. 59–69, Jan. 2018.

[87] A. Klöcker, M. Wiertlewski, V. Théate, V. Hayward, and J.-L. Thonnard, “Physical Factors Influencing Pleasant Touch during Tactile Exploration,” *PLoS One*, vol. 8, no. 11, p. e79085, Nov. 2013.

[88] A. Klöcker, C. Arnould, M. Penta, and J.-L. Thonnard, “Rasch-Built Measure of Pleasant Touch through Active Fingertip Exploration,” *Front. Neurorobot.*, vol. 6, p. 5, Jun. 2012.

[89] W. Kim, Y. Lee, J. H. Lee, G. W. Shin, and M. H. Yun, “A comparative study on designer and customer preference models of leather for vehicle,” *Int. J. Ind. Ergon.*, vol. 65, pp. 110–121, May 2018.

[90] S. Chen and S. Ge, “Experimental research on the tactile perception from fingertip skin friction,” *Wear*, vol. 376–377, pp. 305–314, Apr. 2017.

[91] S. COMAISH and E. BOTTOMS, “The Skin and Friction: Deviations From Amonton’S Laws, and the Effects of Hydration and Lubrication,” *Br. J. Dermatol.*, vol. 84, no. 1, pp. 37–43, Jan. 1971.

[92] A. M. Cottenden, W. K. Wong, D. J. Cottenden, and A. Farbrot, “Development and validation of a new method for measuring friction between skin and nonwoven materials,” *Proc. Inst. Mech. Eng. Part H J. Eng. Med.*, vol. 222, no. 5, pp. 791–803, May 2008.

[93] M. F. Leyva-Mendivil, J. Lengiewicz, and G. Limbert, “Skin friction under pressure. The role of micromechanics,” *Surf. Topogr. Metrol. Prop.*, vol. 6, no. 1, p. 014001, Jan. 2018.

[94] S. Derler and L.-C. Gerhardt, “Tribology of Skin: Review and Analysis of Experimental Results for the Friction Coefficient of Human Skin,” *Tribol. Lett.*, vol. 45, no. 1, pp. 1–27, Jan. 2012.

[95] K. B. Duvefelt, U. L. O. L.-O. Olofsson, and C. M. J. Johannesson, “Towards simultaneous measurements of skin friction and contact area: Results and experiences,” *Proc. Inst. Mech. Eng. Part J J. Eng. Tribol.*, vol. 229, no. 3, pp. 230–242, Mar. 2015.

[96] K. L. Johnson, K. Kendall, and A. D. Roberts, “Surface Energy and the Contact of Elastic Solids,” *Proc. R. Soc. A Math. Phys. Eng. Sci.*, vol. 324, no. 1558, pp. 301–313, 1971.

[97] J. A. Greenwood and D. Tabor, “The friction of hard sliders on lubricated rubber: The importance of deformation losses,” *Proc. Phys. Soc.*, vol. 71, no. 6, pp. 989–1001, 1958.

[98] S. Derler, R. M. Rossi, and G. M. Rotaru, “Understanding the variation of friction coefficients of human skin as a function of skin hydration and interfacial water films,” *Proc. Inst. Mech. Eng. Part J J. Eng. Tribol.*, vol. 229, no. 3, pp. 285–293, 2015.

[99] D. Mahdi, A. Riches, M. Gester, J. Yeomans, and P. Smith, “Rolling and sliding: Separation of adhesion and deformation friction and their relative contribution to total friction,” *Tribol. Int.*, vol. 89, pp. 128–134, Sep. 2015.

[100] J. van Kuilenburg, M. A. Masen, and E. van der Heide, “A review of fingerpad contact mechanics and friction and how this affects tactile perception,” *Proc. Inst. Mech. Eng. Part J J. Eng. Tribol.*, vol. 229, no. 3, pp. 243–258, Mar. 2015.

[101] S. Derler and G. M. Rotaru, “Stick-slip phenomena in the friction of human skin,” *Wear*, vol. 301, no. 1–2, pp. 324–329, Apr. 2013.

[102] G. Man and M.-Q. Man, “Skin Friction Coefficient,” in *Agache’s Measuring the Skin*, Cham: Springer International Publishing, 2017, pp. 203–210.

[103] N. A. Kalebek and O. Babaarslan, “Effect of weight and apllied force on the friction coefficient of the spunlace nonwoven fabrics,” *Fibers Polym.*, vol. 11, no. 2, pp. 277–284, Apr. 2010.

[104] N. K. Veijgen, M. A. Masen, and E. van der Heide, “A novel approach to measuring the frictional behaviour of human skin in vivo,” *Tribol. Int.*, vol. 54, pp. 38–41, Oct. 2012.

[105] X. Liu, M. J. Carré, Q. Zhang, Z. Lu, S. J. Matcher, and R. Lewis, “Measuring contact area in a sliding human finger-pad contact,” *Ski. Res. Technol.*, vol. 24, no. 1, pp. 31–44, Feb. 2018.

[106] S. Derler and L. C. Gerhardt, “Tribology of skin: Review and analysis of experimental results for the friction coefficient of human skin,” *Tribology Letters*, vol. 45, no. 1. pp. 1–27, Jan-2012.

[107] L.-C. L.-C. Gerhardt *et al.*, “Influence of epidermal hydration on the friction of human skin against textiles,” *J. R. Soc. Interface*, vol. 5, no. 28, pp. 1317–1328, Nov. 2008.

[108] M. J. Adams, B. J. Briscoe, and S. A. Johnson, “Friction and lubrication of human skin,” *Tribol. Lett.*, vol. 26, no. 3, pp. 239–253, Apr. 2007.

[109] S. E. Tomlinson, R. Lewis, X. Liu, C. Texier, and M. J. Carré, “Understanding the Friction Mechanisms Between the Human Finger and Flat Contacting Surfaces in Moist Conditions,” *Tribol. Lett.*, vol. 41, no. 1, pp. 283–294, Jan. 2011.

[110] S. Derler, R. M. R. Rossi, and G.-M. M. Rotaru, “Understanding the variation of friction coefficients of human skin as a function of skin hydration and interfacial water films,” *Proc. Inst. Mech. Eng. Part J J. Eng. Tribol.*, vol. 229, no. 3, pp. 285–293, Mar. 2015.

[111] P. Kenins, “Influence of Fiber Type and Moisture on Measured Fabric-to-Skin Friction,” *Text. Res. J.*, vol. 64, no. 12, pp. 722–728, Dec. 1994.

[112] A. R. Gwosdow, J. C. Stevens, L. G. Berglund, and J. A. J. Stolwijk, “Skin Friction and Fabric Sensations in Neutral and Warm Environments,” *Text. Res. J.*, vol. 56, no. 9, pp. 574–580, 1986.

[113] D. Schwartz, Y. K. Magen, A. Levy, and A. Gefen, “Effects of humidity on skin friction against medical textiles as related to prevention of pressure injuries,” *Int. Wound J.*, vol. 15, no. 6, pp. 866–874, May 2018.

[114] W. Ke, G. M. Rotaru, J. Y. Hu, R. M. Rossi, X. Ding, and S. Derler, “In Vivo Measurement of the Friction Between Human Skin and Different Medical Compression Stockings,” *Tribol. Lett.*, vol. 60, no. 1, p. 4, Oct. 2015.

[115] T. André, P. Lefèvre, and J.-L. Thonnard, “A continuous measure of fingertip friction during precision grip,” *J. Neurosci. Methods*, vol. 179, no. 2, pp. 224–229, May 2009.

[116] M. Klaassen, D. J. J. Schipper, and M. A. A. Masen, “Influence of the relative humidity and the temperature on the in-vivo friction behaviour of human skin,” *Biotribology*, vol. 6, pp. 21–28, Jun. 2016.

[117] H. Yokura and M. Niwa, “Objective Hand Measurement of Nonwoven Fabrics Used for the Top Sheets of Disposable Diapers,” *Int. J. Cloth. Sci. Technol.*, vol. 12, no. 3, pp. 184–192, 2003.

[118] M. MATSUDAIRA, J. YOSHIDA, and T. KINARI, “Objective and Subjective Handle Evaluation for Disposable Diaper’s Top Sheets and Reusable Diaper’s Fabrics,” *J. Text. Eng.*, vol. 53, no. 2, pp. 53–57, 2007.

[119] S. Asghari Mooneghi, S. Saharkhiz, and S. Mohammad Hosseini Varkiani, “Surface roughness evaluation of textile fabrics: A literature review,” *J. Eng. Fiber. Fabr.*, vol. 9, no. 2, pp. 1–18, 2014.

[120] W. Li, M. L. Zhan, Q. Y. Yu, B. Y. Zhang, and Z. R. Zhou, “Quantitative assessment of friction perception for fingertip touching with different roughness surface,” *Biosurface and Biotribology*, vol. 1, no. 4, pp. 278–286, Dec. 2015.

[121] C. P. Hendriks and S. E. Franklin, “Influence of Surface Roughness, Material and Climate Conditions on the Friction of Human Skin,” *Tribol. Lett.*, vol. 37, no. 2, pp. 361–373, Feb. 2010.

[122] E. Van Der Heide, X. Zeng, and M. A. Masen, “Skin tribology: Science friction?,” *Friction*, vol. 1, no. 2, pp. 130–142, Jun. 2013.

[123] P. Kenins, “Influence of Fiber Type and Moisture on Measured Fabric-to-Skin Friction,” *Text. Res. J.*, vol. 64, no. 12, pp. 722–728, 1994.

[124] N. K. Veijgen, M. A. Masen, and E. van der Heide, “Relating Friction on the Human Skin to the Hydration and Temperature of the Skin,” *Tribol. Lett.*, vol. 49, no. 1, pp. 251–262, Jan. 2013.

[125] J. R. Ajmeri and C. J. Ajmeri, “Developments in the use of nonwovens for disposable hygiene products,” in *Advances in Technical Nonwovens*, Woodhead Publishing, 2016, pp. 473–496.

[126] S. Mukhopadhyay, “Natural and synthetic fibres for composite nonwovens,” in *Composite Non-Woven Materials*, Woodhead Publishing, 2014, pp. 20–29.

[127] B. P. Subhash K. Batra, “Raw Material: Properties and Use in Fiberweb Nonwovens,” in *Introduction to nonwovens technology*, Lancaster, PA : Destech Publications, c2012., 2012, pp. 307–329.

[128] G. Gierenz and W. Karmann, “Chemical fibers,” in *Nonwoven Fabrics*, Wilhelm Albrecht, Hilmar Fuchs, and Walter Kittelmann, Eds. WILEY-VCH Verlag GmbH & Co, 2003, p. 51.

[129] D. Das, “Composite nonwovens in absorbent hygiene products,” in *Composite Non-Woven Materials*, Woodhead Publishing, 2014, pp. 74–88.

[130] L. M. Vilhena, “Friction Behavior of Human Skin Rubbing against Different Textured Polymeric Materials Obtained by a 3D Printing Microfabrication Technique,” *Tribol. Trans.*, vol. 62, no. 2, pp. 324–336, 2019.

[131] A. Elkhyat, C. Courderot-Masuyer, T. Gharbi, and P. Humbert, “Influence of the hydrophobic and hydrophilic characteristics of sliding and slider surfaces on friction coefficient: in vivo human skin friction comparison,” *Ski. Res. Technol.*, vol. 10, no. 4, pp. 215–221, Nov. 2004.

[132] C. P. Hendriks and S. E. Franklin, “Influence of surface roughness, material and climate conditions on the friction of human skin,” *Tribol. Lett.*, vol. 37, no. 2, pp. 361–373, Feb. 2010.

[133] Y. Kim, F. Limanto, D. H. Lee, R. S. Fearing, and R. Maboudian, “Role of counter-substrate surface energy in macroscale friction of nanofiber arrays,” *Langmuir*, vol. 28, no. 5, pp. 2922–2927, 2012.

[134] D. H. Gracias and G. A. Somorjai, “Continuum Force Microscopy Study of the Elastic Modulus, Hardness and Friction of Polyethylene and Polypropylene Surfaces,” 1998.

[135] N. Yui, Y. Suzuki, H. Mori, and M. Terano, “Surface properties of polypropylene films as biomaterials,” *Polym. J.*, vol. 27, no. 6, pp. 614–622, 1995.

[136] A. Opdahl, S. Hoffer, B. Mailhot, and G. A. Somorjai, “Polymer surface science,” *Chem. Rec.*, vol. 1, no. 2, pp. 101–122, 2001.

[137] K. S. K. Karuppiah, S. Sundararajan, Z. H. Xu, and X. Li, “The effect of protein adsorption on the friction behavior of ultra-high molecular weight polyethylene,” *Tribol. Lett.*, vol. 22, no. 2, pp. 181–188, May 2006.

[138] H. Lim, “A review of spun bond process,” *J. Text. Apparel, Technol. Manag.*, vol. 6, no. 3, pp. 1–13, 2010.

[139] B. P. Subhash K. Batra, “Bonding technologies,” in *Introduction to nonwovens technology*, Lancaster, PA : Destech Publications, c2012., 2012, pp. 87–161.

[140] T. Karthik, R. Rathinamoorthy, and C. Karan Praba, “Nonwoven bonding techniques,” in *Nonwovens : process, structure, properties and applications*, 2016, pp. 95–150.

[141] B. P. Subhash K. Batra, “Staple fiber-based technologies,” in *Introduction to nonwovens technology*, Lancaster, PA : Destech Publications, c2012., 2012, pp. 43–68.

[142] S. S. Falloon, V. Asimakopoulos, and A. M. Cottenden, “An experimental study of friction between volar forearm skin and nonwoven fabrics used in disposable absorbent products for incontinence,” *Proc. Inst. Mech. Eng. Part H J. Eng. Med.*, 2019.

[143] S. S. Falloon and A. Cottenden, “Friction between a surrogate skin (Lorica Soft) and nonwoven fabrics used in hygiene products,” *Surf. Topogr. Metrol. Prop.*, 2016.

CHAPTER 3 Characterization of Topsheet Nonwoven Fabrics of Absorbent Hygiene Products

3.1 Abstract

There is an increasing demand for better skin comfort experiences of using absorbent hygiene products. The topsheet nonwoven fabric of absorbent hygiene products intimately contacts with the skin so its performance can directly affect the tactile sensation and skin comfort. It is beneficial to know about the properties of those fabrics to explore how these properties influence their performance of tactile sensation. A benchmark of commercial topsheet nonwoven fabrics was done to know the basic structure and mechanical properties of those fabrics. The characterized fabrics presented a narrow range of structural properties such as fiber size, thickness, and basis weight. Commercial topsheet fabrics tend to be thin and lightweight. Kawabata evaluation system (KES) was used to measure the surface roughness, friction, compression, and bending properties of topsheet nonwoven fabrics. A sled for friction and a cantilever bending test were compared with KES friction and bending measurements. The fabric type based on the web formation and bonding method showed an impact on the surface roughness and bending properties. The carded, through-air bonded fabric showed a paper-like performance in the KES bending test that leads to a different test result of bending rigidity in cantilever bending test. The compression and friction measurements indicated an influence of pressure on the fabric performance. The fabric can become more indistinguishable under high pressure.

3.2 Introduction

Nonwoven fabrics have been widely used in absorbent hygiene products. Since the products are used for personal care or medical setting, the healthy and comfortable performance of nonwoven fabrics is receiving more and more attention [1][2][3][4]. To understand and explore

the relationship between nonwoven characteristics and tactile sensation, it is necessary to know the fabric properties and performance. The skin comfort evaluation is subjective but an objective or quantitative evaluation is desired for engineering. Kawabata evaluation system (KES) is the most well-known measurement method for fabric hand. It was created by the Hand Evaluation and Standardization Committee (HESC) in Japan. The system consists of compression, bending, surface, shearing, and tensile tests. The measured mechanical properties of fabrics are correlated to the subject evaluation and are identified as tactile properties that can contribute to skin comfort [5]. Although KES is well-developed, drawbacks still exist. The biggest problem is the complexity of the system, the long test time and the high cost. The remaining challenge for the evaluation of skin comfort and tactile perception is not only the individual variance of subjective perception but also the applicability of objective measurements since the measurement results may not work for a certain application , e.g. the methods for hand touch evaluation may not work for the prediction of non-glabrous skin sensations. The KES is originally made for the hand sensation of woven and knitted fabrics. The topsheet nonwoven fabrics used for absorbent hygiene products have different structure and can intimately contact with the skin under a warm, humid environment. The applicability of the KES evaluation to the topsheet nonwoven fabrics needs to be further verified. In this study, commercial topsheet nonwoven fabrics were characterized to know their physical and mechanical properties related to tactile sensation. The measured properties include fiber diameter, basis weight, fabric thickness, bonding area, and fiber orientation. KES was used to characterize the surface, compression, and bending properties. This benchmark can provide the basic information of the different nonwoven fabric types used for topsheet in absorbent hygiene products and help to know the tactile properties of them.

Since there are other methods exist as individual testing and analytic method to simply measure one mechanical parameter, they can be compared with the KES measurements and thus investigate the effectiveness of those methods and the KES measurement [6][7]. The cantilever bending test (WSP 90.5 (05)), and sled test for friction (INDA standard test: IST 140.1) were used to compare with the KES bending and surface friction tests to assess their ability for demonstrating the bending flexibility and friction performance of those topsheet nonwoven fabrics.

3.3 Materials and Methods

3.3.1 Materials

Eight commercial nonwoven fabrics for topsheets were provided by The Nonwovens Institute (Raleigh, U.S.A) and its member companies. A soft paper tissue (single layer) was used as a reference. The fabric information is summarized in Table 3.1 including the polymer type, web formation, and bonding methods, and finish information.

Table 3.1. The information on eight commercial top sheet nonwoven fabrics.

Sample ID	Web formation method	Bonding method	Material	Finish
S1	Spunbond	Thermal calender	PP	Unknown
S2	Spunbond	Thermal calender	PP	Hydrophilic
S3	Spunbond	Thermal calender	PLA	None
S3H	Spunbond	Thermal calender	PLA	Hydrophilic
H1	Spunbond	Hydroentangle	PLA	None
C1	Carding	Through air	PE/PET, sheath/core bicomponent	Hydrophobic
C2	Carding	Through air	PE/PP, sheath/core bicomponent	None
C3	Carding	Through air	PE/PET, sheath/core bicomponent	Hydrophilic
Tissue			Wood pulp	None

3.3.2 Methods

3.3.2.1 Structure Characterization

To understand the structure of these nonwovens, fiber diameter, basis weight, fabric thickness, and bonding area were measured and evaluated. Scanning electron microscope (SEM) images were taken to measure the fiber diameter by using ImageJ software. Three SEM images were taken for each fabric sample and 20 measurements of fiber diameters were taken from them. The mean value with a standard deviation of 20 measurements was used.

The basis weight is the weight of fabric per unit area. Each fabric sample was cut to 10 cm by 10 cm and was weighted and the basis weight calculated in g/m^2. Five replications were done for each sample and the mean and standard deviation for basis weight are reported.

The fabric thickness was measured by an AMES (B.C.Ames Incorporated, U.S.A) thickness gauge with 0.6 psi applied pressure. Five replications were measured for each fabric sample. The fiber orientation distribution (FOD) was done by using the optical fiber orientation analysis system at NWI analytical lab, NC State University. The system used a fast Fourier transfer method to generate a power spectrum and analyze the fiber orientation [8]. The MD/CD ratio was calculated to characterize the anisotropy and it was the ratio of the machine direction (MD) frequencies to cross-machine direction (CD) frequencies. Figure 3.1 illustrates the fiber distribution and the angle ranges from 0° to 180° where the 90° orientation angle represents MD and the 0° and 180° represent CD. The MD/CD ratio was calculated by the frequency of 80° to 100° over the frequency of 0° to 10° and 170° to 180°.

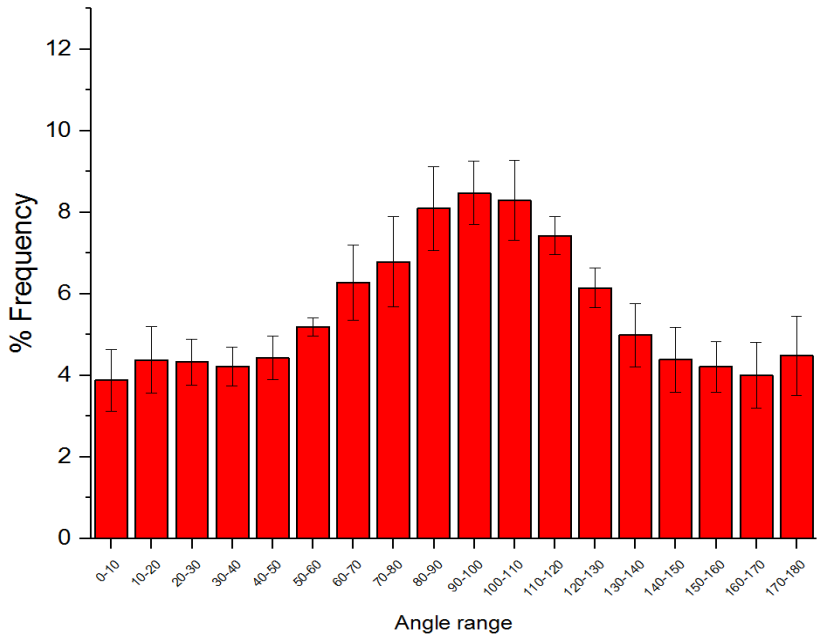

Figure 3.1. Example of fiber orientation distribution (sample S2). 90° orientation angle represents MD and the 0° and 180° represent CD.

The bonding area was measured by using ImageJ based on the images taken by the Keyence VHX-6000 microscope (Keyence, Japan) (Figure 3.2). The percentage of the bonding area was calculated using equation (1). The area of the bonding points are the area circled in Figure 3.2 and the total area is the area of the measured sample.

$$\text{Percentage of bonding area} = \frac{\text{area of the bonding points}}{\text{total area}} \times 100\% \quad (1)$$

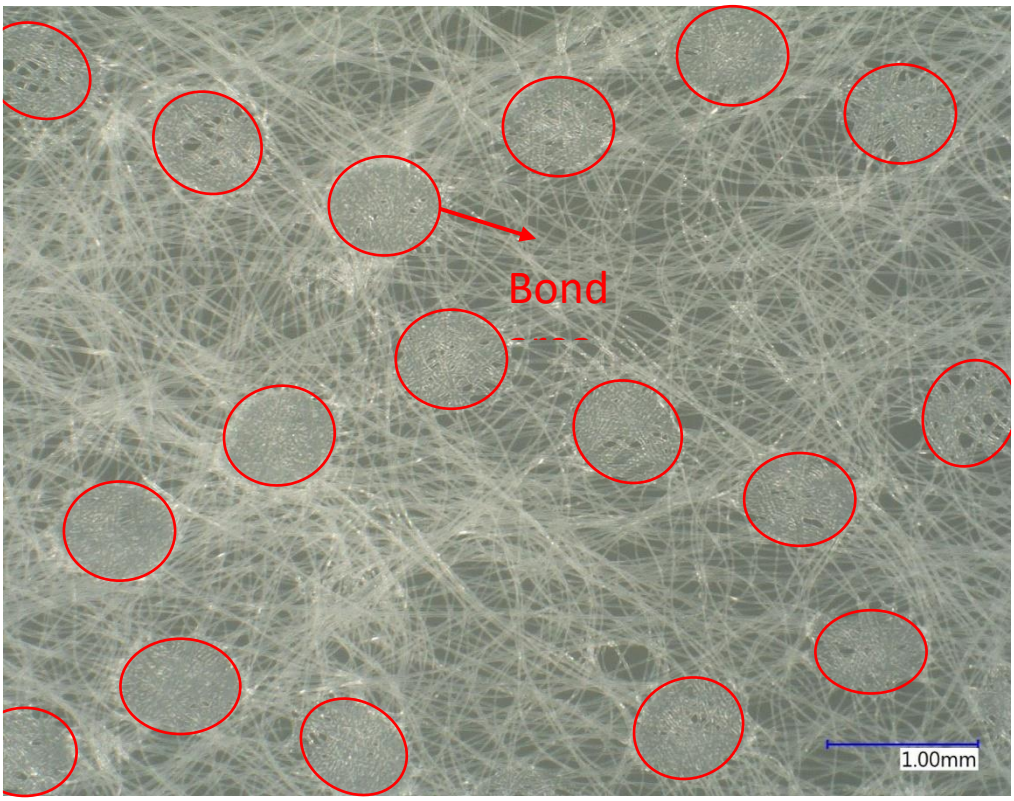

Figure 3.2. Bonding area measurement based on microscope images.

Fabric solidity was the ratio of the fiber volume (V_{fiber}) and fabric volume (V_{fabric}). It was calculated using equation (2).

$$\text{Solidity} = \frac{V\text{fiber}}{V\text{fabric}} = \frac{\text{basis weight } (\text{g/m}^2)}{\text{thickness (mm)} \times \text{fiber density } (\text{g/cm}^3) \times 10^3} \quad (2)$$

The estimated fiber density for PP, PLA, PE/PP, PE/PET were 0.9 g/cm^3, 1.25g/cm^3, 0.9 g/cm^3, 1.13 g/cm^3 respectively [9][10]. The mean values of basis weight and thickness were used.

3.3.2.2 Surface Roughness

KES surface tester was used to measure the surface roughness of all samples. Fabric samples were tested at 70 ± 3˚F (21˚C), 55 ± 5%RH. A tension load of 20 gf/cm and 10 g normal

load was applied to the sample through a single wire probe with a diameter of 0.5 mm. The geometric roughness (SMD) which is the mean deviation of the thickness was obtained.

3.3.2.3 Compression

The KES compression tester was used to measure the compressibility of two spunbond, thermal calender bonded fabrics (S1, S2) and three carded, through-air bonded fabrics (C1, C2, C3). The samples were conditioned and tested at 70 ± 3˚F (21˚C), 65 ± 5%RH. The measured area was 2 cm^2 and the applied force was from 0 to 50 gf/cm^2. The compressibility and compressional resilience were measured based on the compression curve (Figure 3.3). The compressibility is the percentage of thickness change using the initial thickness (T_0, measured at 0.5 gf/cm^2) minus the thickness of the sample at the maximum applied force (T_m, measured at 50 gf/cm^2) and divided by the initial thickness value: $\frac{T_0 - T_m}{T_0} \times 100\%$. The compressional resilience is the extent of recovery when the force is removed. A higher compressional resilience value indicates a higher percent recovery from being compressed. It is calculated by the ratio of the energy for unloading and loading using equation (3):

$$\text{Compressional resilience} = \frac{WC'}{WC} = \frac{\text{area b}}{\text{area a+b}} \quad (3)$$

$WC' = \int_{T_m}^{T_0} P'\,dT$, P' is the pressure measured on the unloading curve

$WC = \int_{T_m}^{T_0} P\,dT$, P is the pressure measured on the loading curve

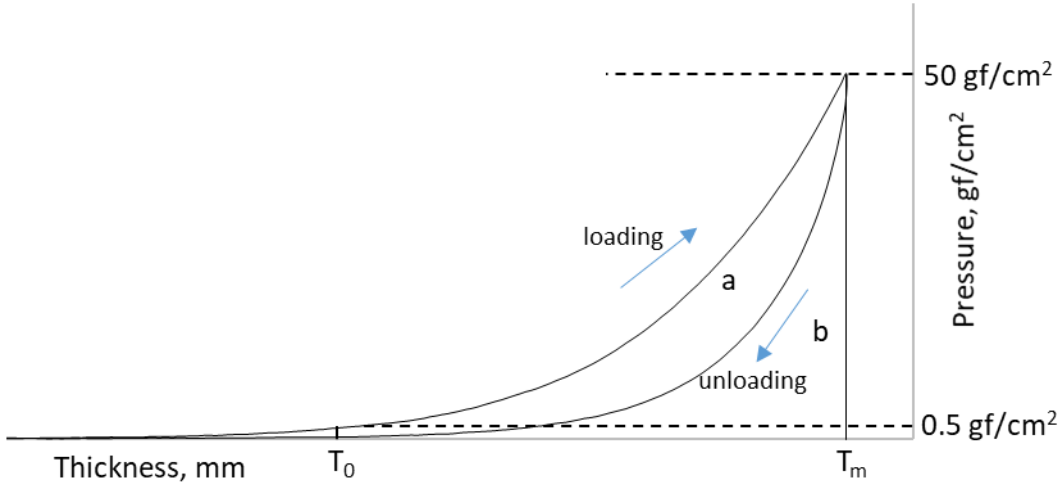

Figure 3.3. Schematic compression curve from KES compression test.

3.3.2.4 Bending Properties

The KES bending test and Cantilever bending test were used to measure bending properties (Figure 3.4). S2, S3, S3H, C1, C3, and H1 were measured to investigate the bending properties of the three fabric types: spunbond, thermal calender bonded fabric, carded, through-air bonded fabric, and spunbond, hydroentangled fabric.

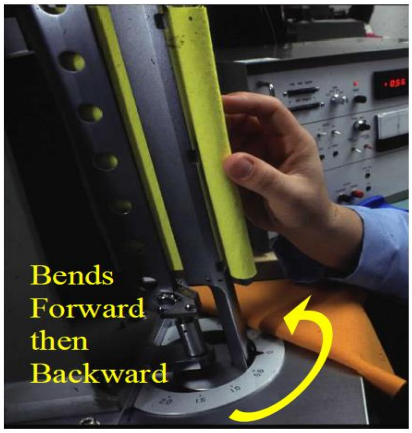

KES-FB2 bending tester
(T-PACC, College of Textiles,
NC State University)

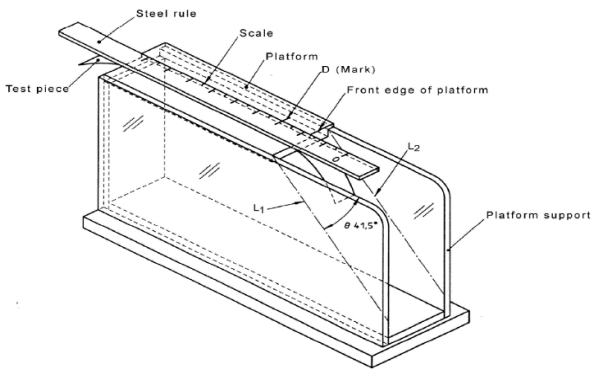

Cantilever bending tester
(EDANA WSP 90.5 (05))

Figure 3.4. KES bending tester and Cantilever bending tester.

KES Bending Test

The specimen size was 20cm×20cm. The fabric sample was clamped by the machine and bent forward and backward to measure the force required to bend the fabric. Bending rigidity (B) and hysteresis of bending momentum (2HB) were obtained from the test. For each test, B and 2HB were obtained during forward and backward movement, respectively (Figure 3.5). Three replications were done for each fabric sample and the mean value of B and 2HB was calculated.

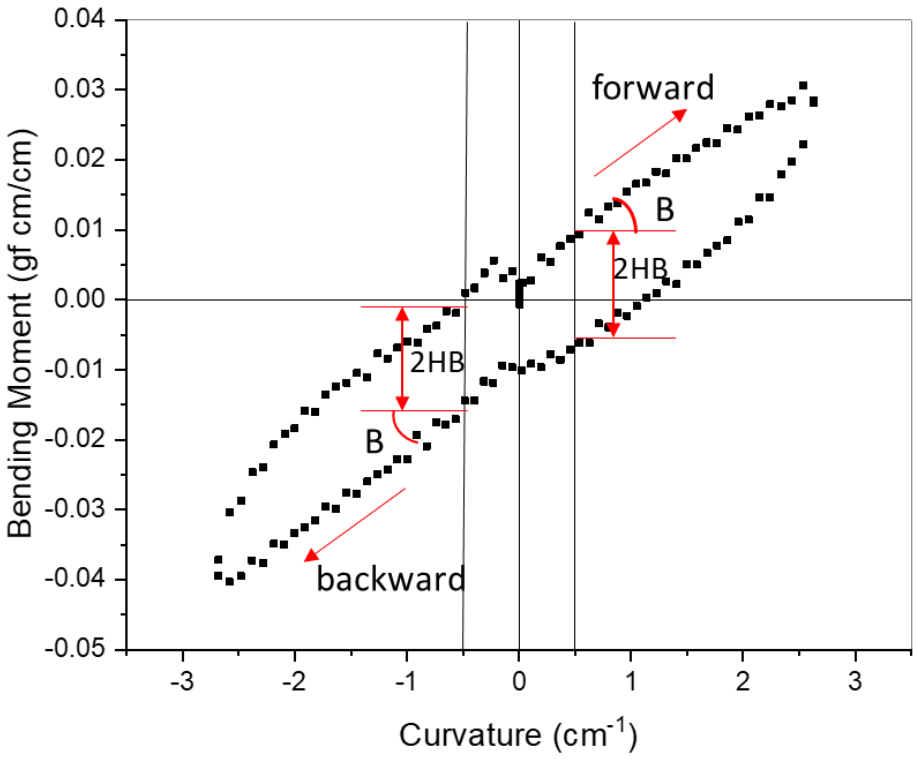

Figure 3.5. Bending curve of KES bending measurement. B is bending rigidity. 2HB is hysteresis of bending momentum.

Cantilever bending test

The cantilever bending test was done based on the standard- INDA/EDANA WSP 90.5(05). All samples were cut to 6 inches by 1 inch. For each fabric sample, three specimens were cut out with the long edges parallel to the machine direction and another three specimens were cut out in the cross-machine direction as the long side. The mean bending length was calculated for machine direction and cross-machine direction respectively. The bending rigidity (G) was calculated using the equation: $G=m\times C^3\times 10^{-3}$ (mN cm). In the equation, m is the basis weight of the sample. C is the mean value of bending length in cm.

3.3.2.5 Coefficient of Friction

Two friction measurement methods were used to evaluate the coefficient of friction: sled of friction test and KES friction test (surface tester). For all measurements, the friction measured was between the fabric and a steel surface. The test conditions are shown in Table 3.2. The pressure for each test was estimated by dividing the normal load by the apparent contact area.

Table 3.2. Test speed and pressure for KES, and sled of friction tests.

	KES friction test	**Sled of friction**
Applied weight	50 g	98 g
Apparent Contact area	25 mm^2	4032.25 mm^2
Pressure	19.65 kpa	0.24 kpa
Speed	1 mm/s	2.5 mm/s

KES Friction Test

In the KES friction test, S1 and S2 and C1, C2, C3 were tested. The kinetic coefficient of friction was measured for both MD and CD of the fabric. A tension load of 20 gf/cm was applied to the sample. The contact probe consists of 10 steel wires to simulate the touch of fingers. Three replications were done for each sample.

Sled of Friction Test

The sled of friction test was done based on the INDA Standard Test: IST 140.1(01). All samples were measured in the machine direction. The fabric was contacted with a flat steel surface. Three replications were done for each sample.

3.4 Results and Discussion

3.4.1 Structure characterization

The structure characterization is summarized in Table 3.3. The fiber diameter range is between 13μm and 17μm. The bicomponent fibers tend to have a bigger fiber diameter than the monocomponent fiber, and the PLA fiber has a lower average fiber diameter than the PP fiber. In

addition, those fabrics are very thin with a low basis weight between 10 g/m^2 to 22 g/m^2. The thickness of all samples is less than 1 mm. The spunbond and spunlaced fabrics have a very low thickness (less than 0.2 mm) which is lower than the soft tissue while the carded, through-air bonded fabrics have higher thickness. The result of solidity shows the S1 sample has the highest solidity while it has the lowest basis weight. The carded, through-air bonded fabric has a lower solidity than the spunbond, thermal calender bonded fabrics and the hydroentangled fabric. The solidity is defined in equation (2) and a higher solidity indicates a denser structure with less spaces between fibers. The structure of the carded, through-air bonded fabric contains more air while the spunbond fabric has a tighter structure. All the spunbond fabric samples have a small bonding area (10%-15%) which can decrease the stiffness of the fabric while the other types of fabric do not have a bond pattern as expected (Figure 3.6). The other fabrics were bonded by through air or hydroentangling rather than thermal calender bonding. The through air method bonds the fibers by the application of heated air and does not have a bond pattern. The hydroentangling is a mechanical bonding method that mechanically entangles fibers by the impingement of water jets. Only the thermal calender bonding has a pattern given by the bonding points on the calender. The MD/CD ratio measures the anisotropy of the fiber orientation. A higher MD/CD ratio means fibers are more MD oriented. It is between 1.7 and 2.6 for all measured samples. Although H1 and C1 have relatively higher MD/CD ratio and the fibers are more machine-direction oriented, most fabrics have a low MD/CD ratio close to 1 that indicates the properties of the fabric can be similar to isotropic.

Table 3.3. Fabric structure properties and surface roughness.

Sample	Basis weight (g/m^2)	Fiber diameter (μm)	Thickness (mm)	Solidity	MD/CD ratio	Surface roughness-MD(μm)	Surface roughness-CD(μm)
S1	9.67±0.15	14.74±0.92	0.067±0.010	0.16	1.85	2.86±0.17	2.56±0.30
S2	15.18±0.25	14.61±1.36	0.183±0.020	0.09	1.98	2.80±0.08	2.60±0.10
S3	16.44±0.21	13.20±1.49	0.114±0.010	0.12	-	3.27±0.16	2.72±0.20
S3H	16.58±0.15	13.56±1.16	0.106±0.016	0.13	-	3.28±0.26	2.74±0.27
H1	19.58±0.17	13.75±1.16	0.119±0.004	0.13	2.55	5.07±0.15	4.57±0.25
C1	19.00±0.28	15.16±1.09	0.702±0.055	0.02	2.65	3.87±0.23	2.48±0.02
C2	20.22±0.50	16.07±1.74	0.538±0.029	0.04	1.74	5.12±0.05	3.03±0.39
C3	21.96±0.68	16.59±1.86	0.362±0.036	0.05	1.88	3.42±0.31	2.42±0.08
Tissue (single layer)	13.33±1.52	-	0.213±0.01	0.01	1.85	1.55±0.12	1.52±0.13

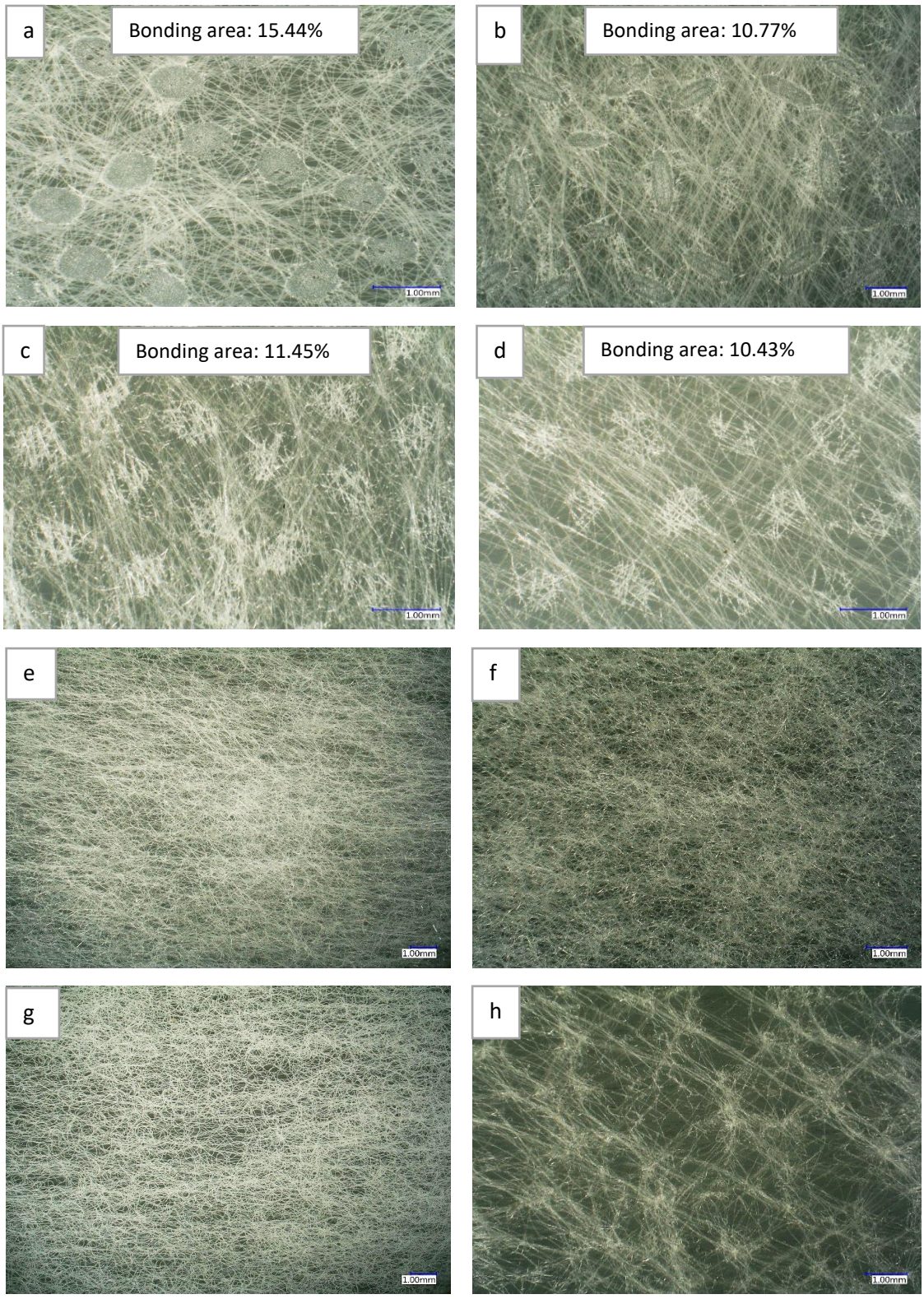

Figure 3.6. Bonding characterization. a: S1;b:S2;c: S3;d:S3H; e: C1; f:C2; g: C3; h: H1.

3.4.2 Surface roughness

The paper tissue has the same roughness in MD and CD while all the nonwoven fabrics have a higher roughness in MD than CD (Table 3.3). The hydroentangled fabric has the roughest surface both in the machine direction and cross-machine direction while the tissue has the smoothest surfaces. The high roughness of hydroentangled fabric may be caused by its more open and less uniform structure based on the bonding characterization (Figure 3.6 h). All the carded, though air bonded fabrics have more different roughness in the two directions than the spunbond, thermal calender bonded fabrics. In addition, the carded, though air bonded fabrics have higher roughness in the MD direction than the spunbond, thermal calender bonded fabrics while the roughness in CD direction is similar for the two types of fabrics. The possible explanation is the surface roughness of spunbond fabrics is more affected by the bond pattern so the difference between MD and CD is small because of the regular bond pattern in both directions but the surface roughness of carded, though air bonded fabrics is dominated by the fiber orientation distribution so the two directions showed a bigger difference.

3.4.3 Compression

The compression properties of topsheet nonwoven fabrics measured by KES are displayed in Table 3.4. Examples of the compression curve are shown in Figure 3.7. All the fabrics have similar compressional resilience between 30% and 40%. This indicates all the topsheet fabrics have a low recovery ability. The range of compressibility is between 58% and 89% which is relatively high. However, the compressibility can be very sensitive to the pressure range. The reciprocal of the slope for each fabric sample at 0.5gf/cm^2 ((0.007 psi)) and 28.83 gf/cm^2 (0.41 psi) was used to indicate the thickness changed at one unit pressure (Figure 3.8). The 0.5 gf/cm^2 is the pressure that the initial thickness is measured in the standard KES testing. The 28.83 gf/cm^2 is the average pressure applied to the diaper for a child (18-24 months) lying on the back [11]. The C1

fabric showed much higher thickness change than the other fabrics at the low pressure but there is negligible thickness change at the high pressure with a small difference between fabrics. Therefore, the main contribution to compressibility occurred at low pressure before the pressure reaches 28.83 gf/cm^2 which is the pressure for a diaper in use.

Table 3.4. Fabric compression properties measured by KES compression test.

Sample	Compressibility (%)	Compressional resilience (%)
S1	76.87±0.82	37.42±0.98
S2	66.56±3.57	38.44±0.26
H1	71.36±0.73	36.81±0.68
C1	88.98±0.76	40.27±1.77
C2	58.83±3.32	34.40±0.62
C3	84.24±0.54	36.84±1.12

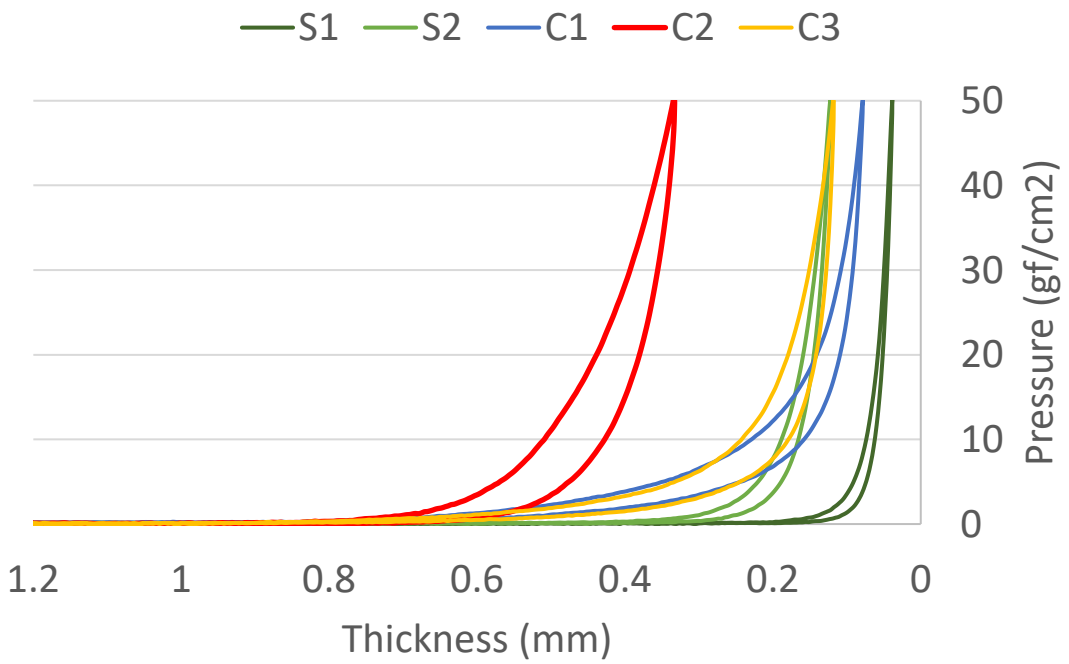

Figure 3.7. Compression curve between 0 and 50 gf/cm2. The initial gap between the fabric and the probe sensor is 1.2 mm.

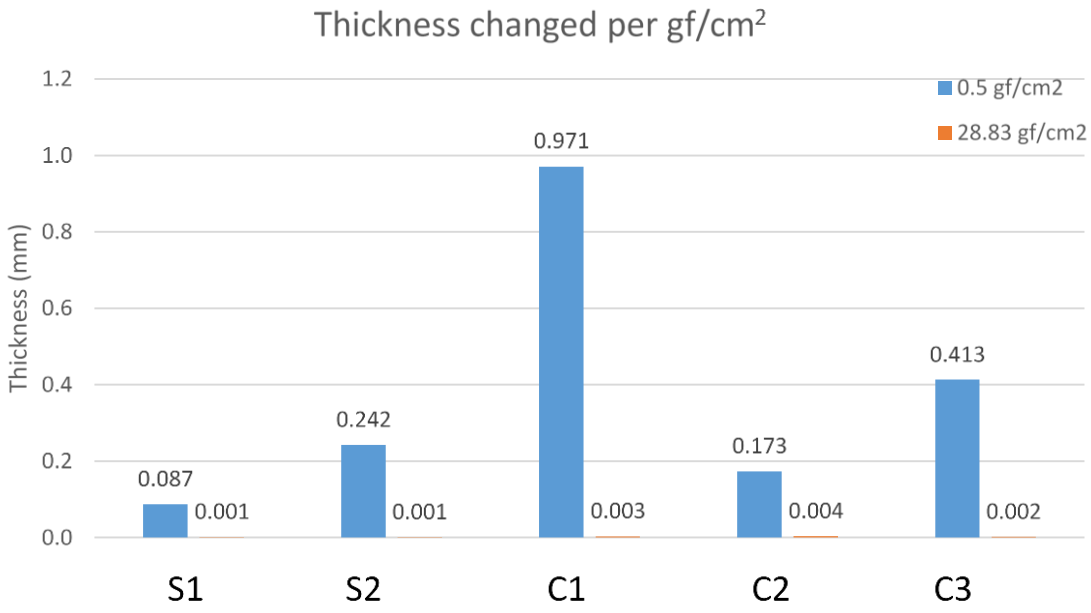

Figure 3.8. Thickness changed at one unit (gf/cm^2) pressure at 0.5gf/cm2 and 28.83 gf/cm^2.

3.4.4 Bending Properties

KES Bending Test

The KES bending results (Table 3.5) show the bending rigidity in cross-machine direction is lower than the machine direction. According to the MD/CD ratio of fiber orientation, there can be more fibers aligned in the machine direction leading to higher stiffness while the cross-machine direction is less stiff. The bending rigidity of the S3H sample with the hydrophilic finish slightly decreased compared to the one without the finish (S3) in the cross-machine direction while it is higher in the machine direction. This indicates the finish may change the bending rigidity especially increase the rigidity in the machine direction. All samples have low bending rigidity in the cross-machine direction and they are more distinguishable in the machine direction. S2, S3, and S3H have the same web and bonding formation methods, and very similar structure (bond area, basis weight, fiber size) but the S3 and S3H present higher bending rigidity than S2. This may indicate PLA fabrics can have higher rigidity than the PP fabric because of the effects of the

material. The hydroentangled PLA fabric (H1) shows a lower rigidity than the spunbond, thermal calender bonded PLA fabric (S3, S3H). The possible reason is the hydroentangling bonding gives fibers higher mobility while the thermal calender bonding fused fibres together at the bonding points. All the fabric samples have indistinguishable low bending hysteresis in the cross-machine direction. In the machine direction, the spunbond, thermal calender bonded fabrics have lower bending hysteresis than the carded, through-air bonded fabrics, which indicates the spunbond fabrics can be better recovered from being bent at a low stress.

Table 3.5. Fabric bending hysteresis and bending rigidity measured by KES bending test.

Sample	Bending hysteresis-MD (gf·cm/cm)	Bending hysteresis -CD (gf·cm/cm)	Bending rigidity-MD (gf·cm^2/cm)	Bending rigidity-CD (gf·cm^2/cm)
S2	0.015±0.001	0.008±0.000	0.010±0.001	0.004±0.000
S3	0.019±0.002	0.009±0.001	0.029±0.003	0.011±0.001
S3H	0.026±0.002	0.005±0.001	0.036±0.001	0.007±0.002
H1	0.020±0.002	0.005±0.000	0.022±0.002	0.003±0.000
C1	0.068±0.002	0.014±0.002	0.015±0.007	0.018±0.002
C3	0.038±0.003	0.006±0.001	0.021±0.001	0.008±0.001

Cantilever Bending Test

Figure 3.9 shows the bending rigidity of cross-machine direction measured in KES and Cantilever test are similar. However, the results show inconsistency in the machine direction. The carded, through-air bonded fabrics have low bending rigidity in the KES measurement while the values are high in the cantilever bending test. One possible explanation for this opposite result is the different bending performance of the carded, through-air bonded fabrics in the two measurement methods. In the KES test, the fabric was clamped by the machine and bent forward and backward by an external force. However, in the cantilever bending test, the fabric was cut to

a rectangular strip and was bent down under its own weight in the horizontal direction. The high bulk and thickness caused the carded, through-air bonded fabric being more rigid with a high moment of inertia. This rigidity presented in the cantilever measurement as it relayed on gravity only while the additional force applied in the KES test can overcome the initial bending moment.

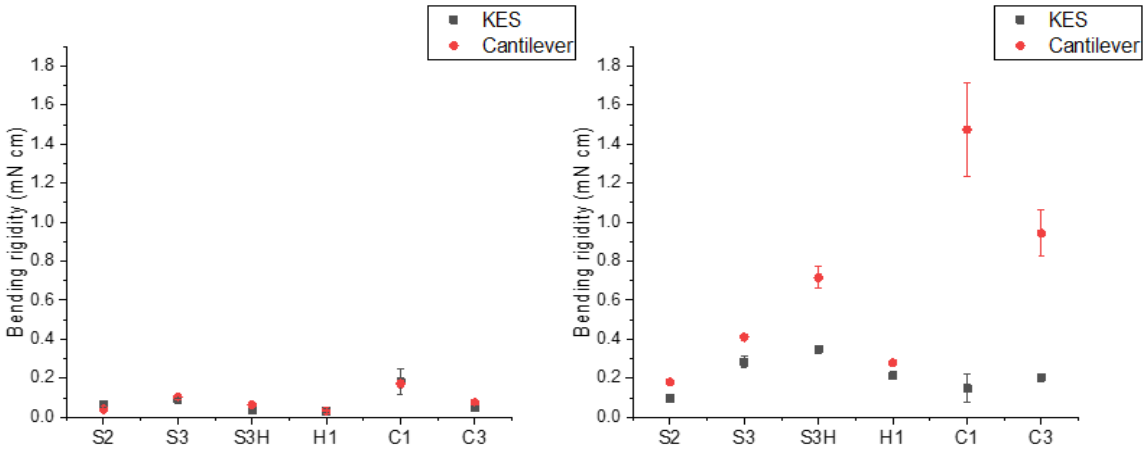

Figure 3.9. Comparison between KES and cantilever test for bending rigidity. Left: cross-machine direction bending rigidity; Right: machine direction bending rigidity.

This bending behavior of the carded, through-air bonded fabric is reflected in the bending hysteresis in KES measurement. The 2HB value is the hysteresis of bending moment and a higher 2HB value indicates a greater fabric inelasticity. Figure 3.10 shows the typical bending curve for the spunbond, thermal calender bonded fabric and the carded, through-air bonded fabric. The curve clearly shows the different behavior between these two fabric types during the bending process. The curve for spunbond, thermal calender bonded fabric is smooth with low hysteresis. This means it is relatively easy to bend the fabric during the whole motion and the fabric can recover easily. However, for the carded, through-air bonded fabric, the curve indicates the curvature requires a higher bending moment in the beginning compared to the spunbond fabric and then the moment decreases. During the measurement, the carded, though-air bonded fabric was forced to be folded

at the beginning and then it became easier to bend the fabric along with the impression of the fold. The impression of the fold can be the reason for the low bending rigidity value that was measured by KES. In other words, the carded, through-air bonded fabric presents a paper-like property compared to the spunbond fabrics. The spunbond fabric is more flexible while the carded, through-air fabric has a buckling performance during the bending motion. Therefore, the fabric type can have an effect on which testing method to use. The bending rigidity of spunbond fabrics shows consistency with additional bending forces (KES test) and with gravity only (cantilever test) while the carded, through-air bonded fabric can perform differently under these two conditions.

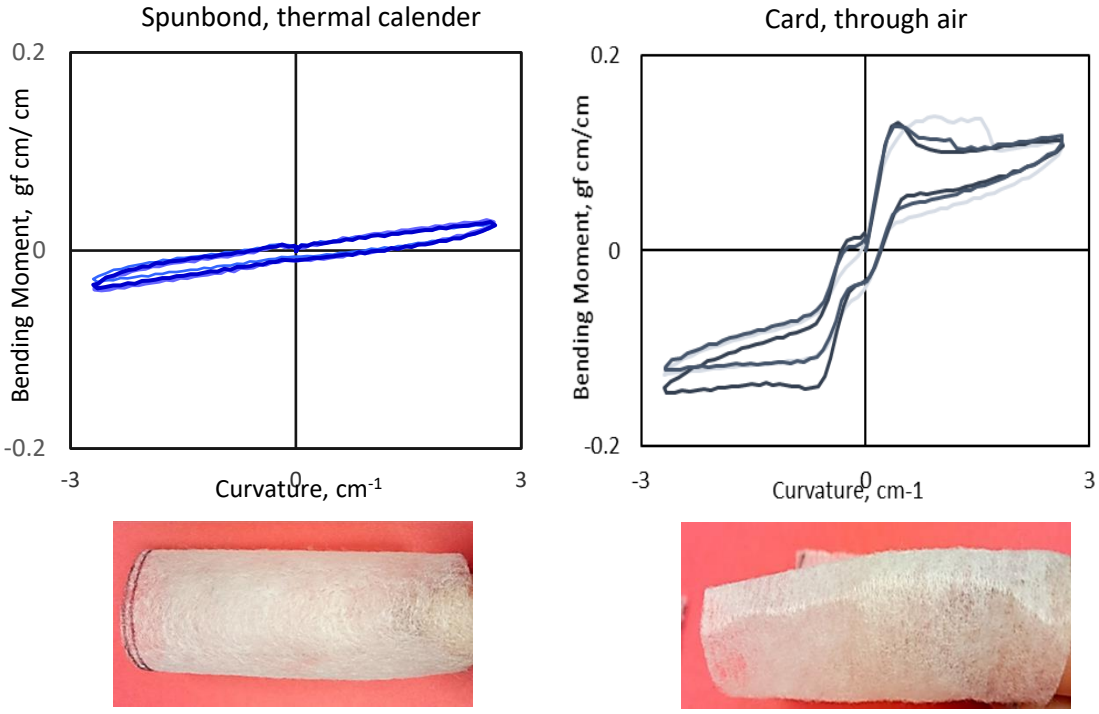

Figure 3.10. KES bending curve for spunbond, thermal calender bonded fabric (S2) and carded, through-air bonded fabric (C1). Each graph includes three replications. Pictures below the graph show the smooth look for the spunbond fabric and the impression of the fold for the carded, through air fabric when they were bent.

3.4.5 Coefficient of Friction

KES Friction Test

The coefficient of friction values for machine direction and cross-machine direction are similar and there is no significant difference between fabrics (Table 3.6). The coefficient of friction value is between 0.2 and 0.25. The performance of the tested fabric samples is not distinguishable based on the friction measurement in KES.

Table 3.6. Coefficient of friction measured by KES surface tester.

Sample	Kinetic friction coefficient-MD	Kinetic friction coefficient-CD
S1	0.24±0.01	0.22±0.01
S2	0.22±0.01	0.22±0.01
C1	0.19±0.01	0.19±0.01
C2	0.21±0.00	0.19±0.01
C3	0.22±0.01	0.22±0.01

Sled Friction Test

The result for the coefficient of friction measured in KES tester were compared with those of the sled friction test (Figure 3.11). In the KES test, there was a small difference between fabrics but the sled friction test showed the spunbond fabrics had a higher coefficient of friction than the carded, through-air bonded fabrics The inconsistent results may have been caused by the different contact pressures and the surface topography of the counter surface. Firstly, the higher pressure in the KES test may have reduced the difference between fabrics because the compression can flatten the fabric. Secondly, the counter surface was a sensor that mimics fingerpads consisting of 10 single steel wires in the KES test while the sled friction tests used a flat surface of stainless steel. According to the surface roughness characterization, the spunbond fabric had a smoother surface than the card, though-air bonded fabric. For the flat surface in the sled friction test, the spunbond fabric may present bigger friction because of a bigger contact area between the two relatively

smooth surfaces. The more uneven surface of carded, though-air bonded fabric may have reduced the contact area thus have reduced the friction. However, the sensor in KES has a surface texture that may decrease the contact area with the smooth surface of spunbond fabrics but it could also create a higher resistant force when sliding against a rougher surface by mechanical interlocking. The similar coefficient of friction for various samples measured in KES suggests the friction performance of top sheet nonwoven fabrics can be indistinguishable under high pressure because the contact area tended to be the same under compression.

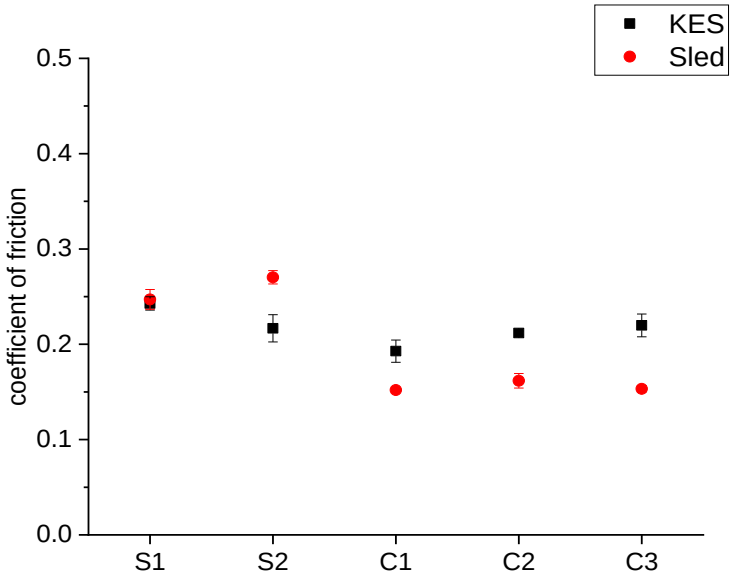

Figure 3.11. Coefficient of friction for machine direction measured by KES and Sled of friction test.

3.5 Conclusions

This study aimed to provide a general understanding of the physical-mechanical properties of nonwoven fabrics used for the topsheet of absorbent hygiene products, which may influence further study of the tactile sensation of these fabrics. The fabric structure characterization showed that the commercial topsheet fabrics had a narrow range of fiber diameter, basis weight, thickness, solidity, bonding area, and MD/CD ratios. The thickness was less than 1mm and the basis weight

was below 22 g/m^2, which reflected the requirement for a thin and lightweight experience. Although the structural parameters were in a narrow range, the fabric types based on web formation and bonding technique, and the fiber types (bicomponent or monocomponent) presented effects on the structural characterization. The KES measurement for surface roughness and bending properties indicated a difference between spunbond fabrics and carded, through-air bonded fabrics. The friction and compression tests showed the effects of pressure on the performance of fabrics. The fabrics became more indistinguishable under high pressure. By comparing the two bending rigidity measurement methods, it was found the spunbond fabric was more flexible with good elasticity while the carded, through-air bonded fabric showed a paper-like behavior or buckling with an external bend force that can generate an impression of the fold. This behavior can cause different test results in cantilever bending test and KES bending test while both methods can work for fabrics without this buckling behavior. Inconsistency was also observed between the KES friction and sled friction tests. It is likely caused by the difference in contact pressure. The different topography of counter surfaces may also be a reason. Because of the limited sample size and the uncontrolled fabric parameters (e.g. web formation and bonding method, basis weight, thickness, etc.), the influence of factors like polymer and finish type was uncertain in this study. Further study will focus on the correlation between the fabric properties and skin sensation and the interpretation of objective measurements for skin comfort. A better-controlled sample group can help to investigate the effects of fabric material and structure parameters. Since the fabric type and test condition can influence the mechanical performance, it is recommended to use a customized measurement system based on the use environment in order to get more relatable and reliable results.

3.6 References

[1] J. R. Ajmeri and C. J. Ajmeri, “Nonwoven personal hygiene materials and products,” in *Applications of Nonwovens in Technical Textiles*, Woodhead Publishing, 2010, pp. 85–102.

[2] “INDA | Hygiene.” [Online]. Available: http://www.inda.org/about-nonwovens/nonwoven-markets/hygiene/. [Accessed: 18-Sep-2017].

[3] R. B, “Skin interaction with absorbent hygiene products,” *Clin. Dermatol.*, vol. 26, no. 1, pp. 45–51, Jan. 2008.

[4] M. Odio and L. Thaman, “Diapering, Diaper Technology, and Diaper Area Skin Health,” *Pediatr. Dermatol.*, vol. 31, no. s1, pp. 9–14, Nov. 2014.

[5] S. Kawabata and M. Niwa, “Objective Measurement of Fabric Mechanical Property and Quality: Its Application To Textile And Clothing Manufacturing,” *Int. J. Cloth. Sci. Technol.*, vol. 3, no. 1, pp. 7–18, 1991.

[6] I. L. Ciesielska-Wróbel and L. Van Langenhove, “The hand of textiles – definitions, achievements, perspectives – a review,” *Text. Res. J.*, vol. 82, no. 14, pp. 1457–1468, Sep. 2012.

[7] V. Sülar and A. Okur, “Objective Evaluation of Fabric Handle by Simple Measurement Methods,” *Text. Res. J.*, vol. 78, no. 10, pp. 856–868, Oct. 2008.

[8] L. B. S. Venu, E. Shim, N. Anantharamaiah, and B. Pourdeyhimi, “Structures and properties of hydroentangled nonwovens: effect of number of manifolds,” *J. Text. Inst.*, vol. 108, no. 3, pp. 301–313, Mar. 2017.

[9] H. H. Cho, K. H. Kim, Y. A. Kang, H. Ito, and T. Kikutani, “Fine structure and physical properties of polyethylene/poly(ethylene terephthalate) bicomponent fibers in high-speed spinning. I. Polyethylene sheath/poly(ethylene terephthalate) core fibers,” *J. Appl. Polym. Sci.*, vol. 77, no. 10, pp. 2254–2266, Sep. 2000.

[10] Fibervisions, “FiberVisions ® Binder Fibers the sensible alternative datasheet,” 2013. [Online]. Available: http://www.fibervisions.com/Repository/Files/Binder_Fiber.pdf.

[11] S. Dey *et al.*, “Exposure Factor considerations for safety evaluation of modern disposable diapers,” *Regul. Toxicol. Pharmacol.*, vol. 81, pp. 183–193, Nov. 2016

CHAPTER 4 Friction Measurement Setups for Topsheet Nonwoven Fabrics

4.1 Abstract

Four different setups for friction measurement between topsheet nonwoven fabrics and metal (stainless steel), skin simulants were used to investigate the effects of the contact surface and deformation on skin-fabric friction. The skin simulants showed the potential to mimic real human skin frictional behavior. The contact with Vitro-skin® that mimics the skin surface topography largely increased the coefficient of friction and displayed the dependence on the normal load while the conventional friction measurement between fabric and stainless steel surface was more independent of the normal load. With the addition of compressible silicone underneath Vitro-skin®, the coefficient of friction was slightly reduced but it amplified the stick-slip phenomena during the dynamic measurement of friction. It indicates the adhesion friction contributes more than deformation to the coefficient of friction value but the deformation can significantly contribute to the stick-slip motion which may affect tactile sensation. It suggested considering the friction dynamics for the discrimination of topsheet nonwoven fabrics for tactile sensation evaluation as the coefficient of friction can be indistinguishable for fabrics and cannot reflect the effects of skin deformation. The skin simulants should be used to replace the conventional measurement setup in order to detect the friction dynamics for the skin-fabric interaction rather than considering the coefficient of friction only.

4.2 Introduction

Absorbent hygiene products like diapers, feminine hygiene products are life necessities and nonwoven fabrics are the main material for their composition. These typically have multilayer structures including the topsheet, acquisition layer, absorbent core, and waterproof backsheet. The topsheets are usually nonwoven fabrics that are fibrous, lightweight, open-structured, and can

quickly pass the liquid through to the absorbent core [1][2][3]. During the intimate contact between the nonwoven fabric and skin at high pressure and humid environment, there are concerns relating to the influence of nonwoven fabrics on skin comfort because of some common issues by using absorbent products such as contact dermatitis [4][5]. To avoid skin damages and to improve skin comfort, it is necessary to study the frictional behavior when the fabric is interacting with human skin.

The conventional standard friction testing methods for fabrics like ASTM standard(ASTM D1894) and the Kawabata Evaluation System are usually carried out between a metal plate like stainless steel or aluminum and the fabric[6][7]. However, the human skin has a multiple-layer construction with intricate surface topography consisting of lines, wrinkles, furrows and it has nonlinear viscoelastic properties while metal is elastic and can be customized with a polished surface [8][9]. In the development of healthcare products that contact skin, the surface features and deformation behavior of the skin can be important factors for the product function and the comfort sensation in use [10]. It is obvious that the metal plate used in the conventional friction measurement cannot provide such investigation. It is questionable how applicable the fabric-metal friction is to the fabric-skin friction. This question has led to a series of studies aimed at measuring friction directly on human skin to investigate the skin frictional behavior [11][12][13]. However, the measurement and analysis of frictional behavior on human skin remain a challenge. The skin friction can be affected by testing conditions such as wetness, interfacial pressure, sliding velocity, the material contacted with skin as well as human subject variants related to the anatomical location, gender, etc.[14]. Experimental studies have shown inconsistent conclusions, and rarely studies can be compared well because of the use of different materials and testing conditions [15][16][17][18]. The fundamental mechanisms of skin friction are not well-understood yet. It is

difficult to obtain reproducible results from human skin because of its inconsistent performance, as it depends on the physiological condition as a living material. Furthermore, it is also much more difficult to perform in vivo studies than in vitro experiments. Therefore, the materials that can simulate the physical and mechanical properties of the skin would help to investigate the skin frictional behavior [19][20][21]. In this study, the frictional behavior of nonwoven fabrics used for topsheet of absorbent hygiene products was investigated through four different setups with the load force from 0.25 N to 1.5 N. Two skin simulants that can mimic skin surface topography and skin deformation respectively were used to evaluate the skin-fabric frictional behavior and were compared to the metal-fabric friction. Additionally, the topsheet nonwoven fabrics are very thin(<1mm) and porous materials. The multiple layers underneath it may influence its frictional behavior. The measurement between topsheet nonwoven fabric and stainless steel with and without the deformable acquisition layer underneath was also carried out to explore the effects of the underneath material on the topsheet frictional behavior.

4.3 Materials and methods

4.3.1 Nonwoven fabric samples

Three commercial nonwoven fabrics used for the topsheet of absorbent hygiene products were provided by different suppliers as representations of the commonly used fabric types of topsheets in absorbent hygiene products. The information on them is summarized in Table 4. 1. The spunbond, thermal calender bonded nonwoven fabric is the most universally used fabric type for topsheets in nonwoven hygiene products. The biggest advantage of this type of fabric is the low thickness and basis weight. Patterns can be designed for the fabric through the design of the calender topography [22][23]. Hydroentanglement is another bonding technique that the spunbond process can be in conjunction with. It uses high-velocity water jets to deliver kinetic energy to the

unbonded nonwoven web and the energy would whirl fibers and cause entanglement so the web is mechanically bonded. The hydroentangled fabric can be produced flexible but the high-pressure water jets can leave jet streaks on the fabric surface that can cause rough and uneven surface [24][25]. Nonwoven fabrics produced by carding with through-air bonding are another dominant fabric type for topsheet. The fabric has no patterns and the fibrous web can retain loft with high bulk because the hot air is used to bond fibers [24][26]. Figure 4. 1 shows the scanning electron microscope (SEM) images of the three topsheet nonwoven fabrics used in this study. A 90 g/m^2 commercial acquisition layer (AQL) was used to evaluate the influence of the underneath material in the friction measurement. The acquisition layer is the second layer underneath the topsheet fabric in an absorbent hygiene product to distribute the liquid.

Table 4.1. Specifications of the tested nonwoven fabrics

Sample ID	Material	Web formation, bonding	Basis weight (g/m^2)	Finish
S-PP	PP	spunbond, thermal calendar bonding	15.2±0.2	Hydrophilic
H-PLA	PLA	spunbond, hydroentangling	19.6±0.2	none
C-PE/PET	PE/PET sheath/core bicomponent	card, through-air bonding	19±0.3	Hydrophobic
AQL	PET/Co-PET side by side bicomponent	card, through-air bonding	90	none

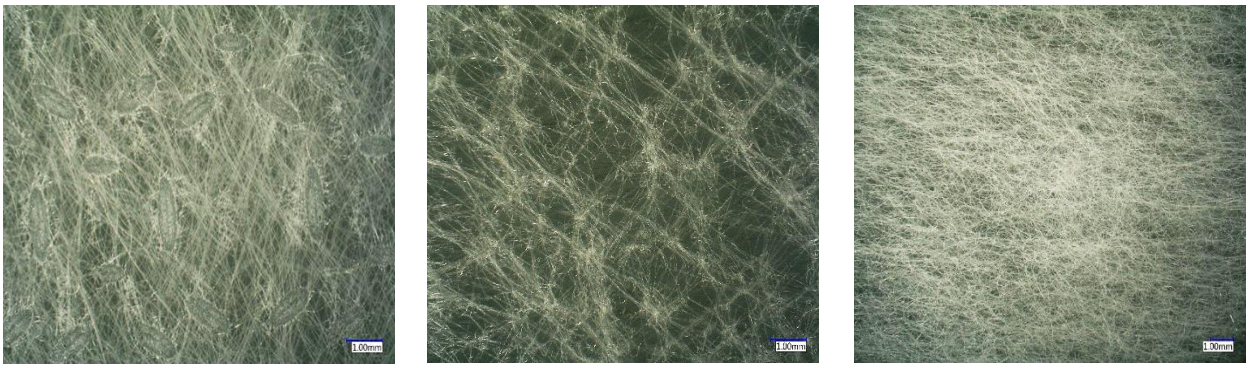

S-PP H-PLA C-PE/PET

Figure 4.1. Microscope images of the three topsheet nonwoven fabrics with different structures. S-PP: spunbond, thermal calender bonded; H-PLA: spunbond, hydroentangled; C-PE/PET: card, though-air bonded. The scale bar represents 1mm and each image shows the same scale.

The surface roughness (SMD, geometrical roughness) of each fabric was measured by the Kawabata Evaluation System (KES) [7]. A higher SMD value stands for a higher roughness. A constant tension load of 20 gf/cm and 10 g normal load was applied to the sample through a single wire probe with a U shape. The diameter of the wire was 0.5 mm. The fabric was moved 3 cm in the forward direction and then the same length in the backward direction with 1mm/s velocity. The vertical displacement of the sensor was detected and transformed into an electrical signal. The sampling rate was 5 Hz. The geometric roughness (SMD) is defined as the mean deviation of the thickness. It was calculated based on the measured vertical displacement. Both the machine direction (MD) and cross-machine direction (CD) of the fabric were measured for three replicates. Each fabric sample was measured with and without the acquisition layer underneath to investigate the effects of the acquisition layer on the detected surface roughness of topsheet fabrics.

4.3.2 Skin simulants

In order to provide the surface texture and viscoelastic mechanical properties of the skin, there were two materials used as skin simulants: Vitro-skin® (IMS, USA) and silicone rubber.

Vitro-skin® (IMS, USA) is a synthetic product to mimic skin surface properties [27]. Figure 4. 2 shows the confocal microscopy image of the Vitro-skin® specimen used in this study. The arithmetic mean roughness (Sa=12.5±0.47 μm) measured by the confocal microscope (Keyence, Japan) was comparable to the surface roughness of Vitro-skin® (Sa=15.4 μm) reported in the work of Eudier et al.[28] and in the range of the arithmetic mean roughness (Sa between 12 and 20 μm) of human skin volar forearm [29], which indicated its potential to simulant the surface topography of human skin.

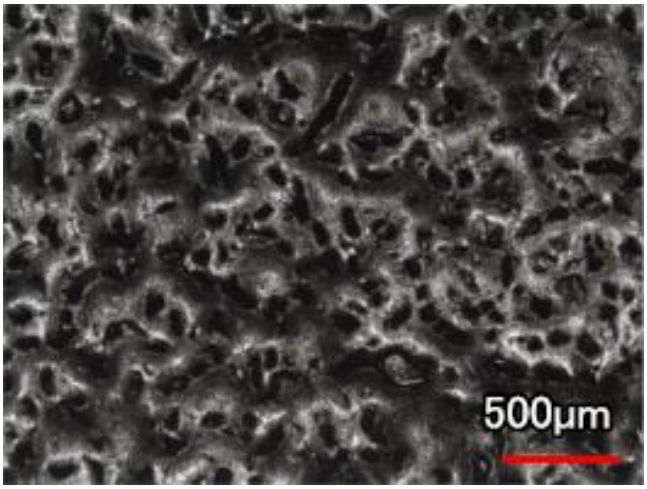

Figure 4.2. Confocal microscopy image of the Vitro-skin® specimen.

EcoflexTM 00-20 (Smooth-On, USA) silicone rubber was used to provide the mechanical properties of human skin, since elastomers like silicone and polyurethane are commonly used as skin substitutes [30][19]. EcoflexTM 00-20 had a shore hardness of 00-20 which was soft and appropriate to simulate the deformation of the skin. The silicone was made by mixing part A and part B with a 1:1 volume ratio. Round-shaped silicone rubber was made with a diameter of 5.5 cm and its thickness was 4.3 mm which agrees with the thickness of human skin (1.5 mm to 4 mm) [31][8]. A compression test (KES-FB3 Compression Tester, Japan) was done to estimate its

Young's modulus. The thickness of the sample was recorded as a function of the applied normal force (0 to 50 gf/cm^2) during the loading and unloading process. The force versus thickness was converted into stress (equation 1) versus strain (equation 2) by using the following equations:

$$Stress(Pa) = force\ \left(\frac{gf}{cm^2}\right) \times 10 \times 9.8\ m/s^2 \quad (1)$$

$$Strain = \frac{initial\ thickness - \ thickness\ of\ the\ sample}{initial\ thickness} \quad (2)$$

The converted stress-strain curve was shown in Figure 4. 3. The value of Young's modulus was obtained from the initial slope of the linear region in the loading curve, which was 11.2 kPa. It was in the range of the skin Young's modulus reported by Pailler-Mattei et al. [32].

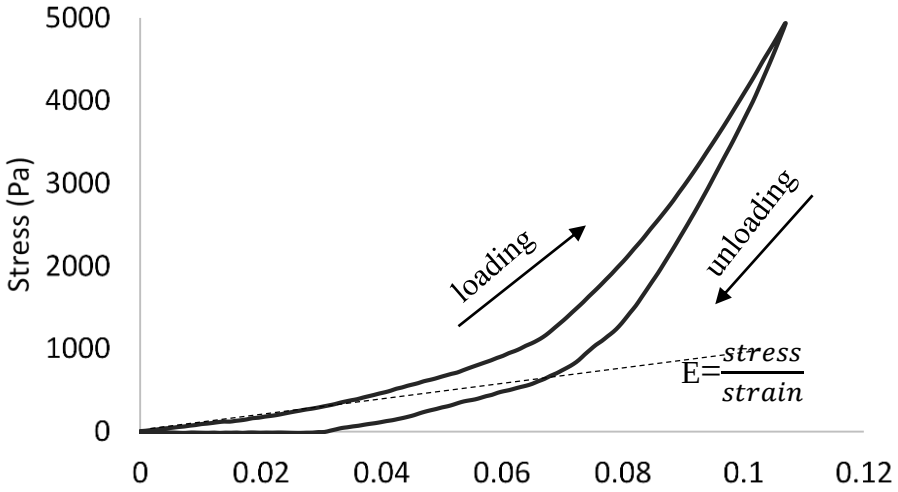

Figure 4.3. Stress-strain curve of EcoflexTM 00-20 silicone used in this study.

4.3.3 Friction measurement

Friction measurements were conducted using the Discovery HR-3 (TA Instruments, USA) with the Tribo-Rheometry accessory. The device consisted of a flat plate geometry on which a ring head would rotate on the plate surface base to measure friction. The ring had an outer diameter of 32 mm and an inner diameter of 29 mm. The normal load could be adjusted with a 0.1 N

tolerance and the normal loads used in this study were 0.25N, 0.5N, 1N, and 1.5N. The corresponding apparent pressures were 1.74 kPa, 3.48 kPa, 6.96 kPa, and 10.44 kPa. It covered the range of the pressure applied by children when diapers in use. According to the work of Dey et al., the average pressure applied by children in the age between 2 weeks and 52 months while lying or sitting is from 0 to 1.5 psi [33], which is from 0 to 10.3 kPa. The rotational speed used in this study was 1 rad/s. The measurement time was 60 seconds for each test.

Figure 4. 4 shows the four experimental setups used to evaluate the effects of the deformable acquisition layer underneath the topsheet, skin topography, and skin deformation for the friction measurement of the topsheet nonwoven fabric. Setup A and B were the conventional testing setups that friction was measured between the fabric and a metal plate. Both the rotational head and the metal plate base were stainless steel. The nonwoven fabric was mounted on the metal base by tapes and the fabric surface was kept flat. Setup A only had the topsheet nonwoven fabric contacting the rotational head while setup B had the acquisition layer underneath the topsheet nonwoven fabric to investigate whether and how the underneath material affects the frictional performance between the topsheet nonwoven fabric and the stainless steel surface. The skin simulants were added to setup C and D to mimic the skin-fabric interaction. Because the Vitro-skin® and silicone were stiffer than the fabrics, it was better to keep them in place on the base while the fabric sample was adhered to the rotational head by tapes. In setup C, only the Vitro-skin® was used to replace the metal surface. In setup D, the silicone was placed underneath the Vitro-skin®. A fresh new fabric sample, AQL, and Vitro-skin® were used for each test, and the silicone was the same one for all setup D tests. Each measurement was performed three times.

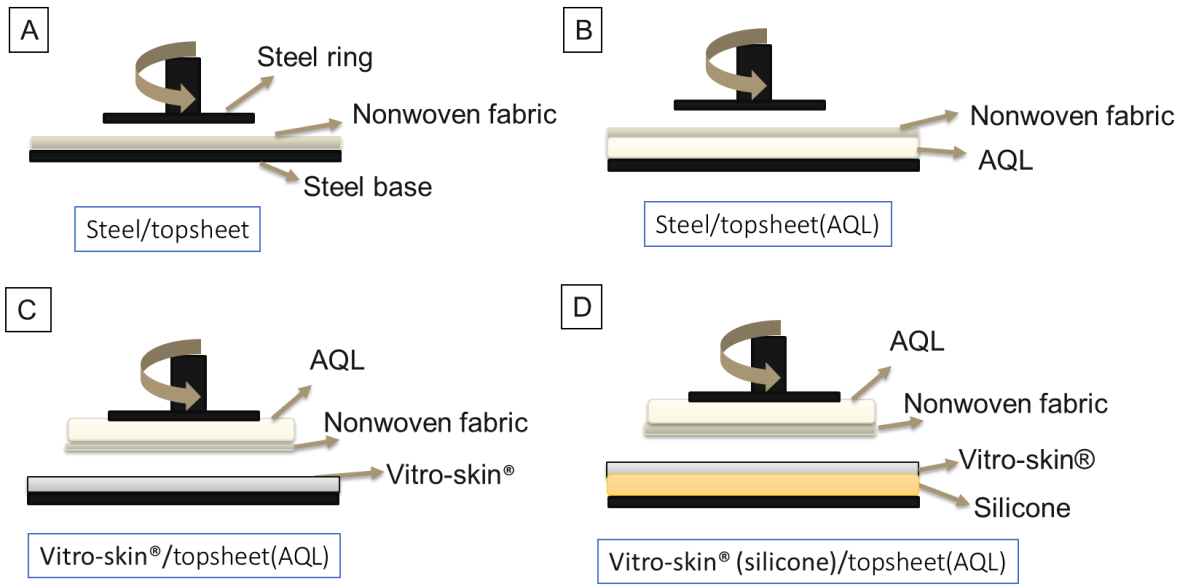

Figure 4.4. Four setups for friction measurement: A) friction measurement between steel and topsheet fabric; B) friction measurement between steel and topsheet fabric with AQL(acquisition layer) underneath; C) friction measurement between Vitro-skin® and topsheet fabric with AQL underneath; D) friction measurement between Vitro-skin® with silicone underneath and topsheet fabric with AQL underneath.

An example of the measured force signals is shown in Figure 4. 5. The rotational head started with a low velocity for a few seconds and then remained constant for the rest of the measurement. The coefficient of friction was calculated by dividing the friction force by normal force and it was calculated continuously during the measurements. The coefficient of friction was analyzed at the stable period, excluding the initial 20 seconds. The mean value of the coefficient of friction with standard deviation and the dynamic frictional force were reported. The variation of the applied normal load was within 0.1 N for all measurements.

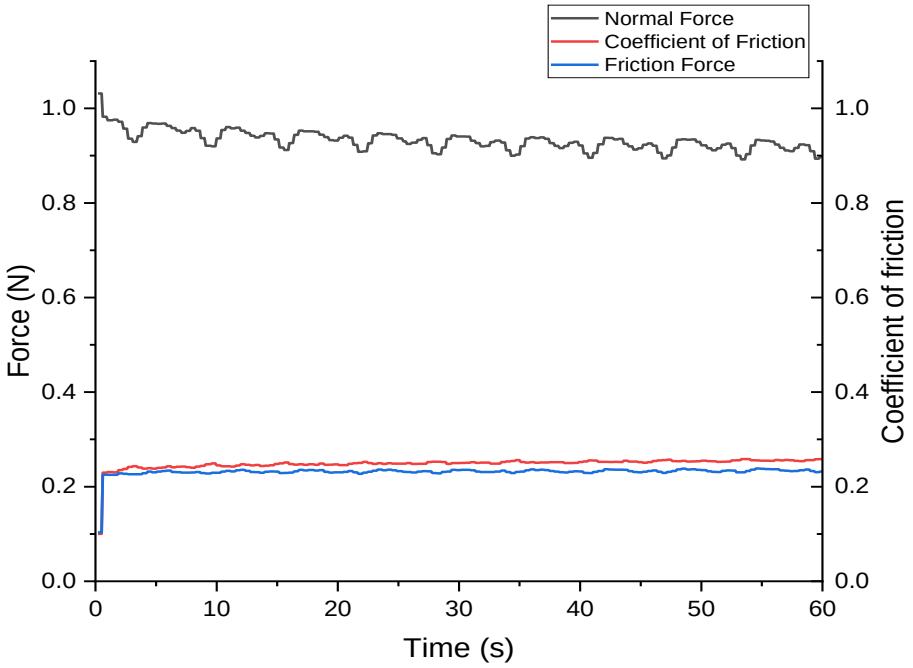

Figure 4.5. Example of the measured signal of normal force, coefficient of friction, and friction force in one minute (friction measurement between S-PP fabric (without acquisition layer) and stainless steel with a normal load at 1 ±0.1 N). In the first few seconds, the velocity was not stable so the friction force and coefficient of friction at the beginning were not counted for the analysis of friction.

4.4 Results and discussion

4.4.1 Coefficient of friction

Figure 4.6 shows the coefficient of friction for the four setups. In setup A (Figure 4. 6A), the coefficient of friction between topsheet and stainless steel was independent of normal load for the fabric S-PP, and C-PE/PET but not for the H-PLA. The spunbond, hydroentangled fabric, H-PLA, has a higher coefficient of friction at the middle (at normal loads of 0.5 N, and 1 N) and a lower coefficient of friction with the normal load of 0.25 N and 1.5 N. The SEM images in Figure 4. 1 shows the H-PLA had a more open structure and lower uniformity because there were fewer fibers covering the surface than with the other two fabrics. This may have led to a larger change in the contact area within the applied normal force range and have caused the varying coefficient

of friction. The stainless steel surface might contact the highest asperities of the fabric only at the low normal force with a small contact area. When the normal load increased, it started to contact the layers lower than the highest asperities because of the compression of the fibrous multilayer structure. The contact area likely increased so the friction increased. At an even higher normal load, the fabric was fully compressed and the surface became smoother with less interlocking between two surfaces. This may then have led to a lower coefficient of friction. The relatively dense and uniform structure of the fabrics S-PP, and C-PE/PET (Figure 4. 1) gave them a more stable contact area that had a neglectable change within this load range thus the friction force was proportional to the normal load.

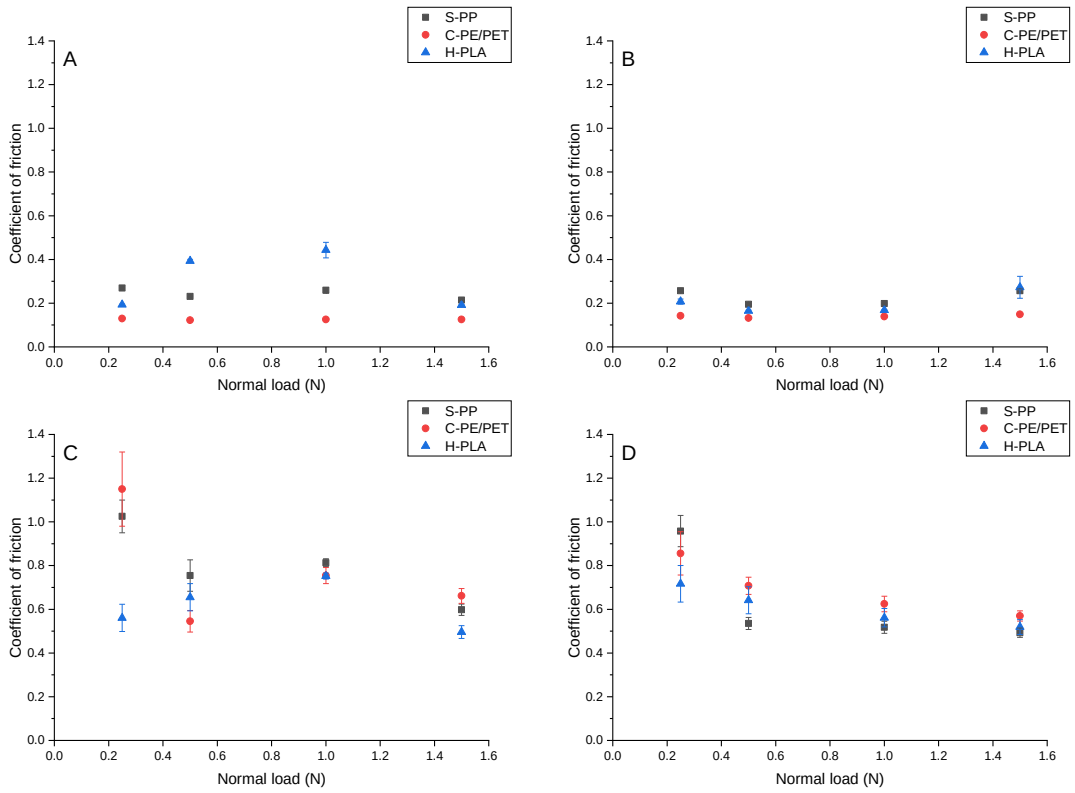

Figure 4.6. Coefficient of friction as a function of the normal load of topsheet nonwoven fabrics against A) stainless steel, B) stainless steel but the topsheet fabric had acquisition layer(AQL) underneath, C) Vitro-skin® (topsheet fabric with AQL), D) Vitro-skin® with silicon underneath (topsheet fabric with AQL).

With the deformable acquisition layer underneath topsheet fabric in setup B (Figure 4. 6B), the coefficient of friction value was not significantly different for the three topsheet fabrics. The coefficient of friction was between 0.1 and 0.3 which was comparable to the coefficient of friction measured without the acquisition layer. However, the H-PLA performed differently with the acquisition layer underneath. The coefficient of friction became constant and independent of the normal load. The similar friction coefficients of the fabrics may be explained by the surface roughness measurements in Figure 4. 7. It shows the surface roughness with and without the acquisition layer underneath the topsheet fabric. With the acquisition layer, the surface roughness of three topsheet fabrics was reduced and became similar, especially in the machine direction. The topsheet fabric with the acquisition layer underneath likely tends to perform as a smoother plane because of the addition of the deformation layer. The addition of the deformation layer may compress the surface protuberances of topsheet fabric compacting the fabric with decreased pore size [34]. Additionally, the fibrous acquisition layer may fill out the spaces between fibers of the topsheet layer. As a result of that, the variation of surface height reduces and the surface is flattened. The H-PLA fabric was most affected by the underneath layer as it had the most open structure while the other two fabrics were less porous. The change of the surface roughness supported the effects of the acquisition layer on friction. A more uniform and dense structure of nonwoven fabrics seemed less affected by the underneath layer. Conversely, the acquisition layer underneath the topsheet in an absorbent hygiene product could smooth the top-layer fabric that contacts the skin.

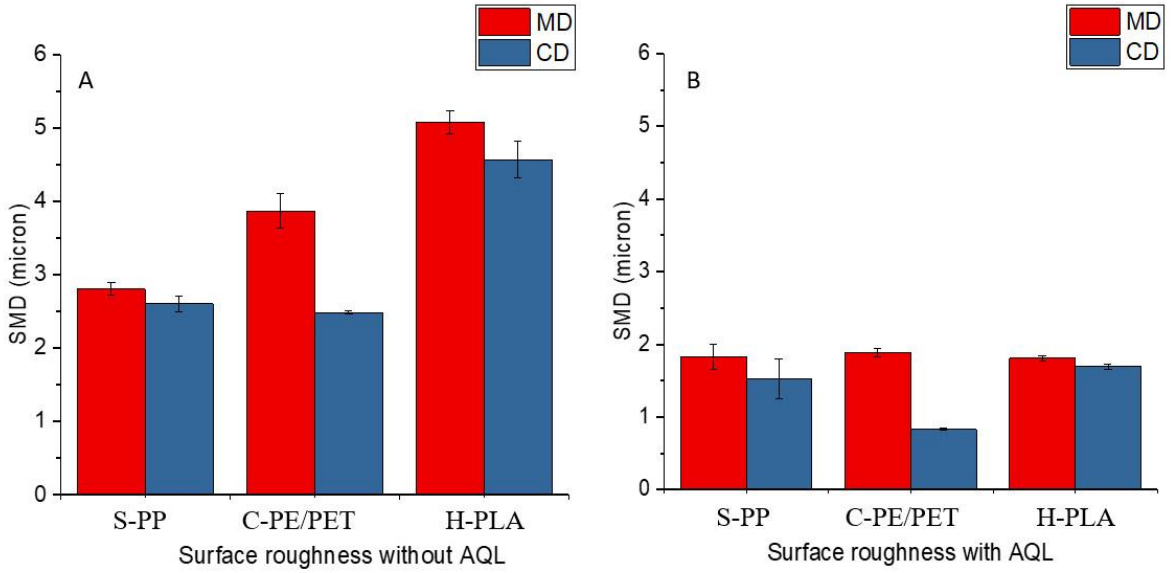

Figure 4.7. KES measured surface roughness of topsheet nonwoven fabrics without the acquisition layer (graph A) and with the acquisition layer (graph B) for the machine direction (MD) and cross-machine direction (CD).

In the setups of skin simulants contacting the fabric (Figure 4. 6 C and D), the coefficient of friction significantly increased and it was within the same range as the coefficient of friction measured on human skin when the normal load was below 2 N [20][35][11]. In setup C (Figure 4. 6 C), the Vitro-skin® film was used to replace the stainless steel surface that contacted the nonwoven fabric. The coefficient of friction was not constant at different normal loads, while the interaction between the metal surface and the fabric presented a constant coefficient of friction. It suggests the skin may increase the coefficient of friction compared to a metal surface and the normal load could have an influence. Interestingly, the hydroentangled fabric showed a different relationship between the coefficient of friction and normal load compared to the other two fabrics. It displayed higher friction at the middle and lower friction at the lowest and the highest normal load which was similar to the tendency presented in setup A, while the other two fabrics tended to have lower friction with an increased normal load. It is likely that the surface texture of the Vitro-

skin® eliminated the smoothening effects of the acquisition layer when interacting with the flat metal surface, because of mechanical interlocking between asperities on both surfaces as the asperities were both within a few microns of the same order of magnitude (fabric:~2μm to 5μm; Vitro-skin®:~12μm).

In setup D (Figure 4. 6 D), all fabrics show a decreased coefficient of friction with the increase of normal load which agrees with the effects of normal force on friction coefficient measured in vivo as reported in some previous works [36][37][11][20]. In this setup, the decrease of friction coefficient with the increase of normal load could be expressed by a power law equation: $\mu = kN^n$, where μ is the coefficient of friction, k is the friction coefficient at unit normal load, N is the applied normal load, and n is the load index. This equation was used to fit the data obtained in setup D and the k value and load index n are displayed in Table 4. 2. The exponent n was around -0.2 which was consistent with the typical exponents(-0.2 to -0.5) calculated from experiments of human skin friction [38][39]. Derler et al. made the point that the exponent close to -1/3 indicated the adhesion component of friction contributed more than the deformation friction based on the expression derived by Wolfram and Johnson[40]. This is supported by the four-setup experiments in our study. The significant change of coefficient of friction occurred when the contact surface changed from steel to Vitro-skin®. As the adhesion friction is more related to surface properties, this change of surface supported the significant contribution of adhesion friction. The addition of deformation layers did not change the coefficient of friction significantly when the contact surface was the same. It indicated the friction coefficient was more determined by the surface properties that were more relevant to adhesion force while the bulk deformation had less effects. However, it was notable that the addition of deformation silicone showed significant influence on the frictional behavior of the H-PLA fabric with the change of normal load compared

to the other two fabrics. It was hypothesized that the deformable silicone reduced the roughness of the Vitro-skin® surface similar to the reduction of surface roughness of topsheet fabrics with deformable acquisition layer as shown in Figure 4. 7. This reduction of surface roughness showed more influence on the interaction with the H-PLA, as it did in setup B.

Table 4.2. Parameters determined from the equation $\mu = kN^n$ for friction between three fabrics and the skin simulants in setup D. μ is the coefficient of friction and N is the normal load. r^2 is the coefficient of determination.

Fabric	k	n	r^2
S-PP	0.52	-0.23	0.50
C-PE/PET	0.62	-0.21	0.99
H-PLA	0.56	-0.18	0.99

At increased normal load the coefficient of friction for all fabrics appeared to converge as contact surfaces were compressed and the contact became smooth. The coefficient of friction tended to be independent of the normal load at a high normal load range. The silicone compound used in this study had increased elastic modulus with increased normal force (Figure 4. 3) which was similar to the performance of human skin [35][32]. This nonlinear mechanical property resulted in the deformation of the skin/silicone decreasing friction with increased normal load. In other words, the surface would be harder and the change of contact area would become smaller. Therefore, the effect of the normal load on the coefficient of friction was smaller at high loads.

4.4.2 Dynamic frictional behavior

Figure 4. 8 shows the friction force for the four setups at 1 N normal load. The friction force between stainless steel and fabric (Figure 4. 8 a, b) is more constant than the friction force between the Vitro-skin® and fabric (Figure 4. 8 c, d). With the skin simulants, considerable variation in the friction force occurred. This oscillating motion, stick-slip, is displayed with the

skin simulants especially with the deformable silicone underneath. When the fabric contacted the stainless steel surface, the dynamic friction force was steady with a negligible variation. Therefore, the coefficient of friction was constant and that can be used as a material feature.

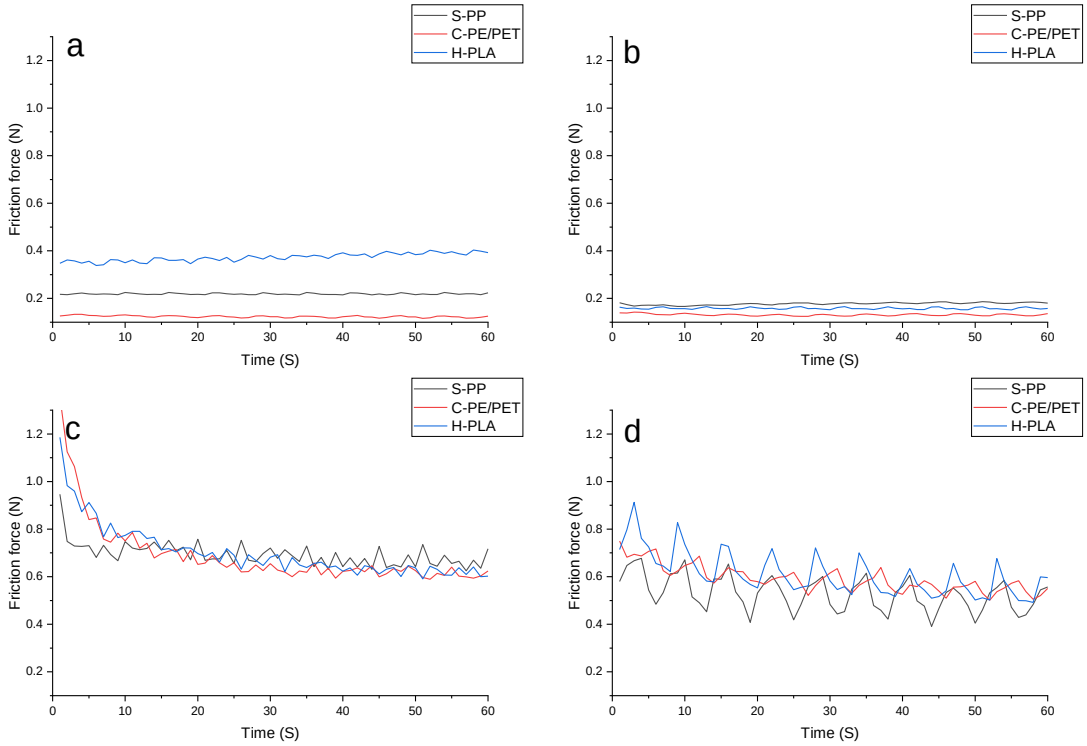

Figure 4.8. Representative friction at 1 N normal load as a function of time of the nonwoven topsheet fabrics against a) stainless steel, b) stainless steel but the topsheet fabric had acquisition layer(AQL) underneath, c) Vitro-skin® (topsheet fabric with AQL), d) Vitro-skin® with silicon underneath (topsheet fabric with AQL).

However, when the fabric was in contact with the skin simulants, it showed considerable stick-slip frictional behavior. In this case, the coefficient of friction calculated from the mean value of the friction force might lose information that reflects the variation of the friction force. In addition, the stick-slip phenomena have also been reported in many studies investigating skin sliding over a surface in vivo, which means the stick-slip behavior is more likely to be observed in the dynamic contact between the real human skin and a counter surface [37][41][10]. The

variation of friction that occurred in the contact with the Vitro-skin® was likely to be caused by the textured surface of the Vitro-skin® compared to the relatively smooth stainless steel surface. Ding and Bhushan reported a lower variation of friction force of skin with skin cream treatment than the skin without the treatment and believed the smoothness was the reason for the decrease of variation [10]. Das et al. used polydimethylsiloxane to mimic gecko toe pads and observed variation of friction when it contacted a rough glass surface rather than a smooth glass surface [42]. Therefore, the textured surface of the skin simulant is likely to cause a higher variation of friction force than a smooth metal surface. In our experiments, a distinct higher initial friction force when the fabric was observed when the fabric contacted the skin simulants rather than the stainless steel (Figure 4. 8). The distinct higher friction force at the beginning of the motion can be recognized as the static friction and this is consistent with what Berman et al. mentioned: higher static friction than kinetic friction was a sufficient condition for the occurrence of stick-slip motion [43].

In addition to the effects of the surface texture, the addition of silicone rubber underneath showed an even stronger influence of deformation on the fluctuation of friction force. This is consistent with the phenomenon observed by Kondo that the skin with a higher stratum corneum water content, which was softer, showed more distinct stick-slip [44]. Dong et al. also found a significant stick-slip phenomena for plastics when the deformation was significant [45]. Therefore, a more deformable or softer material is likely to cause stick-slip friction. The effects come from the hysteresis of the viscoelastic property of the deformable material. The material stores energy when it resists deformation during the stick phase and it dissipates energy at the slip phase. It is commonly found in a soft solid material with a rough surface in biological surfaces [46][47][48]. The energy storage and dissipation results in the differences between static and kinetic friction of the stick-slip motion and this difference was proposed as an important factor that contributes to

the tactile perception [49]. Figure 4. 9 shows the amplitude of stick-slip friction in the contact between fabric and Vitro-skin® with silicone underneath at different normal loads. The fabrics showed distinguishable amplitudes of the stick-slip motion, especially at a relatively high normal load. Nonomura et al. showed the drastic change in the static and kinetic friction contributed to the stick-slip feel which can affect the perception of water on the skin [49]. Ajayi observed that the woven or knitted fabric with high protuberances caused by yarn structure or surface hairness perceived rougher had a higher amplitude of stick-slip friction than fabric with more plane surfaces [50]. Brörmann and Tomimoto reported that a smaller contact area could not only reduce the frictional force but also decreased the amplitude of stick-slip motion [51][52]. According to these previous studies, a big stick-slip amplitude is likely to cause more impact on the tactile sensation, so the speculation would be the carding, through air fabric would have less influence on tactile sensation through the interaction with the skin, while the spunbond, thermal calender bonded fabric would be perceived as more textured. Based on the current study and some previous studies on the friction between nonwoven fabrics and skin or skin simulant[53][54], the nonwoven fabrics used in hygiene products can have a remarkably similar coefficient of friction regardless of the properties of structure and material, especially at high normal load. In the current study, the coefficient of friction tended to be similar for the nonwoven fabrics with the increased normal load (Section 3.1, Figure 4. 6 D) but the stick-slip amplitude at high normal load was different between fabrics. This may give the opportunity to indicate the friction-related perception in dynamic tests when the coefficient of friction cannot. Furthermore, it implies the need for considering deformation friction for the purpose of skin sensation evaluation. Moreover, the stick-slip can potentially cause skin damages. Lee et al. reported damage and wear of articular cartilage was more related to stick-slip sliding rather than friction coefficient [55]. Thus, the variation of friction

can both relate to skin sensation and abrasion or further damages. It can cause vibration and displacement of skin, and then exciting the mechanoreceptors in the skin [41][56].

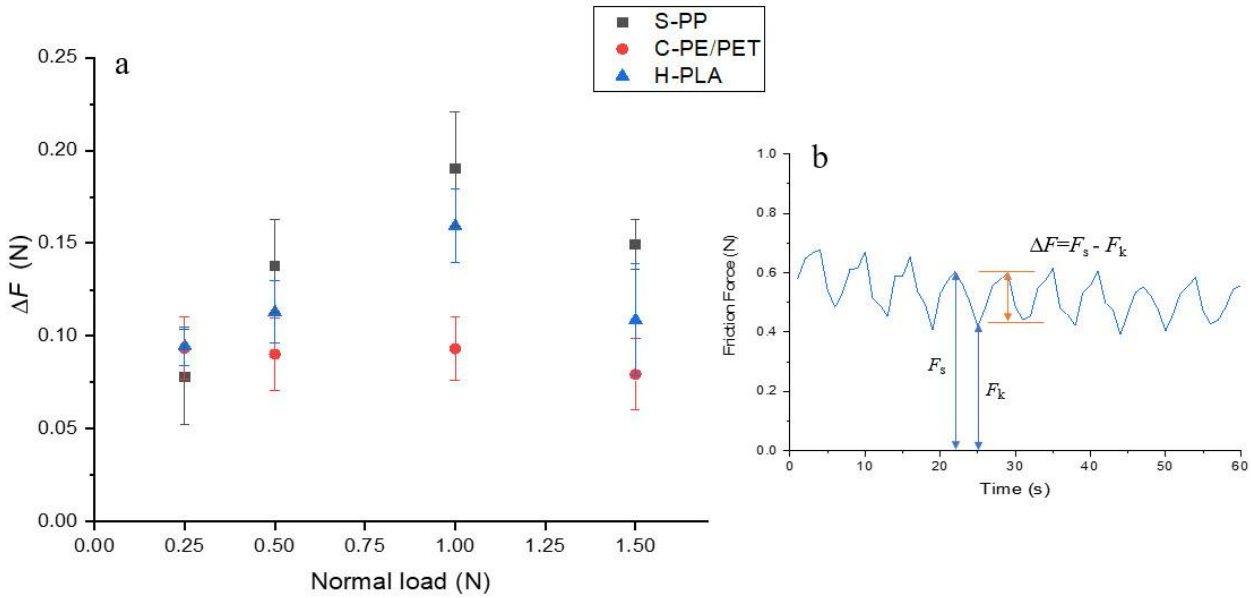

Figure 4.9. a. the amplitude of stick-slip friction by calculating $\Delta F = F_s - F_k$ for three nonwoven fabrics contacting Vitro-skin® with silicone underneath at different normal loads. b. the calculating for ΔF. F_s is the static friction force which is the maximum force peak during each stick-slip period. F_k is the kinetic friction force which is the minimum force peak during each stick-slip period.

4.5 Conclusions

Four different setups for friction measurements were studied. The conventional measurement between fabric and metal plate was compared with the measurement between fabric and skin simulants. The effects of the counter surface and the deformation layer on the frictional behavior were displayed. The top-layer skin simulant that provides a surface texture of human skin largely increased the coefficient of friction compared to a stainless steel surface but the addition of deformation layers underneath fabric and top-layer skin simulant showed much less influence on the coefficient of friction. Nevertheless, the addition of a deformation layer underneath can make fabrics with different structures perform similarly by reducing the surface roughness.

Although the addition of silicone rubber did not present influence the coefficient of friction, it displayed a considerable contribution to stick-slip motion.

The coefficient of friction and the adhesion friction force received a lot of attention in the literature while the deformation friction was usually neglected. However, this study suggests the dynamic frictional behavior, stick-slip, and skin deformation can be important for the discrimination of fabrics interacting with skin. The coefficient of friction of topsheet nonwoven fabrics tended to be indistinguishable at a high normal load whereas a high normal load or pressure is usually expected when using absorbent hygiene products. However, the fluctuation of friction can be significant with a distinct amplitude of stick-slip for different fabrics. It suggests the potential of analyzing the variation of friction to distinguish the interaction between fabric and human skin and not taking the coefficient of friction as the ultimate parameter. In this study, the skin simulants showed potential to mimic human skin and detect the frictional dynamics of skin-fabric interaction while the conventional friction measurement setup can miss such information. As the stick-slip friction can potentially impact tactile sensation and cause damages, in vivo human studies should be carried out to explore the dynamic frictional behavior for the interaction between skin and fabric and the relationship between it and tactile sensation.

4.6 References

[1] J. R. Ajmeri and C. J. Ajmeri, “Nonwoven personal hygiene materials and products,” in *Applications of Nonwovens in Technical Textiles*, Woodhead Publishing, 2010, pp. 85–102.

[2] D. Das, “Composite nonwovens in absorbent hygiene products,” in *Composite NonWoven Materials*, Woodhead Publishing, 2014, pp. 74–88.

[3] J. L. Counts, C. T. Helmes, D. Kenneally, and D. R. Otts, “Modern disposable diaper construction: Innovations in performance help maintain healthy diapered skin,” *Clin. Pediatr. (Phila).*, vol. 53, no. 9, pp. 10S-13S, Aug. 2014.

[4] S. Bağlam and B. Engin, “Diaper (napkin) dermatitis: A fold (intertriginous) dermatosis,” *Clin. Dermatol.*, vol. 33, no. 4, pp. 477–482, Jul. 2015.

[5] J. K. Bender, J. Faergemann, and M. Sköld, “Skin Health Connected to the Use of Absorbent Hygiene Products: A Review,” *Dermatol. Ther. (Heidelb).*, vol. 7, no. 3, pp. 319–330, Sep. 2017.

[6] ASTM International, “ASTM D1894, Standard Test Method for Static and Kinetic Coefficients of Friction of Plastic Film and Sheeting.” ASTM International, p. 7, 2014.

[7] S. Kawabata and M. Niwa, “Objective Measurement of Fabric Mechanical Property and Quality: Its Application To Textile And Clothing Manufacturing,” *Int. J. Cloth. Sci. Technol.*, vol. 3, no. 1, pp. 7–18, 1991.

[8] M. A. Abellan, H. Zahouani, and J. M. Bergheau, “Contribution to the determination of in vivo mechanical characteristics of human skin by indentation test,” *Comput. Math. Methods Med.*, vol. 2013, p. 814025, 2013.

[9] U. Jacobi *et al.*, “In vivo determination of skin surface topography using an optical 3D device,” *Ski. Res. Technol.*, vol. 10, no. 4, pp. 207–214, Nov. 2004.

[10] S. Ding and B. Bhushan, “Tactile perception of skin and skin cream by friction induced vibrations,” *J. Colloid Interface Sci.*, vol. 481, pp. 131–143, Nov. 2016.

[11] N. K. Veijgen, M. A. Masen, and E. van der Heide, “A novel approach to measuring the frictional behaviour of human skin in vivo,” *Tribol. Int.*, vol. 54, pp. 38–41, Oct. 2012.

[12] L.-C. Gerhardt, A. Lenz, N. D. Spencer, T. Münzer, and S. Derler, “Skin-textile friction and skin elasticity in young and aged persons,” *Ski. Res. Technol.*, vol. 15, no. 3, pp. 288–298, Aug. 2009.

[13] M. A. Masen, N. Veijgen, M. Klaassen, M. A. Masen, N. Veijgen, and · M Klaassen, “Experimental Tribology of Human Skin,” in *Skin Biophysics*, G. Limbert, Ed. Springer, Cham, 2019, pp. 281–295.

[14] E. Van Der Heide, X. Zeng, and M. A. Masen, “Skin tribology: Science friction?,” *Friction*, vol. 1, no. 2, pp. 130–142, Jun. 2013.

[15] A. M. Cottenden, W. K. Wong, D. J. Cottenden, and A. Farbrot, “Development and validation of a new method for measuring friction between skin and nonwoven materials,”

Proc. Inst. Mech. Eng. Part H J. Eng. Med., vol. 222, no. 5, pp. 791–803, May 2008.

[16] M. F. Leyva-Mendivil, J. Lengiewicz, and G. Limbert, “Skin friction under pressure. the role of micromechanics,” *Surf. Topogr. Metrol. Prop.*, vol. 6, no. 1, p. 014001, Jan. 2018.

[17] S. Derler and L. C. Gerhardt, “Tribology of skin: Review and analysis of experimental results for the friction coefficient of human skin,” *Tribol. Lett.*, vol. 45, no. 1, pp. 1–27, Jan. 2012.

[18] K. B. Duvefelt, U. L. O. L.-O. Olofsson, and C. M. J. Johannesson, “Towards simultaneous measurements of skin friction and contact area: Results and experiences,” *Proc. Inst. Mech. Eng. Part J J. Eng. Tribol.*, vol. 229, no. 3, pp. 230–242, Mar. 2015.

[19] A. K. Dąbrowska *et al.*, “Materials used to simulate physical properties of human skin,” *Ski. Res. Technol.*, vol. 22, no. 1, pp. 3–14, Feb. 2016.

[20] A. Dąbrowska *et al.*, “A water-responsive, gelatine-based human skin model,” *Tribol. Int.*, vol. 113, pp. 316–322, Sep. 2017.

[21] M. Nachman and S. E. E. Franklin, “Artificial Skin Model simulating dry and moist in vivo human skin friction and deformation behaviour,” *Tribol. Int.*, vol. 97, pp. 431–439, May 2016.

[22] H. Fuchs and W. Kittelmann, “Characteristics and application of nonwovens,” in *Nonwoven Fabrics: Raw Materials, Manufacture, Applicaion, Characteristics, Testing Processes*, 2003, pp. 489–493.

[23] H. Lim, “A review of spun bond process,” *J. Text. Apparel, Technol. Manag.*, vol. 6, no. 3, pp. 1–13, 2010.

[24] B. P. Subhash K. Batra, “Bonding technologies,” in *Introduction to nonwovens technology*, Lancaster, PA : Destech Publications, c2012., 2012, pp. 87–161.

[25] G. Li, A. Sankaran, A. L. Yarin, and B. Pourdeyhimi, “Hydroentangled polymer nonwovens: Prediction of jet streaks and surface roughness,” *Polymer (Guildf).*, vol. 180, p. 121731, Oct. 2019.

[26] B. P. Subhash K. Batra, “Staple fiber-based technologies,” in *Introduction to nonwovens technology*, Lancaster, PA : Destech Publications, c2012., 2012, pp. 43–68.

[27] S. Chen and B. Bhushan, “Nanomechanical and nanotribological characterization of two synthetic skins with and without skin cream treatment using atomic force microscopy,” *J. Colloid Interface Sci.*, vol. 398, pp. 247–254, May 2013.

[28] F. Eudier, G. Savary, M. Grisel, and C. Picard, “Skin surface physico-chemistry: Characteristics, methods of measurement, influencing factors and future developments,” *Adv. Colloid Interface Sci.*, vol. 264, pp. 11–27, Feb. 2019.

[29] L. C. Gerhardt, A. Schiller, B. Müller, N. D. Spencer, and S. Derler, “Fabrication, characterisation and tribological investigation of artificial skin surface lipid films,” *Tribol. Lett.*, vol. 34, no. 2, pp. 81–93, 2009.

[30] M. Azmi, Nurul Nadiah; Azhar, Ilya Izyan Shahrul; Jamaluddin, “A Brief Review and

Framework towards Synthesising Silicone-Hydrogel Materials that Mimic Skin Deformation Behaviour," *Appl. Mech. Mater.*, vol. 680, pp. 70–73, 2014.

[31] V. B. Mountcastle, "The Evolution and Structure of the Hand," in *The sensory hand: Neural mechanisms of somatic sensation.*, Harvard University Press., 2005, pp. 41–50.

[32] C. Pailler-Mattei, S. Bec, and H. Zahouani, "In vivo measurements of the elastic mechanical properties of human skin by indentation tests," *Med. Eng. Phys.*, vol. 30, no. 5, pp. 599–606, Jun. 2008.

[33] S. Dey *et al.*, "Exposure Factor considerations for safety evaluation of modern disposable diapers," *Regul. Toxicol. Pharmacol.*, vol. 81, pp. 183–193, Nov. 2016.

[34] S. Jaganathan, H. Vahedi Tafreshi, E. Shim, and B. Pourdeyhimi, "A study on compression-induced morphological changes of nonwoven fibrous materials," *Colloids Surfaces A Physicochem. Eng. Asp.*, vol. 337, no. 1–3, pp. 173–179, 2009.

[35] M. Nachman and S. E. Franklin, "Artificial Skin Model simulating dry and moist in vivo human skin friction and deformation behaviour," *Tribol. Int.*, vol. 97, pp. 431–439, May 2016.

[36] G. Man and M.-Q. Man, "Skin Friction Coefficient," in *Agache's Measuring the Skin*, Cham: Springer International Publishing, 2017, pp. 203–210.

[37] S. Derler and G. M. Rotaru, "Stick-slip phenomena in the friction of human skin," *Wear*, vol. 301, no. 1–2, pp. 324–329, Apr. 2013.

[38] S. Derler, L.-C. Gerhardt, A. Lenz, E. Bertaux, and M. Hadad, "Friction of human skin against smooth and rough glass as a function of the contact pressure," *Tribiology Int.*, vol. 42, no. 11–12, pp. 1565–1574, Dec. 2008.

[39] M. J. Adams, B. J. Briscoe, and S. A. Johnson, "Friction and lubrication of human skin," *Tribol. Lett.*, vol. 26, no. 3, pp. 239–253, Jun. 2007.

[40] S. Derler, L. C. Gerhardt, A. Lenz, E. Bertaux, and M. Hadad, "Friction of human skin against smooth and rough glass as a function of the contact pressure," *Tribol. Int.*, vol. 42, no. 11–12, pp. 1565–1574, Dec. 2009.

[41] R. Fagiani, F. Massi, E. Chatelet, Y. Berthier, and A. Akay, "Tactile perception by friction induced vibrations," *Tribol. Int.*, vol. 44, no. 10, pp. 1100–1110, 2011.

[42] S. Das *et al.*, "Stick–slip friction of gecko-mimetic flaps on smooth and rough surfaces," *J. R. Soc. Interface*, vol. 12, no. 104, p. 20141346, Mar. 2015.

[43] A. D. Berman, W. A. Ducker, and J. N. Israelachvili, "Origin and Characterization of Different Stick-Slip Friction Mechanisms," *Langmuir*, vol. 12, no. 19, pp. 4559–4563, 1996.

[44] S. Kondo, "The Frictional Properties Between Fabrics and the Human Skin," *J. Japan Res. Assoc. Text. End-Uses*, vol. 43, no. 264, pp. 264–275, 2002.

[45] C. Dong, C. Yuan, X. Bai, H. Qin, and X. Yan, "Investigating relationship between deformation behaviours and stick-slip phenomena of polymer material," *Wear*, vol. 376–

377, pp. 1333–1338, Apr. 2017.

[46] S. N. Patek, “Spiny lobsters stick and slip to make sound: These crustaceans can scare off predators even when their usual armour turns soft,” *Nature*, vol. 411, no. 6834, pp. 153–154, May 2001.

[47] M. Urbakh, J. Klafter, D. Gourdon, and J. Israelachvill, “The nonlinear nature of friction,” *Nature*, vol. 430, no. 6999. pp. 525–528, 29-Jul-2004.

[48] K. Viswanathan, N. K. Sundaram, and S. Chandrasekar, “Stick-slip at soft adhesive interfaces mediated by slow frictional waves,” *Soft Matter*, vol. 12, no. 24, pp. 5265–5275, Jun. 2016.

[49] Y. Nonomura *et al.*, “Tactile impression and friction of water on human skin,” *Colloids Surfaces B Biointerfaces*, vol. 69, no. 2, pp. 264–267, Mar. 2009.

[50] J. 0 Ajayi’, “Fabric Smoothness, Friction, and Handle,” *Text. Res. J.*, vol. 62, no. 1, pp. 52–59, 1992.

[51] K. Brörmann, I. Barel, M. Urbakh, and R. Bennewitz, “Friction on a microstructured elastomer surface,” *Tribol. Lett.*, vol. 50, no. 1, pp. 3–15, Apr. 2013.

[52] M. Tomimoto, “The frictional pattern of tactile sensations in anthropomorphic fingertip,” *Tribol. Int.*, vol. 44, pp. 1340–1347, 2011.

[53] S. S. Falloon and A. Cottenden, “Friction between a surrogate skin (Lorica Soft) and nonwoven fabrics used in hygiene products,” *Surf. Topogr. Metrol. Prop.*, vol. 4, no. 3, 2016.

[54] S. S. Falloon, V. Asimakopoulos, and A. M. Cottenden, “An experimental study of friction between volar forearm skin and nonwoven fabrics used in disposable absorbent products for incontinence,” *Proc. Inst. Mech. Eng. Part H J. Eng. Med.*, vol. 233, no. 1, pp. 35–47, 2019.

[55] D. W. Lee, X. Banquy, and J. N. Israelachvili, “Stick-slip friction and wear of articular joints,” *Proc. Natl. Acad. Sci. U. S. A.*, vol. 110, no. 7, p. E567, Feb. 2013.

[56] R. I. Leine, D. H. Van Campen, A. De Kraker, and L. Van Den Steen, “Stick-Slip Vibrations Induced by Alternate Friction Models,” *Nonlinear Dyn.*, vol. 16, no. 1, pp. 41–54, 1998.

CHAPTER 5 A Study of Skin Physiology, Sensation and Friction of Nonwoven Fabrics Used in Absorbent Hygiene Products in Neutral and Warm Environments

*This chapter was published as: "L. Yin, E. Shim, and E. DenHartog, "A Study of Skin Physiology, Sensation and Friction of Nonwoven Fabrics Used in Absorbent Hygiene Products in Neutral and Warm Environments," Biotribology, vol. 24, Sep. 2020.

5.1 Abstract

Absorbent hygiene products like diapers, feminine hygiene, and wet wipes are life necessities. These products commonly use nonwoven fabrics as the layer that is in contact with the skin. Their performance in terms of skin health and comfort is receiving increased attention because of the existence of concerns for skin health issues such as skin irritation and dermatitis, and the large influence of skin sensation on individuals' preference. Friction is usually recognized as an important factor for skin comfort and dermatitis issues, but there is a lack of understanding of the relationship between friction and skin physiology, skin sensation, in the use of absorbent hygiene products. This study reports a measurement of friction in vivo with the evaluation of skin physiology and sensation in neutral and warm environments to explore the effects of fabric and friction on skin comfort. Friction tests between the volar forearm and nonwoven fabrics were conducted with the measurement of transepidermal water loss, skin redness, and the evaluation of subjective skin sensation. The interaction between skin and eight nonwoven fabrics with a surface roughness (arithmetic mean height) between 3μm and 20μm was evaluated in neutral (22℃) and warm (35℃) environments. Skin physiological changes after friction were able to be detected quantitatively by the transepidermal water loss and skin redness measurement. In the warm environment, there was significantly higher friction, less pleasantness, more changes in transepidermal water loss but not in skin redness. The friction can only relate to skin physiology and sensation in the neutral environment while the surface roughness of fabrics related to them in

both neutral and warm environments. Both rough and smooth fabrics caused high friction in the warm environment, but the rough fabric caused a higher adverse impact on skin physiology and sensation than smooth fabrics that suggested the adhesion and deformation friction could have different effects on skin comfort. Deformation friction is more likely to have effects on skin physiology and pleasantness sensation than adhesion friction. The pleasantness sensation has a negative relationship with skin physiology. A more unpleasant sensation can indicate more impact on skin physiology. This provides a potential that the unpleasant sensation can be a precaution signal for the adverse effects on skin physiology.

5.2 Introduction

Nonwoven fabrics have been selected to use for absorbent hygiene products such as diapers, feminine hygiene, and adult incontinence because of the low cost, disposability, and feasibility to be engineered for various purposes. The main components of absorbent hygiene products include the topsheet, acquisition/distribution layer, absorbent core, and backsheet. A fibrous, thin, and lightweight nonwoven fabric is commonly used as the top sheet material that contacts the skin. Although the functional performance of hygiene products has dramatically improved over the past 40 years, users still experience discomfort caused by unpleasant sensation, skin damages, and irritation during the contact between the skin and nonwoven fabrics. Diaper dermatitis and incontinence-associated dermatitis are common problems that people suffer from when they use hygiene products [1][2]. The warm and humid environment can be important for the interaction between fabric and skin and make the skin more vulnerable. It has been reported that the temperature of the air and the skin surface can increase in the use of absorbent hygiene products after a period of time [3][4]. In such a warm environment, sweat is expected on the skin surface and a higher friction force has been reported when there is sweat or water on the skin surface [5][6].

It also can lead to higher skin hydration that would decrease the elastic modulus of skin. Due to the change of mechanical properties, the skin surface can become more compliant with more deformation and slower recovery, and the skin is more likely to be injured [4][5][7][8].

Friction is widely recognized as one of the main reasons for contact dermatitis and a key property in the evaluation of textiles' comfort [9][10]. However, there is no experimental work to demonstrate if friction can lead to skin damages, injuries, and discomfort for the use of absorbent hygiene products in a warm environment. Although some experiments showed the abraded skin particles and blisters were generated under friction, the relationship between friction and dermatitis or rash was only speculated by the observation that redness occurred in the fabric contact area [1][9][11][12]. To keep skin health and comfort, it is necessary to learn more about the interaction between nonwoven fabric and skin and how the interaction is related to tactile pleasantness and skin health in the use environment.

The friction force between the skin and a counter surface is commonly demonstrated using a two-term model consisting of adhesion and deformation components. The adhesion friction is generated on the interface by the shearing force between the two surfaces while the deformation relates to the bulk hysteresis of the contacting surfaces [13][14][15][16][17][18]. The coefficient of friction is widely used to study the effects of friction on skin comfort which is related to the total friction force but does not separate the adhesion and deformation components [12][19][20][21][22]. Therefore, it is unknown whether the deformation and adhesion components have the same effects on skin physiology and sensation. In the literature, the adhesion force is usually considered the primary component of the friction of human skin, and the deformation component is generally neglected [23]. Nevertheless, the contribution of deformation can change depending on the contact material, lubrication state, and the normal load. Mahdi et al. and

Kuilenburg et al. have suggested taking the deformation into account when the skin is sliding against a rough surface under wet conditions, especially when the normal load is high [18][24]. It could be helpful to investigate the changes of friction and skin comfort between neutral-dry and warm-humid environments to understand if the two components could have different influences on the skin because the contribution of adhesion and deformation force can be different under the different environments which may lead to different effects on skin comfort.

The frictional behavior of skin is expected to be largely affected by the surface roughness of the counter surface [8][25][26], and a smooth surface may facilitate electrostatic attractions and the formation of capillary bridges that increase adhesion force between two surfaces in the intimate contact while the rough surface could be less affected by adhesion [27][28]. It is also known the smoothness is reported as one of the most useful indicators for the sense of touch of nonwovens [29][30], and the surface roughness of fabric is strongly related to the smoothness sensation [31]. Therefore, the surface roughness was used to control fabric samples in this study, and investigate its effects on friction, skin physiology, and sensation.

The skin health condition can be indicated by physiological measurement. The typical parameters used for skin physiological condition evaluation include transepidermal water loss (TEWL), hydration of the Stratum Corneum (SC), pH, and skin color. TEWL is typically used to indicate the skin barrier function [32]. It is the passive flux of water from the dermis and epidermis to the surface of the SC. The water loss is a result of the increased permeability of the stratum corneum, so a higher TEWL value indicates the skin is more permeable. An elevated TEWL value indicates altered skin barrier function and it has been observed in several skin diseases like contact diaper dermatitis [33][34][35]. Skin hydration is the water content of the SC and a high hydration level is usually found in the dermatitis area [34][36]. Skin pH can also represent the integrity of

the skin barrier function as an acidic skin surface helps to ensure the barrier function [35]. Skin color analysis is another way to quantify skin response. Erythema or skin redness is a common sign of dermatitis area[36][37]. At the early stage of dermatitis, skin redness is the most obvious observation. The area of redness will increase with the increase of severity degree. To a moderate and severe situation, there can be pustules, desquamation, and edema. When a diaper rash lasts more than 72 hours, a more severe infection could occur[38][39][40]. The skin color can be assessed using a spectrophotometer [41] and images with color analysis [42][42][43][44].

Skin sensation is a complex subjective perception based on physical, physiological, and psychological factors. Psychological and physiological factors are dynamic factors such as the state of being, mood, feelings, physical fitness, and thermal strain. Physical factors include fabric properties, environment temperature, and humidity, which are relatively steady and measurable compared to psychological and physiological factors [45]. In the current study, the relationship between subjective sensation and physical factors including friction, fabric properties, and environment were explored on the human forearm, and the pleasantness sensation of topsheet nonwoven fabrics was investigated in a warm environment. In the work of Zimmerer et al. and Akin et al., a comparable TEWL value of adult volar forearm(mean value: 4.3 $g/m^2/h$) and child diaper area(mean value: 5.6 $g/m^2/h$ respectively) with similar kinetics of TEWL after hydration of the skin were reported. Zimmerer et al. also investigated coefficient of friction in dry and wet conditions are comparable (dry condition: adult:0.30±0.09, infant:0.30±0.14; wet condition: adult: between 1.18±0.2 and 1.22±0.29; infant:0.96±0.3). Thus the performance of the volar forearm can be a reference of the buttocks skin [11][46].

The objective of the work presented in this paper is to explore the impact of friction on skin physiology and sensation and explore if there is a quantitative correlation between them for

the use of absorbent hygiene products. In this study, the skin physiology and sensation in neutral and warm environments were investigated through non-invasive parameters- TEWL and skin color, and subjective evaluation using ordinal scales. The warm environment was 35℃, which is close to the temperature of the skin region covered by absorbent hygiene products[3]. An in vivo friction measurement was conducted between volar forearms and nonwoven fabrics because of the easy access of this anatomical site and the comparable skin condition of adult volar forearms and buttocks.

5.3 Materials and methods

5.3.1 Nonwoven fabrics characterization

5.3.1.1 Basis weight

The basis weight is the weight of fabric (gram) per square meter. The fabric was cut into a circle using a template with an area of 100 cm^2. The basis weight was calculated by the measured fabric weight(gram) times 100. Five replications were tested for each fabric sample. The mean value ± standard deviation is displayed in Table 5. 1.

5.3.1.2 Surface roughness

The surface roughness (SMD, geometrical roughness) of each fabric was measured by the Kawabata Evaluation System (KES) [47]. Only the machine direction of the nonwoven fabrics was tested on the human subjects, therefore, the surface roughness was measured in this direction as well (Table 5. 1). The SMD is the arithmetic mean of the surface heights in the evaluation length. The sensor contacts the fabric surface and the vertical displacement of the sensor was measured. The sampling rate was 5 Hz and the traveling distance was 30 mm. The geometric roughness (SMD) is defined as the mean deviation of the measured vertical displacement. It was calculated as below:

$$SMD = \frac{1}{L}\int_0^L \left|\mathrm{T} - \mathrm{T}'\right| dL$$

Where L is the total evaluation length, T is the local surface height and T' is the mean fabric surface height [48][49]. A higher SMD value stands for a higher roughness. Fabric samples were tested at 21±2 ˚C, 55 ± 5% RH. A constant tension load of 19.6 N/m (20 gf/cm) and 0.098 N (10 g) normal load was applied to the sample through a single wire probe with a U shape. The diameter of the wire was 0.5 mm. The fabric was moved 3 cm in the forward direction and then the same length in the backward direction with 1 mm/s velocity. Three replications were done for each fabric sample.

5.3.1.3 Nonwoven fabrics used for in vivo skin test

Eight nonwoven fabrics were selected for the experiments. The nonwoven manufacturing methods, materials, basis weight, and surface roughness are summarized in Table 5. 1. This study primarily focused on the performance of topsheet nonwoven fabrics used for absorbent hygiene products. There were two rough fabrics (M1, M2) with high basis weight were used as a contrast because the topsheet fabrics were all relatively smooth within a narrow range of roughness. The other six nonwoven fabrics were made for topsheet that were lightweight and thin. C1 and C2 were two commercial samples provided by different suppliers. PP1, PE1, PP3, and PE3 were made in the Nonwoven Institute (North Carolina State University, U.S.A.) with controlled materials and bond area. They were produced with the Reicofil single beam spunbond line in the Nonwoven Institute and thermally calender bonded by the facility in Fiber Visions (Fiber Visions Manufacturing, GA, U.S.A.). PP1 and PP3 were made from polypropylene (ExxonMobile PP3155) fibers. PE1 and PE3 were made from polyethylene (Dow PE-ASPUN 6855A)/Polypropylene (ExxonMobile PP3155) sheath/core bicomponent fibers. The sheath/core ratio was 10 to 90. Code 1 was a small bond area of 8.7% while the code 3 represented a bigger bond area of 24.5%. The acquisition layer is the second layer in absorbent hygiene products, underneath the topsheet and

usually much thicker than the topsheet. To simulate the structure of absorbent hygiene products, a commercial acquisition layer nonwoven fabric with a basis weight of 90 g/m^2 was used as the background material.

The spunbond technology is the most universal method used for disposable products and hygiene products. It combines the process of filament extrusion and web formation. Filaments are obtained from molten polymer extrusion and then directly laid on a conveyor to form a web [50][51]. The achievement of low basis weight nonwovens is one of its biggest advantages [52][53]. The thermal calender bonding is a typically used bonding technology combined with spunbond because it is suitable to be used for fabrics with low thickness. In addition, it can give a well-designed texture for the fabric surface by adjusting the pattern on the roll surface [54][55]. The meltblown process is similar to spunbond but it uses hot and high-velocity air to draw the molten polymer and can achieve much finer fibers than the spunbond process[56]. Nonwoven fabrics produced by carding with through-air bonding are another dominant fabric type for topsheet. The fabric has no patterns and the fibrous web can retain loft with high bulk because hot air is used to bond fibers [54][57].

Table 5.1. Specifications of the tested nonwoven fabrics. The surface roughness was measured by the Kawabata Evaluation System.

Sample ID	Nonwoven manufacturing methods	Materials	Basis weight (g/m^2)	Surface roughness (μm)
M1	Meltblown	PP	48.2±2	18.34±0.75
M2	Meltblown	PP	48.8±2.3	8.69±0.21
PE1	Spunbond, thermal calender,	PE/PP sheath/core bicomponent	19.4±1	6.21±0.24
PP1	Spunbond, thermal calender	PP	19.8±0.4	4.85±0.39
PP3	Spunbond, thermal calender	PP	20±0	4.77±0.39
PE3	Spunbond, thermal calender	PE/PP sheath/core bicomponent	18±0.9	4.29±0.09
C2	Carding, through-air	PE/PET sheath/core bicomponent	19±0.3	3.87±0.23
C1	Spunbond, thermal calender	PE/PP sheath/core bicomponent	20±0.5	3.73±0.39
AQL (acquisition layer)	Carding, through-air	PET/Co-PET bicomponent	90	N/A

5.3.2 In vivo skin physiology and sensation evaluation

5.3.2.1 Friction measurement

A friction measurement device was made to measure the friction force in vivo (Figure 5. 1). The mechanism was similar to the Instron friction testing. The main components include a motorized test stand and a force gauge. The eTrack X linear stage with the NSC A2L two-axis stepper motor controller (Newmark systems Inc., U.S.A.) was used as the motorized test stand to control the horizontal movement. A force sensor with a digital force gauge (Omega Engineering Inc., U.S.A.) was mounted on the linear stage to record the friction force during the sliding movement. A 3 cm by 3 cm plastic cube, that allowed attachment of the fabrics, was connected to the force sensor. The subject's arm could be placed on an adjustable platform to allow the tested fabrics to contact the skin. The tested skin area was on the volar forearm, which was 3 cm to 5 cm from the elbow to the palm direction as that was a relatively flat area which helped to maintain a

constant normal force. The sliding distance was 5 cm. The fabric slid on the skin back and forth for 12 cycles with a velocity of 15 mm/s. The resolution of the acquired friction force was 0.01N with a sampling rate of 10Hz. The normal force applied to the skin was 1.32 ±0.1 N that was measured by a capacitive force sensor (SingleTact, U.S.A.). This normal force was accepted by all subjects without causing any pain during the test. The test fabric was attached to entirely cover the plastic cube so the apparent contact area was 9 cm^2. A typical measurement of friction force was displayed in Figure 5. 2. The positive values were the force generated when the fabric slid towards the face (proximal) side while the negative values were the force generated when the fabric slid towards the palm (distal) side. The force was slightly bigger on the positive side because the surface of the arm was not perfectly flat and there was a higher resistance when the fabric moved towards the upper arm. It was hypothesized a bigger force could have more effects on the skin so the mean value of the maximum positive force for each cycle was used.

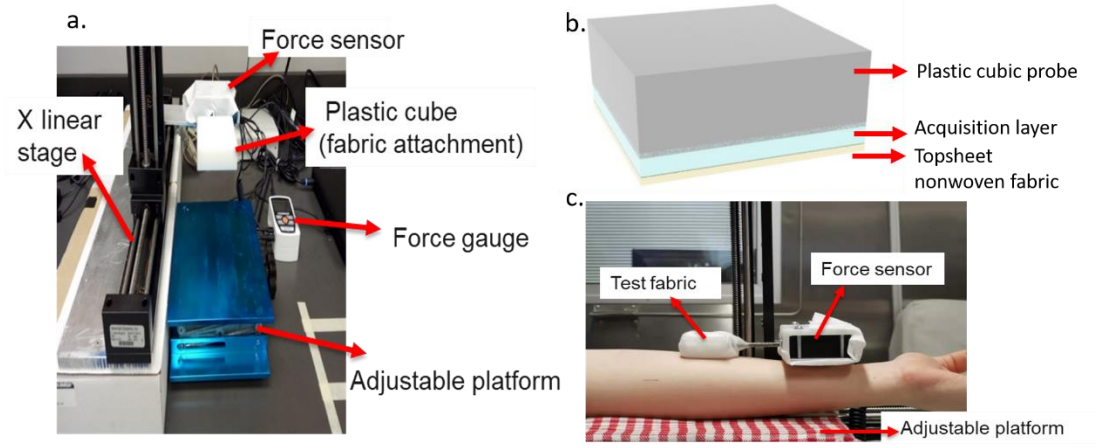

Figure 5.1. a. the construction of the friction measurement device. b. schematic of the probe that contacts skin with the fabric layout. c. photograph of the skin-fabric contact on the friction measurement device.

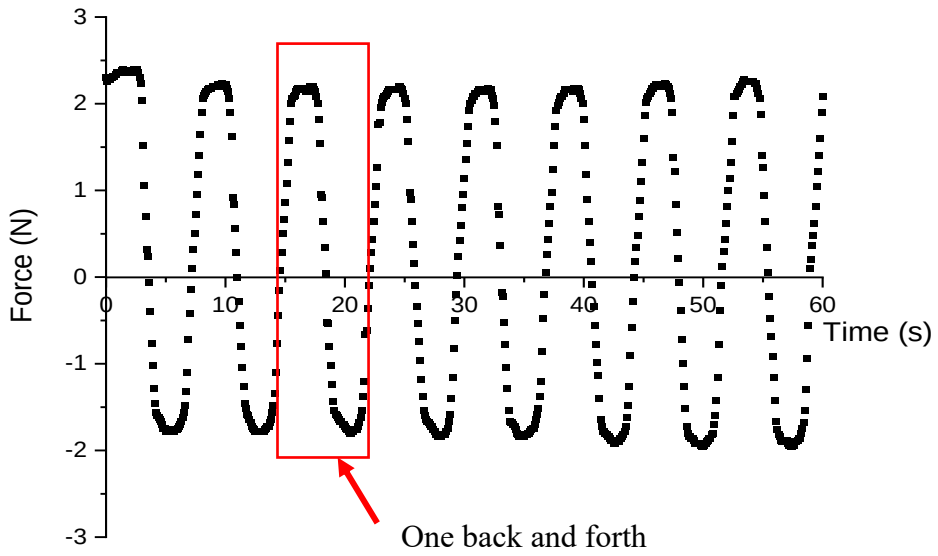

Figure 5.2. Friction force of one of the friction tests in a minute.

5.3.2.2 Transepidermal water loss (TEWL) measurement

TEWL measurements were taken using a Tewameter TM300 (Courage & Khazaka electronic GmbH, Germany). To get more stable and accurate readings, the Tewameter probe was constantly warmed up to 30℃ which is close to skin temperature by using the Probe Heater PR100 (Courage & Khazaka electronic GmbH, Germany) before each measurement. Two measurements were taken at the test skin area before and after the friction test and each measurement was recorded over 30 seconds to provide a stable average reading. The measured epidermal water loss was expressed in $g/m^2/h$. The mean value of the two measurements before friction was taken as the water loss amount at the normal skin condition. The mean value of the two measurements after friction was taken as the water loss amount of skin after the impact of friction. The difference

between the after-friction value and the before-friction value was taken as TEWL change to indicate the influence of friction on the skin barrier function.

5.3.2.3 Skin redness measurement

Images of the skin were taken using a digital handheld microscope Aven 26700 (Aven, U.S.A.). The diameter of the lens was 30 mm. The microscope was placed on the skin perpendicularly without any gaps between it and the skin. There were 8 LED lights built-in and the transparent part of the microscope was covered using opaque black tape, therefore, the light was consistent when taking images. The spatial resolution was 14 microns. A skin image was taken at the tested skin area before and after each friction test. The CIE (Commission Internationale de l'Eclairage) L*a*b* color space is widely used to identify the color differences. The L* value is for lightness while the a* and b* are color dimensions. It has been reported that the a* value linearly correlates with skin erythema [58]. The a* value is the red/green coordinate. A bigger a* value on the positive coordinate indicates the color is redder. Each image was processed by Matlab (The MathWorks, U.S.A.) to get the a* value. The difference between the after-friction a* value and the before-friction a* value was used to present the color difference in terms of redness. A positive difference indicates the skin is redder after the friction test and negative values would indicate a decrease in redness of the skin.

5.3.2.4 Skin sensation evaluation

To evaluate the subjective skin sensation during the friction test, a questionnaire was used. The sensation was assessed from five perspectives: pleasantness, localized sensation, texture sensation, wetness sensation, and stickiness sensation. For each sensation, an ordinal scale was used (Figure 5. 3). The pleasantness perception and the localized sensation were evaluated using a bipolar balanced scale based on ISO 10551(2001). In the pleasantness scale, middle point 0 was

neither pleasant nor unpleasant. The ratings from 0 to 4 were the increase in pleasantness while from 0 to -4 present the reduction in pleasantness. The localized sensation demonstrated the specific sensation on the skin especially for an uncomfortable sensation such as itch and tingle. The scale ranged from 0 to 5 with an increase in uncomfortable levels. The scales for texture, wetness, and stickiness sensations were adapted from literature [31]. The texture sensation scale was used to evaluate the perception of fabric smoothness and roughness. The neutral sensation (neither rough nor smooth) was 0. The positive ratings present an increase in roughness whereas the negative ratings were the different levels of smoothness. The ordinal scale of wetness sensation ranged from 0 to 6 corresponding to extremely dry to extremely wet. The sensation of fabric stickiness was assessed by 5 magnitudes ranged from 0 (not sticky) to 4 (extremely sticky).

1. Pleasantness sensation

Rating	
4	Extremely Pleasant
3	Very Pleasant
2	Pleasant
1	Somewhat pleasant
0	Neutral
-1	Slightly unpleasant/uncomfortable
-2	Unpleasant/uncomfortable
-3	Very unpleasant/uncomfortable
-4	Extremely unpleasant/uncomfortable

2. Localized sensation

Rating	
0	Comfortable/Neutral Touch
1	Tickle
2	Itch
3	Tingle
4	Prickle
5	Abrasive

3. Texture sensation

Rating	
3	Very rough
2	Rough
1	Sligtly rough
0	Neither rough nor smooth
-1	Slightly smooth
-2	Smooth
-3	Very smooth

4. Wetness sensation

Rating	
6	Extremely wet
5	Very wet
4	Wet
3	Slightly wet
2	Barely wet
1	Dry
0	Extremely Dry

5. Stickiness sensation

Rating	
4	Extremely sticky
3	Very sticky
2	Sticky
1	Slightly sticky
0	Not sticky

Figure 5.3. Skin sensation scales for pleasantness, localized sensation, texture sensation, wetness sensation, and stickiness sensation.

5.3.2.5 Study Protocol

Eleven healthy volunteers were recruited from North Carolina State University. There were 10 females and 1 male, all with ages between 18 and 21. All participants had no prior history of diagnosed dermatological illnesses and no open wounds or skin infections. The content and test procedure were explained to them verbally before their consent to participate. The study was

reviewed and approved by the North Carolina State University Institutional Review Board for the Use of Human Subjects in Research (protocol #15425) and written informed consent was obtained from each participant. Subjects were instructed not to apply body care products like lotions to the forearm skin on the day of testing. For all studies, the subjects were acclimatized for 15 minutes in a thermoneutral room (22^{o}C) and read the questionnaire to familiarize themselves with the questions in a waiting room prior to measurements. After the subject left the waiting room, they entered the climatic chamber where the temperature and humidity were controlled. The experiments of neutral and warm environments were conducted on different days for each subject. The temperature was 22℃ for the neutral and 35℃ for the warm environment. The relative humidity was between 45% to 50% for both environments. During the experiments, the subjects sat comfortably wearing T-shirts and positioned their forearm on an adjustable platform. The nonwoven fabric faced to the skin surface with the acquisition layer as a background layer behind it. They were taped on the plastic cube and the contact surface was kept flat. The machine direction of the fabric was parallel to the longitudinal axis of the forearm. Fresh fabric samples were used for each test. To keep the measurements consistent for each subject and guide the measurements for skin physiology, the test skin area was marked with washable ink (only the boundary, not affecting the test area). The subject was instructed to keep the arm still during the test. The friction test was carried out on the left arm and right arm alternatively to give enough time for the skin to recover from the previous friction test. Two subjects were tested on the right arm only because it was uncomfortable for them to keep the left volar forearm flat and the arm would rotate during the friction test. The interval time between two tests on the same skin region was 10 minutes to allow the skin to recover (no skin redness observed, low TEWL value). The eight fabric samples were tested in random order.

5.3.3 Statistical Analysis

All statistical analyses were performed with SPSS (IBM, U.S.A.). All data were tested for normal distribution and homogeneity of variance using the Shapiro-Wilk test and Levene's test respectively. To assess if there was a significant difference between neutral and warm environments, a paired t-test was used for ΔTEWL and Δa* respectively. The distribution of the differences in friction between fabrics was not normally distributed so the nonparametric Wilcoxon Signed Rank test was used to identify significant differences between neutral and warm environments. The skin sensation data were ordinal therefore the nonparametric Wilcoxon Signed Rank test was used as well. Repeated measures ANOVA tests were used to analyze whether there were significant differences in ΔTEWL and Δa* in both environments as well as the friction in the warm environment between fabric samples. Data were tested for sphericity and if the sphericity assumption was violated, the Greenhouse-Geisser corrections were taken. The main effects and pairwise comparisons were based on estimated marginal means. When a significant main effect was found, the Bonferroni post-hoc analyses were used to assess the difference between each pair of fabrics. When the Bonferroni correction did not show where the differences occurred, the least significant difference (LSD) test was conducted to do pairwise comparisons. The effect of fabric on friction in the neutral environment and the skin sensation ratings in both environments were analyzed using nonparametric tests and the Friedman test was performed with the Dunn-Bonferroni post hoc test for pairwise comparison. To explore the relationships between different variables, linear regression analyses were performed using data from the group means with standard errors. A P value <0.05 was recognized as statistically significant.

5.4 Results and Discussion

5.4.1 Surface roughness and friction in neutral and warm environments

The friction force between the skin and eight nonwoven fabrics in the neutral and warm environments are shown in Figure 5. 4. The friction was significantly ($P<0.001$) higher in the warm environment than in the neutral environment, corresponding to what has been reported in the literature [6][5][59]. On average, the friction force in the warm environment was 2 to 5 times larger than it in a neutral environment. The increased friction is likely caused by more sweat produced by the skin in the warm environment. The production of sweat can increase the skin hydration that softens and plasticizes the skin surface. The softened skin is more compliant that can lead to an increase of contact area [5][60][61]. The sweat on the skin surface can also facilitate the formation of capillary bridges on the interface that can increase the adhesion force [62][63]. In addition, a higher environment temperature tends to cause a slightly lower skin pH because of the sweat secretion caused by increased skin temperature [64]. It has been reported a lower pH of lubricants applied to the skin surface could cause higher friction as well [14]. The fabric surfaces were all made of polypropylene and polyethylene that have a negative surface charge while the skin surface would tend to become more positive when the pH is smaller than 5. The attraction between the two surfaces could then become stronger because of an enhanced electrostatic effect [65].

A linear positive relationship ($r^2=0.81$, $p<0.001$) was observed between friction and surface roughness measured by KES in the neutral environment so a higher surface roughness tended to cause higher friction. This would be the result of the plowing interaction that the skin and the surface asperities of fabric are embedded into each other, and higher amplitude of asperities can increase the resistance force during the sliding movement [25]. However, this relationship did not present in the warm environment (Figure 5. 5). The topsheet fabrics with relatively low surface

roughness caused about the same friction to the very rough fabrics. It is known that the liquid on the interface may increase the adhesion force [66][67]. The sweat on the skin produced in the warm environment may have altered the interaction between the two surfaces due to a larger contribution of the adhesion force. That may explain the changes in the relationship between the surface roughness and friction compared to the neutral environment. In addition, it is noticeable that the relationship was highly influenced by the two rough fabrics, M1 and M2. The linear relationship was absent when excluding the two rough fabrics. The topsheet smooth fabrics performed similarly.

In the neutral environment, the roughest fabric M1 showed statistically significantly higher friction than the other fabrics ($P<0.02$) except for fabric PE3($P=0.086$) and M2($P=1$). Fabric M2 showed significantly higher friction than fabrics C1($P<0.001$), C2($P=0.001$), and PP3($P=0.001$) but there was no significant difference($P=0.069$) between friction across all the fabrics in the warm environment. This indicated the significant difference in friction between rough fabrics and smooth fabrics did not exist in the warm environment. In addition, the ratio of the friction in the warm environment to the friction in the neutral environment showed the smooth fabric had a much higher increase in friction than the rough fabric (M1 and M2) when the ambient condition changed from neutral to warm (Figure 5. 6). The possible reason for the increased friction of smooth fabrics would be that the smooth fabric was more affected by the capillary adhesion and electrical attraction because of a bigger contact area[68] and a closer average distance between the fabric and skin surface compared to the rough fabrics. The rough fabric can reduce the formation of capillary bridging and separate the interfaces because of the “valleys” and “hills” on the surface so it can be less influenced by the adhesion friction[27][66]. From this point of view, higher friction could be generated by either a rough fabric or a smooth fabric which may be altered in different environments due to the contribution of adhesion force. The high friction in the warm environment

of smooth fabrics could then be attributed to a high adhesion force while the rough fabrics were less influenced by the adhesion because of bigger separation between the skin and fabric surface.

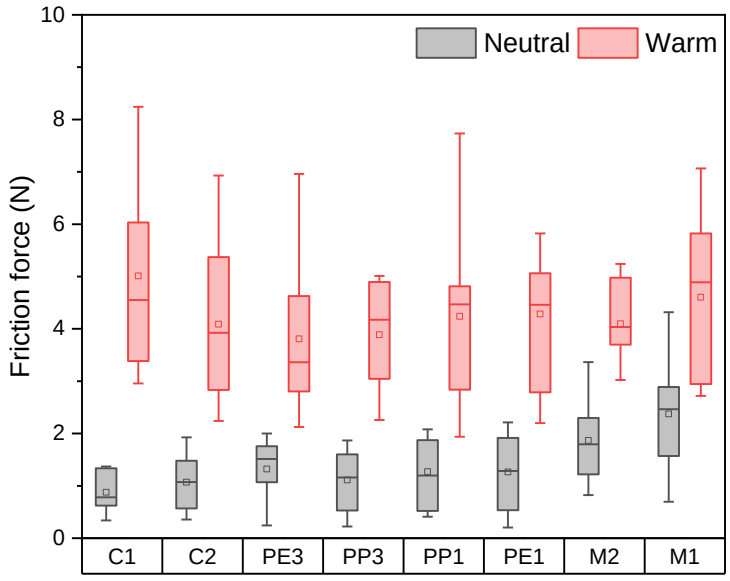

Figure 5.4. Friction of different fabrics in neutral and warm environments. The fabrics are ranked by surface roughness (C1-the lowest roughness to M1-the highest roughness). The length of the box is the interquartile range (25% to 75%). The upper whisker and lower whisker are determined by the 5th and 95th percentiles, respectively. The line in the box is the median mark. The hollow square is the mean value.

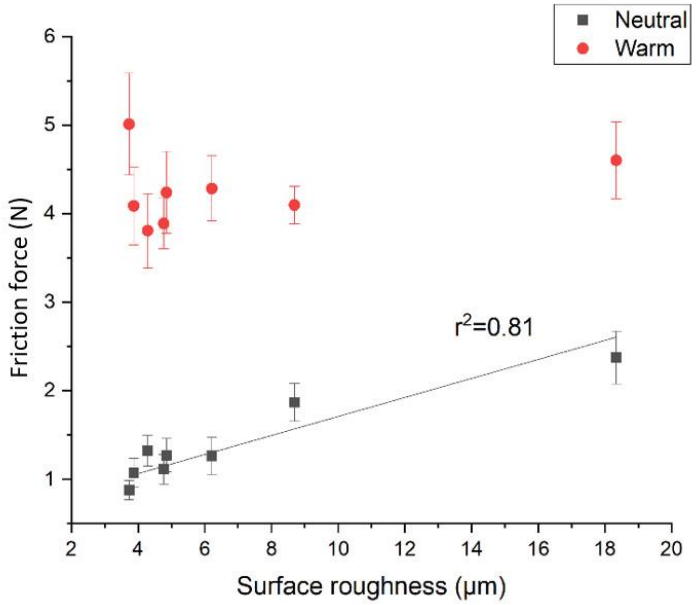

Figure 5.5. Relationship between surface roughness (x-axis) of fabrics and friction force (y-axis) in neutral and warm environments. The error bar is the standard error of the friction force measured on 11 subjects.

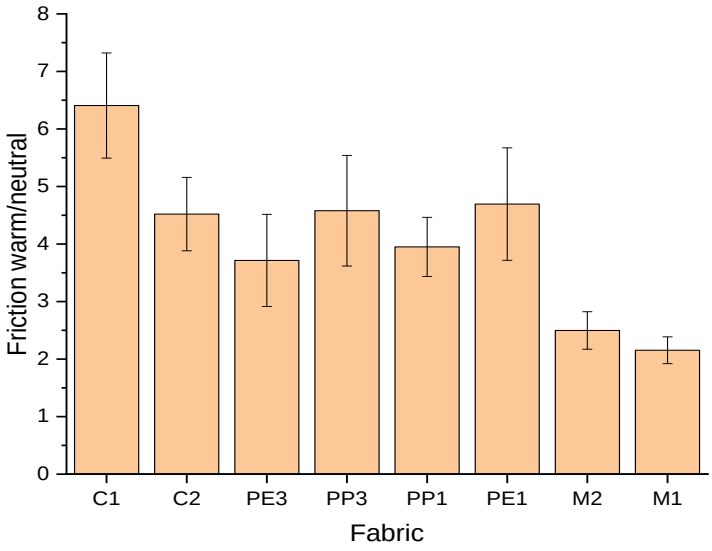

Figure 5.6. The ratio (mean±SE) of friction force in the warm environment to the friction force in the neutral environment for each fabric. The fabrics are ranked by surface roughness (C1-the lowest roughness to M1-the highest roughness). The error bar is the standard error of the ratio of friction force in the warm environment to the friction force in the neutral environment obtained from the 11 subjects.

5.4.2 Skin physiology in neutral and warm environments

The TEWL and skin redness measurements in this study were able to demonstrate the physiological changes quantitatively. Figure 5. 7 shows the change of TEWL after friction for different fabrics. The results showed a general increase of the TEWL after the friction test both in the neutral and warm environments (paired t-test for the TEWL before and after the friction test showed there was a statistically significant increase of the TEWL after friction test, in both environments $P<0.001$). In the neutral environment, the increase of TEWL ranged from 0 $g/m^2/h$ to 5 $g/m^2/h$ while the majority of the data were distributed between 0 $g/m^2/h$ and 20 $g/m^2/h$ in the warm environment. The increase of TEWL value in the warm environment was significantly ($P< 0.001$) higher than that in the neutral environment. This indicated the friction would cause more water loss from the skin, especially in the warm environment. However, one limitation was the higher increase of TEWL in the warm environment may have been due to the high production of sweat which may also lead to higher TEWL measurements. The change of TEWL was used to reduce the interference, but the sweat might still influence the assessment of the actual impact of friction on the skin barrier function and obscure the relationship between ΔTEWL and friction.

The linear relationship between ΔTEWL and frictional force only approached the significance in the neutral environment ($r^2=0.45$, $p = 0.007$) and showed no linear relationship in the warm environment (Figure 5. 8). In the warm environment, both the roughest and the smoothest fabric caused high friction but the smoothest fabric caused much less change of TEWL than the roughest fabric. This suggests a higher frictional force does not necessarily mean a higher impact on skin barrier function in the warm environment. Nevertheless, the surface roughness presented a relationship with ΔTEWL in both environments (neutral environment: $r^2=0.68$, $p=0.01$, warm environment: $r^2=0.81$, $p=0.002$) (Figure 5. 8) so the surface roughness played a bigger role than

frictional force in influencing the skin barrier function. In addition, there were no significant differences between the topsheet fabrics. The only significant differences between fabrics occurred between the rough fabrics, M1 and M2, and some of the smoother topsheet fabrics (Table 5. 2), which indicate the rough fabrics can cause a significantly higher impact on the skin barrier function than the topsheet fabrics regardless of the environments.

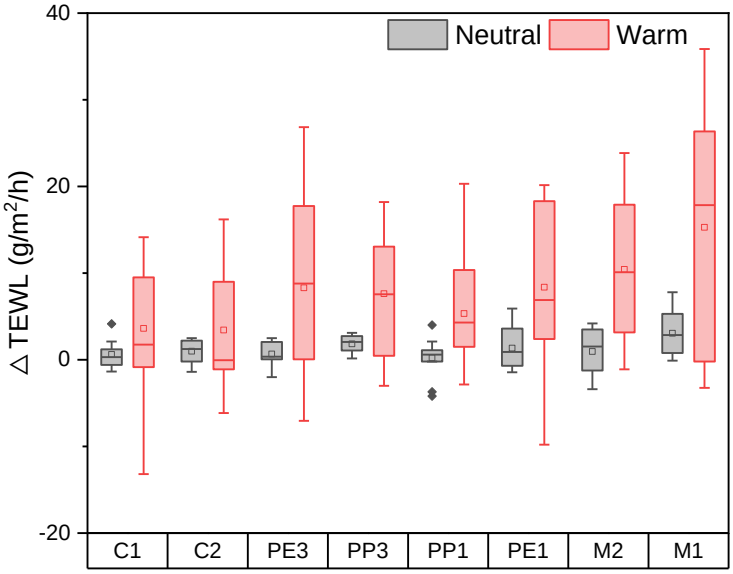

Figure 5.7. Change of TEWL after friction test of different fabrics in neutral and warm environments. The fabrics are ranked by surface roughness (C1-the lowest roughness to M1-the highest roughness). The length of the box is the interquartile range (25% to 75%). The upper whisker and lower whisker are determined by the 5th and 95th percentiles respectively. The line in the box is the median mark. The hollow square is the mean value and the solid dot are outliers.

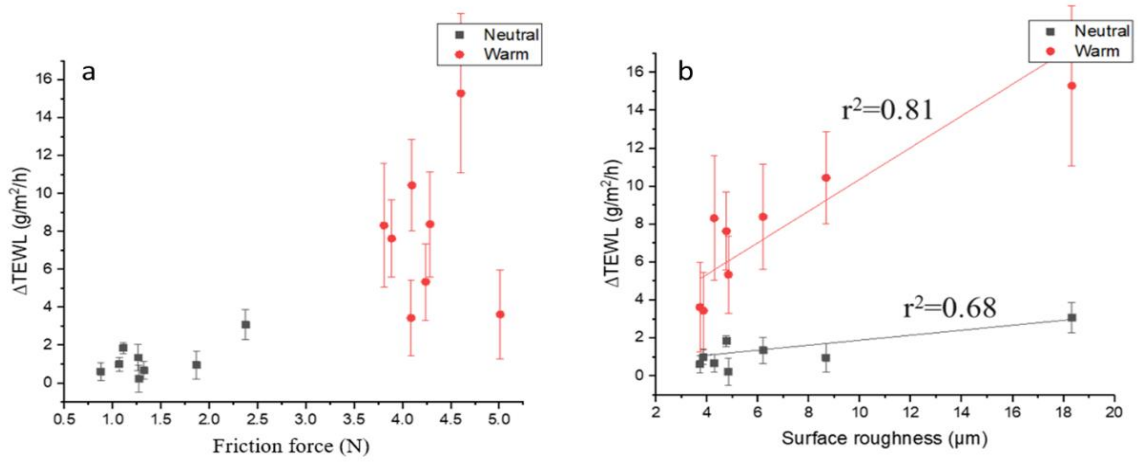

Figure 5.8. Graph a: the relationship between friction force and the change of TEWL value in the neutral and warm environment. Graph b: the relationship between surface roughness and the change of TEWL value in the neutral and warm environment.

Table 5.2. Significant differences between rough (M1, M2) and smooth topsheet fabrics (there were no significant differences between rough fabrics or between smooth topsheet fabrics).

Sample 1-Sample 2	ΔTEWL		Δa*	
	Neutral	warm	neutral	warm
M1-C1	0.025*	0.012*	0.027*	0.006**
M1-C2	0.023*	0.009**	-	0.026*
M1-PE1	-	-	0.041*	0.009**
M1-PE3	0.021*	-	-	0.002**
M1-PP1	0.018*	0.03*	-	0.004**
M1-PP3	-	-	0.001**	0.003**
M2-C1		-		
M2-C2		0.006**		
M2-PE1		-		
M2-PE3	-	-	-	-
M2-PP1		0.022*		
M2-PP3		-		

*Significant at the 0.05 level. **Significant at the 0.01 level.

The measurement of skin redness change after friction is shown in Figure 5. 9. The environment did not present a significant influence on the change of skin redness (P=0.515). In other words, the increased friction in the warm environment did not lead to a higher increase in skin redness (also no significant difference (P=0.19) between the initial a* value of the neutral and warm environment). On average, friction presented a linear relationship (r^2=0.86, p=0.003) to the Δa* in the neutral environment whereas no relationship was observed in the warm environment (Figure 5. 10). Similar to the ΔTEWL in the warm environment, both the smoothest and roughest fabric caused high friction but the smoothest fabric did not lead to a high impact on skin redness as the roughest fabric did. The surface roughness showed stronger relationship to Δa* in both environments (neutral: r^2=0.86, p<0.001, warm: r^2=0.96, p<0.001). However, the linear relationships were highly dominated by the two rough fabrics since all the topsheet fabrics had an indistinguishable influence on skin redness. The differences between fabrics (Table 5. 2) suggests the roughest fabric M1 had a prominent influence on skin redness, especially in the warm environment.

Considering the significant larger impact of rough fabrics on TEWL and skin redness than smooth topsheet fabrics, the impact on skin physiology may come from a deeper interaction between fabric and skin such as plowing effects, which can cause stresses and strains on deeper tissues other than a superficial abrasion only [69]. This suggests the deformation friction could have a big impact on skin physiology. In addition, the smoothest fabric showed high friction but a lower impact on skin physiology than the rough fabric in the warm environment. Since the increase of friction for smooth fabric is likely caused by the dominate contribution of adhesion force, it indicates the adhesion force may have very limited effects on skin barrier function and redness while the larger proportion of deformation component of friction for the interaction between skin

and rough fabrics can impact more on the skin physiology. Therefore, a separation of adhesion and deformation force may give a better indicator of the impact on skin physiology condition than the total friction. Furthermore, there can be limitations by using linear regression to explore the relationships between friction and skin physiological changes because the effects of friction on the skin could have a threshold and not perform linearly. In this study, the effects were artificially controlled to avoid skin damages and injuries for subjects which limited the range of skin physiology changes. In reality, the effects and relationships could change with a different surface roughness range, higher normal load, or longer contact time if a physiological threshold exists and the effects of friction reach and exceed the threshold.

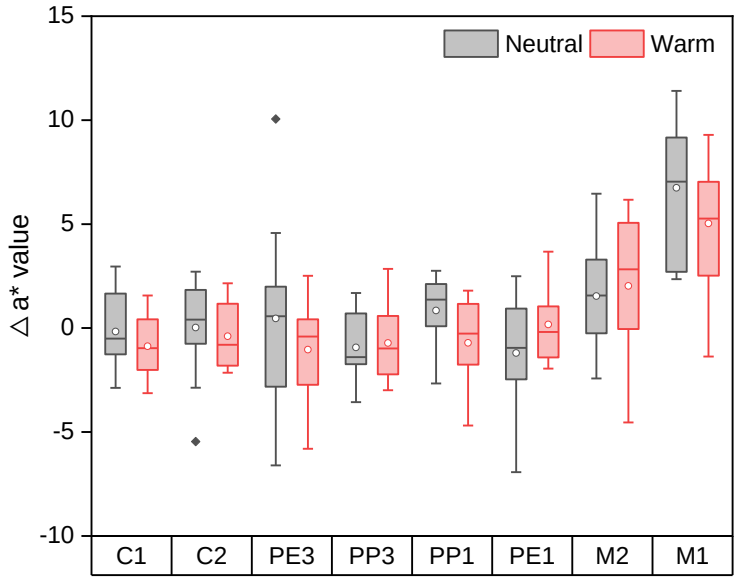

Figure 5.9. Change of skin redness after friction test of different fabrics in neutral and warm environments. The fabrics are ranked by surface roughness (C1-the lowest roughness to M1-the highest roughness). The length of the box is the interquartile range (25% to 75%). The upper whisker and lower whisker are determined by the 5th and 95th percentiles respectively. The line in the box is the median mark. The hollow square is the mean value and the solid dot are outliers.

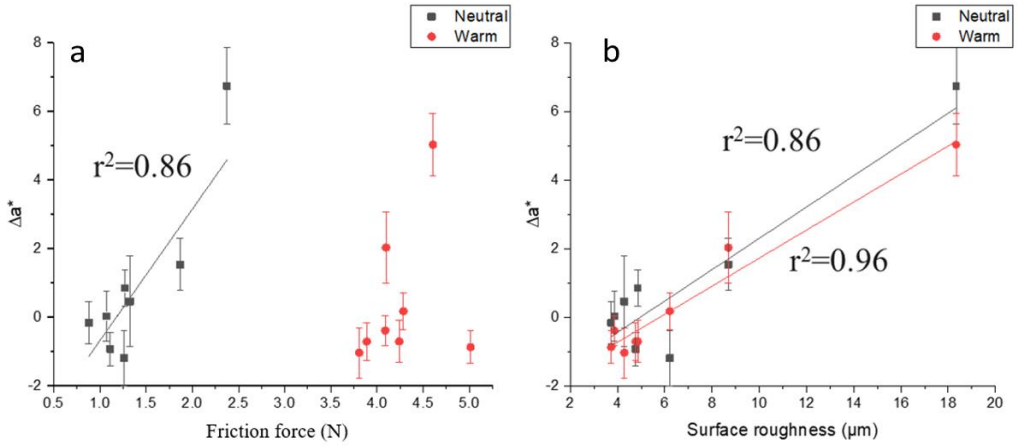

Figure 5.10. Graph a: the relationship between friction and the change of skin redness in the neutral and warm environment. Graph b: the relationship between surface roughness and the change of skin redness in the neutral and warm environment.

5.4.3 Skin sensation in neutral and warm environments

The skin sensation was significantly ($P<0.001$) more pleasant in the neutral environment than in the warm environment (Figure 5. 11). The rough fabrics were unpleasant in both environments while all the topsheet fabrics were perceived pleasant in the neutral environment but approached the neutral sensation (neither pleasant nor unpleasant) in the warm environment. The differences between the neutral environment and warm environment were also significant for localized sensation ($P=0.001$), texture sensation ($P<0.001$), and stickiness sensation ($P<0.001$) but not for the wetness sensation ($P=0.098$). Thus, the absence of pleasant sensation of topsheet fabrics in the warm environment was accompanied by a localized tickle sensation, the absence of smooth sensation, and a slightly sticky sensation. The wetness sensation was not affected.

A negative linear relationship ($r^2=0.88$, $P<0.001$) between pleasantness sensation and friction was displayed in the neutral environment only. In the warm environment, the smoothest fabric had high friction similar to the roughest fabric, but it was perceived as much less unpleasant. Nevertheless, a linear relationship between surface roughness and pleasantness sensation was

displayed in both neutral (r^2=0.87, P<0.001) and warm environments (r^2=0.78, P=0.003) (Figure 5. 12). Friction and surface roughness showed a comparable correlation to pleasantness sensation in the neutral environment that corresponded with the linear relationship between them in the neutral environment, but friction did not indicate the pleasantness sensation in the warm environment. In addition, the texture sensation presented a very strong relationship to the pleasantness sensation (neutral: r^2=0.97, P<0.001; warm: r^2=0.98, P<0.001) (Figure 5. 13). This suggests the texture sensation is important for the assessment of pleasantness. A higher sensation of roughness can diminish the pleasantness sensation significantly, which agrees with what Raccuglia et al. reported [31]. Furthermore, this indicates the KES surface roughness measurement method did not correlate well with the texture sensation of human subjects for these nonwoven fabrics. Since the KES surface roughness measurement mimics the finger touch, the texture sensation can be different between the fingers and skin of volar forearms because of different surface topography. In addition, the texture sensation relates to several sensations like softness and coldness so the measurement of roughness only might decrease the correlation to the complex texture sensation [70]. The KES surface roughness measurement may need to be revised and be improved to match the texture sensation better, and then the surface roughness measurement could play a bigger role to predict the pleasantness sensation.

There were no significant differences between rough fabrics M1 and M2, and between topsheet fabrics for all the sensations in both neutral and warm environments but by comparing to rough fabrics, the smoothest fabrics had relatively higher tickle sensation in the neutral environment and relatively higher stickiness sensation than the other topsheet fabrics in the warm environment. The rough fabrics were sensed rougher and less pleasant in both environments but they caused less wetness and stickiness sensation than some topsheet fabrics in the warm

environment. If the roughness could represent the contribution of deformation force in total friction as mentioned before, it indicates the deformation effects would influence texture and pleasantness sensation while the adhesion effects raised by smooth fabrics are likely to cause stickiness and wetness sensation. The relative differences between smooth topsheet fabrics are likely to be influenced by the surface roughness as well as fabric material and structure but cannot only be explained by the friction measured on human subject skin.

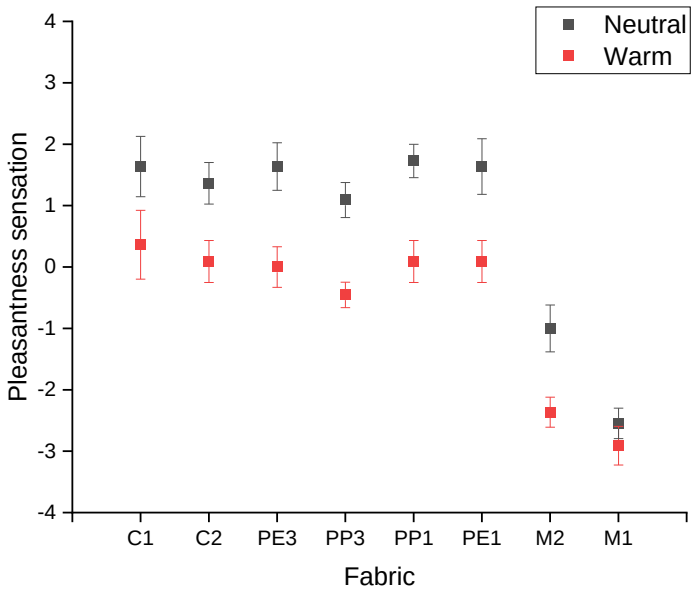

Figure 5.11. Pleasantness sensation of fabrics in neutral and warm environments. The fabrics are ranked by surface roughness (C1-the lowest roughness to M1-the highest roughness). Pleasantness scale: 0-neutral, positive side- increase in pleasantness, negative side- increase in unpleasantness.

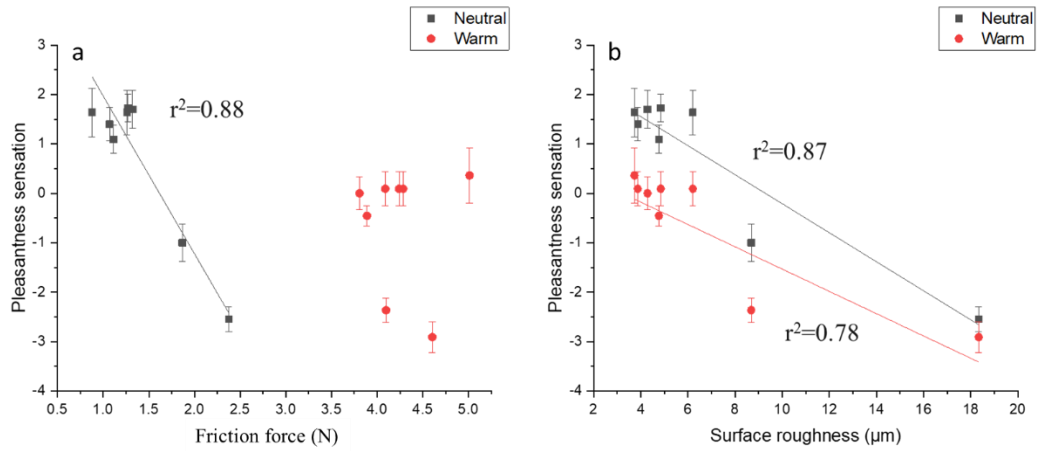

Figure 5.12. Graph a: the relationship between friction force and pleasantness sensation. Graph b: the relationship between surface roughness and pleasantness sensation (0-neutral, positive side- increase in pleasantness, negative side- increase in unpleasantness).

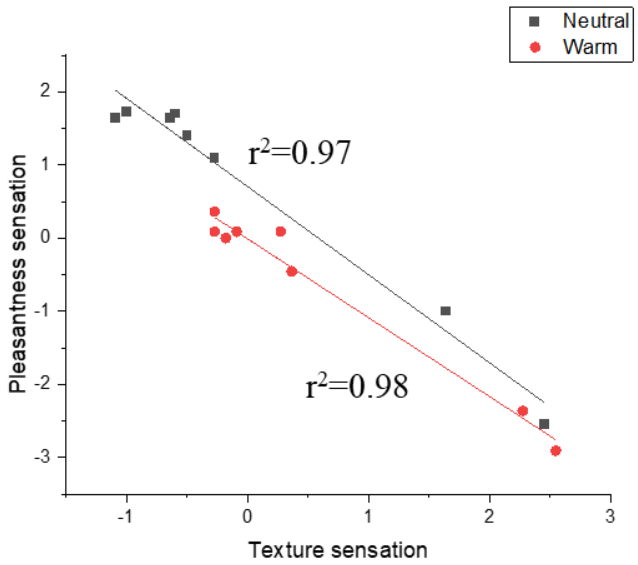

Figure 5.13. Relationship between texture sensation (negative side-smooth, positive side-rough) and pleasantness sensation (negative side- unpleasantness, positive side- pleasantness) in neutral and warm environments.

5.4.4 Relationship between skin physiology and pleasantness sensation

It was found there was a negative relationship between pleasantness sensation and TEWL changes as well as the skin redness change regardless of the environment (Figure 5. 14). The relationship was more significant for the warm environment than the neutral environment for both ΔTEWL (warm: r^2=0.76, P=0.005; neutral: r^2=0.56, P=0.03) and Δa* (warm: r^2=0.86, P<0.001; neutral: r^2=0.78, P=0.004) . This indicates a less pleasant sensation tends to correlate with a higher water loss from the skin and redder skin especially in a warm environment, and thus it would be correlated with physiological changes. This suggests our perception could be a precaution signal even though individuals may not be aware of the effects on their skin health condition. When there is less pleasantness sensation, it is more likely that there is a negative impact on skin physiology even though the impact cannot be seen by the naked eye and no pain is perceived. This can be recognized as a protection mechanism of our body. In addition, the methodology in this study proposed a way to quantify the physiological effects before skin damage happens. It showed a potential for early detection which can help to take corrective actions to prevent skin damages.

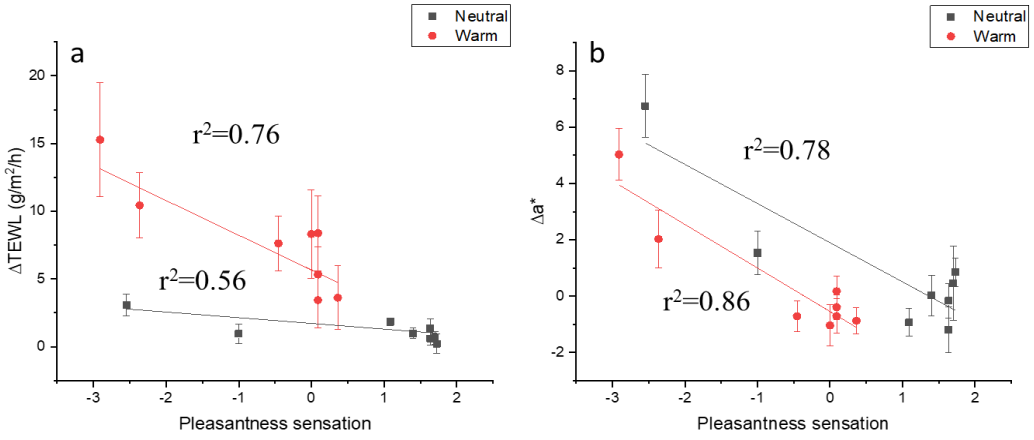

Figure 5.14. Graph a: the relationship between pleasantness sensation (positive side- pleasantness, negative side- unpleasantness) and TEWL change (bigger value, more transepidermal water loss) in the neutral and warm environment. Graph b: the relationship between pleasantness sensation and a* value change (i.e. skin redness change) in the neutral and warm environment.

5.5 Discussion

This study showed higher friction did not necessarily cause a higher impact on skin physiology and sensation. The rougher surface showed a higher impact than the smooth surface on the skin when they had comparable friction force. Based on this observation, we speculated this difference was caused by a different contribution of adhesion and deformation friction to smooth and rough surfaces. The effects of adhesion friction and deformation friction on skin physiology and sensation might be different. However, we did not directly evaluate the adhesion and deformation friction in this study such as the formation of capillary bridging on the interface. Further investigation should be done to demonstrate the contribution of adhesion and deformation friction of fabrics with varying roughness and correspond to the effects on skin physiology and sensation.

The topsheet nonwoven fabrics used in this study showed a pleasant skin sensation can be promising in the neutral environment for the contact between skin and the topsheet fabric but the warm environment can significantly decrease the pleasantness with more vulnerable skin barrier caused by rubbing. This indicates the improvement of absorbent hygiene products should focus more on their performance on skin comfort in high temperature and humid environments. Since the skin condition can be influenced by many factors such as age and gender, the effects on different groups of people should be further investigated. In addition, the performance of topsheet fabrics in this study was not significantly distinguishable. More various topsheet fabrics should be investigated and evaluation of them may need to be more sensitive including the evaluation of skin physiology, sensation, and the measurement of fabric surface profile.

5.6 Conclusions

The performance of nonwoven fabrics in terms of skin physiology and sensation was studied in neutral and warm environments through friction on human subject skin. In the tested surface roughness range (3μm to 20μm, measured by Kawabata Evaluation System) of nonwoven fabrics, higher surface roughness can cause higher friction in the neutral environment, but this relationship did not remain in the warm environment. The warm environment can cause higher friction, more loss of water from the skin surface, reduced pleasantness sensation, but not influence the change of skin redness. Fabric surface roughness has a strong relationship with the impact on skin physiology and sensation. Since there is a positive linear relationship between surface roughness and friction, both higher roughness and friction tend to cause a higher impact on skin physiology and sensation in the neutral environment, but higher friction in the warm environment is not necessarily bound up with higher influence on skin physiology and sensation. In the warm environment, a smooth fabric can have less impact on the skin physiology condition and be less unpleasant than the rough fabric even though they have the same high friction. It is proposed that when the smooth and rough fabrics have the same friction, the deformation component will be larger on the rough fabric than on the smooth fabric. The higher deformation component of friction tends to cause larger effects on skin physiology and sensation, while the adhesion force is dominant in the smooth fabric friction and this has smaller effects on skin physiology and sensation.

The nonwoven fabrics used for the topsheet of absorbent hygiene products with a roughness range between 3μm and 7μm are sensed pleasant and have small impacts on skin physiology in the neutral environment. However, the warm environment can cause a significant increase of transepidermal water loss and reduction in pleasantness sensation with more tickle sensation, less smooth sensation, and slightly sticky sensation; it does not affect the wetness

sensation though. The topsheet nonwoven fabrics are not significantly distinguishable for their performance of skin physiology and sensation, and the linear relationships between skin friction, surface roughness, and skin sensation are highly dominated by rough fabrics and fit less well for the topsheet fabrics within a small surface roughness range. However, the strong correlation between texture sensation and pleasantness sensation suggests a distinguishable texture of topsheet fabrics could provide a distinctive pleasantness sensation.

The significant physiological changes were able to be measured and associated with subjective sensation. The negative relationship between pleasantness sensation and skin physiology suggests the sensation can be a precaution signal for the adverse effects on the skin health conditions. These methods could be further explored and refined to detect early levels of skin damages and predict skin discomfort.

5.7 References

[1] U. Blume-Peytavi and V. Kanti, “Prevention and treatment of diaper dermatitis,” *Pediatr. Dermatol.*, vol. 35, pp. s19–s23, Mar. 2018.

[2] H. Beele, S. Smet, N. Van Damme, and D. Beeckman, “Incontinence-Associated Dermatitis: Pathogenesis, Contributing Factors, Prevention and Management Options,” *Drugs and Aging*, vol. 35, no. 1, pp. 1–10, Jan. 2018.

[3] M. Saadatmand *et al.*, “Skin hydration analysis by experiment and computer simulations and its implications for diapered skin,” *Ski. Res. Technol.*, vol. 23, no. 4, pp. 500–513, Nov. 2017.

[4] M. Igaki, T. Higashi, S. Hamamoto, S. Kodama, S. Naito, and S. Tokuhara, “A study of the behavior and mechanism of thermal conduction in the skin under moist and dry heat conditions,” *Ski. Res. Technol.*, vol. 20, no. 1, pp. 43–49, Feb. 2014.

[5] M. Klaassen, D. J. Schipper, and M. A. Masen, “Influence of the relative humidity and the temperature on the in-vivo friction behaviour of human skin,” *Biotribology*, vol. 6, pp. 21–28, Jun. 2016.

[6] A. R. Gwosdow, J. C. Stevens, L. G. Berglund, and J. A. J. Stolwijk, “Skin Friction and Fabric Sensations in Neutral and Warm Environments,” *Text. Res. J.*, vol. 56, no. 9, pp. 574–580, 1986.

[7] M. Geerligs, C. Oomens, P. Ackermans, F. Baaijens, and G. Peters, “Linear shear response of the upper skin layers,” *Biorheology*, vol. 48, no. 3–4. pp. 229–245, 2011.

[8] M. Klaassen, E. G. de Vries, and M. A. Masen, “Friction in the contact between skin and a soft counter material: effects of hardness and surface finish,” *J. Mech. Behav. Biomed. Mater.*, Jan. 2019.

[9] D. J. Atherton, “Understanding irritant napkin dermatitis,” *Int. J. Dermatol.*, vol. 55, pp. 7–9, Jul. 2016.

[10] I. L. Ciesielska-Wróbel and L. Van Langenhove, “The hand of textiles – definitions, achievements, perspectives – a review,” *Text. Res. J.*, vol. 82, no. 14, pp. 1457–1468, Sep. 2012.

[11] R. E. Zimmerer, K. D. Lawson, and C. J. Calvert, “The Effects of Wearing Diapers on skin,” *Pediatr. Dermatol.*, vol. 3, pp. 95–101, 1986.

[12] P. F. D. NAYLOR, “Experimental Friction Blisters,” *Br. J. Dermatol.*, vol. 67, no. 10, pp. 327–342, Oct. 1955.

[13] J. A. Greenwood and D. Tabor, “The friction of hard sliders on lubricated rubber: The importance of deformation losses,” *Proc. Phys. Soc.*, vol. 71, no. 6, pp. 989–1001, 1958.

[14] M. J. Adams, B. J. Briscoe, and S. A. Johnson, “Friction and lubrication of human skin,” *Tribol. Lett.*, vol. 26, no. 3, pp. 239–253, Apr. 2007.

[15] M. F. Leyva-Mendivil, J. Lengiewicz, and G. Limbert, “Skin friction under pressure. the role of micromechanics,” *Surf. Topogr. Metrol. Prop.*, vol. 6, no. 1, p. 014001, Jan. 2018.

[16] S. Derler and L.-C. Gerhardt, “Tribology of Skin: Review and Analysis of Experimental Results for the Friction Coefficient of Human Skin,” *Tribol. Lett.*, vol. 45, no. 1, pp. 1–27, Jan. 2012.

[17] K. B. Duvefelt, U. L. O. L.-O. Olofsson, and C. M. J. Johannesson, “Towards simultaneous measurements of skin friction and contact area: Results and experiences,” *Proc. Inst. Mech. Eng. Part J J. Eng. Tribol.*, vol. 229, no. 3, pp. 230–242, Mar. 2015.

[18] D. Mahdi, A. Riches, M. Gester, J. Yeomans, and P. Smith, “Rolling and sliding: Separation of adhesion and deformation friction and their relative contribution to total friction,” *Tribol. Int.*, vol. 89, pp. 128–134, Sep. 2015.

[19] S. Derler, M. Preiswerk, G.-M. Rotaru, J.-P. Kaiser, and R. M. Rossi, “Friction mechanisms and abrasion of the human finger pad in contact with rough surfaces,” *Tribol. Int.*, vol. 89, pp. 119–127, Sep. 2015.

[20] A. Klöcker, M. Wiertlewski, V. Théate, V. Hayward, and J. L. Thonnard, “Physical factors influencing pleasant touch during tactile exploration,” *PLoS One*, vol. 8, no. 11, pp. 1–9, Nov. 2013.

[21] W. Kim, Y. Lee, J. H. Lee, G. W. Shin, and M. H. Yun, “A comparative study on designer and customer preference models of leather for vehicle,” *Int. J. Ind. Ergon.*, vol. 65, pp. 110–121, May 2018.

[22] S. Chen and S. Ge, “Experimental research on the tactile perception from fingertip skin friction,” *Wear*, vol. 376–377, pp. 305–314, Apr. 2017.

[23] S. Derler, R. M. Rossi, and G. M. Rotaru, “Understanding the variation of friction coefficients of human skin as a function of skin hydration and interfacial water films,” *Proc. Inst. Mech. Eng. Part J J. Eng. Tribol.*, vol. 229, no. 3, pp. 285–293, 2015.

[24] J. van Kuilenburg, M. A. Masen, and E. van der Heide, “A review of fingerpad contact mechanics and friction and how this affects tactile perception,” *Proc. Inst. Mech. Eng. Part J J. Eng. Tribol.*, vol. 229, no. 3, pp. 243–258, Mar. 2015.

[25] W. Li, M. L. Zhan, Q. Y. Yu, B. Y. Zhang, and Z. R. Zhou, “Quantitative assessment of friction perception for fingertip touching with different roughness surface,” *Biosurface and Biotribology*, vol. 1, no. 4, pp. 278–286, Dec. 2015.

[26] C. P. Hendriks and S. E. Franklin, “Influence of surface roughness, material and climate conditions on the friction of human skin,” *Tribol. Lett.*, vol. 37, no. 2, pp. 361–373, Feb. 2010.

[27] O. S. Dinç, C. M. Ettles, S. J. Calabrese, and H. A. Scarton, “Some parameters affecting tactile friction,” *J. Tribol.*, vol. 113, no. 3, pp. 512–517, Jul. 1991.

[28] A. Emblem and M. Hardwidge, “Adhesives for packaging,” in *Packaging Technology*, Elsevier, 2012, pp. 381–394.

[29] H. Yokura and M. Niwa, “Objective Hand Measurement of Nonwoven Fabrics Used for the Top Sheets of Disposable Diapers,” *Int. J. Cloth. Sci. Technol.*, vol. 12, no. 3, pp. 184–192, 2003.

[30] M. MATSUDAIRA, J. YOSHIDA, and T. KINARI, “Objective and Subjective Handle Evaluation for Disposable Diaper’s Top Sheets and Reusable Diaper’s Fabrics,” *J. Text. Eng.*, vol. 53, no. 2, pp. 53–57, 2007.

[31] Raccuglia *et al.*, “Human wetness perception of fabrics under dynamic skin contact,” *Text. Res. J.*, vol. 88, no. 19, pp. 2155–2168, 2018.

[32] Q. Zhang, M. Murawsky, T. LaCount, G. B. Kasting, and S. K. Li, “Transepidermal water loss and skin conductance as barrier integrity tests,” *Toxicol. Vitr.*, vol. 51, pp. 129–135, Sep. 2018.

[33] V. Rogiers, “EEMCO Guidance for the Assessment of Transepidermal Water Loss in Cosmetic Sciences,” *Skin Pharmacol. Appl. Skin Physiol.*, vol. 14, no. 2, pp. 117–128, 2001.

[34] J. du Plessis *et al.*, “International guidelines for the *in vivo* assessment of skin properties in non-clinical settings: Part 2. transepidermal water loss and skin hydration,” *Ski. Res. Technol.*, vol. 19, no. 3, pp. 265–278, Aug. 2013.

[35] L. Ludriksone, N. Garcia Bartels, V. Kanti, U. Blume-Peytavi, and J. Kottner, “Skin barrier function in infancy: a systematic review,” *Arch. Dermatol. Res.*, vol. 306, no. 7, pp. 591–599, Sep. 2014.

[36] G. N. Stamatas, C. Zerweck, G. Grove, and K. M. Martin, “Documentation of Impaired Epidermal Barrier in Mild and Moderate Diaper Dermatitis In Vivo Using Noninvasive Methods,” *Pediatr. Dermatol.*, vol. 28, no. 2, pp. 99–107, Mar. 2011.

[37] A. R. Matias, M. Ferreira, P. Costa, and P. Neto, “Skin colour, skin redness and melanin biometric measurements: Comparison study between Antera 3D, Mexameter and Colorimeter,” *Ski. Res. Technol.*, vol. 21, no. 3, pp. 346–362, Aug. 2015.

[38] S. Borkowski, “Diaper Rash Care and Management,” *Pediatr. Nurs.*, vol. 30, no. 6, pp. 467–70, 2004.

[39] G. N. Stamatas and N. K. Tierney, “Diaper Dermatitis: Etiology, Manifestations, Prevention, and Management,” *Pediatr. Dermatol.*, vol. 31, no. 1, pp. 1–7, Jan. 2014.

[40] S. Bağlam and B. Engin, “Diaper (napkin) dermatitis: A fold (intertriginous) dermatosis,” *Clin. Dermatol.*, vol. 33, no. 4, pp. 477–482, Jul. 2015.

[41] R. P. Chilcott and R. Farrar, “Biophysical measurements of human forearm skin in vivo: Effects of site, gender, chirality and time,” *Ski. Res. Technol.*, vol. 6, no. 2, pp. 64–69, 2000.

[42] I. D. Stephen, M. J. Law Smith, M. R. Stirrat, and D. I. Perrett, “Facial skin coloration affects perceived health of human faces,” *Int. J. Primatol.*, vol. 30, no. 6, pp. 845–857, 2009.

[43] M. Nischik and C. Forster, “Analysis of skin erythema using true-color images,” *IEEE Trans. Med. Imaging*, vol. 16, no. 6, pp. 711–716, 1997.

[44] M. Sommers, B. Beacham, R. Baker, and J. Fargo, “Intra- and inter-rater reliability of digital image analysis for skin color measurement,” *Ski. Res. Technol.*, vol. 19, no. 4, pp. 484–491, 2013.

[45] G. J. Pontrelli, “Comfort by Design,” *Text. Asia*, no. 21, pp. 52–61, 1990.

[46] F. J. Akin, J. T. Lemmen, D. L. Bozarth, M. J. Garofalo, and G. L. Grove, “A refined method to evaluate diapers for effectiveness in reducing skin hydration using the adult forearm,” *Ski. Res. Technol.*, vol. 3, no. 3, pp. 173–176, Aug. 1997.

[47] S. Kawabata and M. Niwa, “Objective Measurement of Fabric Mechanical Property and Quality: Its Application To Textile And Clothing Manufacturing,” *Int. J. Cloth. Sci. Technol.*, vol. 3, no. 1, pp. 7–18, 1991.

[48] O. Troynikov, E. Ashayeri, and F. K. Fuss, “Tribological evaluation of sportswear with negative fit worn next to skin,” *J. Eng. Tribol.*, vol. 226, no. 7, pp. 588–597, 2011.

[49] S. Asghari Mooneghi, S. Saharkhiz, and S. Mohammad Hosseini Varkiani, “Surface roughness evaluation of textile fabrics: A literature review,” *J. Eng. Fiber. Fabr.*, vol. 9, no. 2, pp. 1–18, 2014.

[50] H. Lim, “A review of spun bond process,” *J. Text. Apparel, Technol. Manag.*, vol. 6, no. 3, pp. 1–13, 2010.

[51] J. Rupp, “Spunbond & Meltblown Nonwovens,” *Text. World*, vol. 158, no. 3, 2008.

[52] H. Fuchs and W. Kittelmann, “Characteristics and application of nonwovens,” in *Nonwoven Fabrics: Raw Materials, Manufacture, Applicaion, Characteristics, Testing Processes*, 2003, pp. 489–493.

[53] J. R. Ajmeri and C. J. Ajmeri, “Nonwoven personal hygiene materials and products,” in *Applications of Nonwovens in Technical Textiles*, Woodhead Publishing, 2010, pp. 85–102.

[54] B. P. Subhash K. Batra, “Bonding technologies,” in *Introduction to nonwovens technology*, Lancaster, PA : Destech Publications, c2012., 2012, pp. 87–161.

[55] T. Karthik, R. Rathinamoorthy, and C. Karan Praba, “Nonwoven bonding techniques,” in *Nonwovens : process, structure, properties and applications*, 2016, pp. 95–150.

[56] B. S. Gupta and D. K. Smith, “Nonwovens in Absorbent Materials,” in *Absorbent Technology*, vol. 13, Elsevier, 2002, pp. 349–388.

[57] B. P. Subhash K. Batra, “Staple fiber-based technologies,” in *Introduction to nonwovens technology*, Lancaster, PA : Destech Publications, c2012., 2012, pp. 43–68.

[58] A. Fullerton, T. Fischer, A. Lahti, K.-P. Wilhelm, H. Takiwaki, and J. Serup, “Guidelines for measurement skin colour and erythema A report from the Standardization Group of the European Society of Contact Dermatitis *,” *Contact Dermatitis*, vol. 35, no. 1, pp. 1–10, 1996.

[59] N. K. Veijgen, M. A. Masen, and E. van der Heide, “Variables influencing the frictional behaviour of in vivo human skin,” *J. Mech. Behav. Biomed. Mater.*, vol. 28, pp. 448–461, Dec. 2013.

[60] S. Derler, L.-C. Gerhardt, A. Lenz, E. Bertaux, and M. Hadad, “Friction of human skin against smooth and rough glass as a function of the contact pressure,” *Tribiology Int.*, vol. 42, no. 11–12, pp. 1565–1574, Dec. 2008.

[61] L. C. Gerhardt, V. Strässle, A. Lenz, N. D. Spencer, and S. Derler, “Influence of epidermal hydration on the friction of human skin against textiles,” *J. R. Soc. Interface*, vol. 5, no. 28, pp. 1317–1328, Nov. 2008.

[62] S. E. Tomlinson, R. Lewis, X. Liu, C. Texier, and M. J. Carré, “Understanding the Friction Mechanisms Between the Human Finger and Flat Contacting Surfaces in Moist Conditions,” *Tribol. Lett.*, vol. 41, no. 1, pp. 283–294, Jan. 2011.

[63] M. Morales-Hurtado, E. G. de Vries, M. Peppelman, X. Zeng, P. E. J. van Erp, and E. van der Heide, “On the role of adhesive forces in the tribo-mechanical performance of ex vivo human skin,” *Tribol. Int.*, vol. 107, pp. 25–32, Mar. 2017.

[64] T. ABE, J. MAYUZUMI, N. KIKUCHI, and S. ARAI, “Sensonal Variations in Skin Temperature, Skin pH, Evaporative Wter Loss and Skin Surface Lipid Values on Human Skin,” *Chem. Pharm. Bull. (Tokyo).*, vol. 28, no. 2, pp. 387–392, 1980.

[65] S. A. Johnson, D. M. Gorman, M. J. Adams, and B. J. Briscoe, “The friction and lubrication of human stratum corneum,” *Tribol. Ser.*, vol. 25, no. C, pp. 663–672, Jan. 1993.

[66] H. M. Stanley, I. Etsion, and D. B. Bogy, “Adhesion of contacting rough surfaces in the presence of sub-boundary lubrication,” *J. Tribol.*, vol. 112, no. 1, pp. 98–104, Jan. 1990.

[67] C. Pailler-Mattéi and H. Zahouani, “Study of adhesion forces and mechanical properties of human skin in vivo,” *J. Adhes. Sci. Technol.*, vol. 18, no. 15–16, pp. 1739–1758, 2004.

[68] G. P. Chimata and C. J. Schwartz, “Investigation of friction mechanisms in finger pad sliding against surfaces of varying roughness,” *Biotribology*, vol. 3, pp. 11–19, Sep. 2015.

[69] T. Jee and K. Komvopoulos, “In vitro investigation of skin damage due to microscale shearing,” *J. Biomed. Mater. Res. Part A*, vol. 102, no. 11, pp. 4078–4086, Nov. 2014.

[70] G. P. Chimata and C. J. Schwartz, “Investigation of the Role of Diminishing Surface Area on Friction-Based Tactile Discrimination of Textures,” *Biotribology*, vol. 15, pp. 1–8, Sep. 2018.

CHAPTER 6 Effects of Wetness and Fabric Parameters on Skin Physiology and Sensation from Topsheet Nonwoven Fabrics Rubbing Against Skin

6.1 Introduction

As absorbent hygiene products are in widespread use in modern life, both skin health and the skin sensations relating to the use of it are important to improve the user experience. Diaper dermatitis (DD) and incontinence-associated dermatitis (IAD) are the two most common issues related to the usage of hygiene products. The high skin humidity with shear forces between the nonwoven fabric and the skin is reported to be a primary cause of contact dermatitis. If there is long-time skin contact with urine and feces, there is a higher risk for the skin to be exposed to micro-organisms and bacteria that leads to skin infection [1]. Therefore, it is important to study the interaction between the fabrics and skin in a wet condition for the improvement of absorbent hygiene products and investigate how the skin physiology and sensation can be affected by the interaction. In the previous study of skin-fabric friction in a neutral and warm environment (Chapter 5), the relationship between friction and skin physiology, skin sensation was studied. Sweat was found to be an important factor that contributed to the significant differences that occurred between the two environments. However, the exact amount of sweat produced in the warm environment was not controlled or monitored. In this study, a controlled water amount was applied to the skin surface to investigate the effects of wetness on the interaction with the topsheet fabrics. The commercial topsheet nonwoven fabrics have very narrow ranges of properties and structures and the engineering of them has low flexibility because of the restrictions on economics and manufacturing. Although there is low flexibility of fabric engineering, it is believed there are differences regarding the tactile perception for those fabrics in the industry. Since the selection of fiber types and the control of bonding sites are most practicable [2], topsheet fabrics with

controlled fiber types and bond areas were used to investigate the effects in this study. Polypropylene (PP) and polyethylene (PE), the two most widely used fiber types in nonwoven fabrics, were investigated to explore if there was a difference between them regarding interaction with the skin. The PP monocomponent fibers were compared to PE/PP sheath/core bicomponent fibers with PE as the surface material with a PP core. Fabrics with big and small bond areas were evaluated as the bond area may influence the surface texture sensation of fabrics. The effects were evaluated with respect to friction, skin permeability, skin redness, and skin sensation.

6.2 Materials and Methods

6.2.1 Materials

The spunbond technology is the most commonly used method for the manufacturing of the topsheet of disposable hygiene products [3]. Four spunbond nonwoven fabrics with controlled material and bond area were used for these experiments. All of them were produced with a Reicofil single beam spunbond line in the Nonwoven Institute (North Carolina State University, U.S.A.) and thermal calender bonded (Fiber Visions Manufacturing, GA, U.S.A.). Since polypropylene and polyethylene are the most widely used polymers for the topsheet fabrics, these two fiber types were investigated in this study. Fabric samples were named PP1, PP3, PE1, and PE3. PP1 and PP3 were made from polypropylene (ExxonMobile PP3155) fibers. PE1 and PE3 were made from polyethylene (Dow PE-ASPUN 6855A)/Polypropylene (ExxonMobile PP3155) sheath/core bicomponent fibers. The sheath/core ratio was 10 to 90. The fabric samples had the same pattern shape created by the different bond areas. The information of bond pattern is given in Table 6. 1. In the sample ID, the code 1 represents a small bond area of 8.7% while the code 3 was a bigger bond area of 24.5%. The bigger bond area was achieved by higher density of the bond points while the shape and size of each bond point was the same. The bonding temperature for PP fabrics was

138℃, and for PE/PP fabrics was 130 ℃.

Table 6.1. Bond pattern information for the tested fabric samples.

Sample ID	Bond area	Bond Shape	Spots/cm^2	Bond pattern images
PP1, PE1	8.7%	diamond	40.9	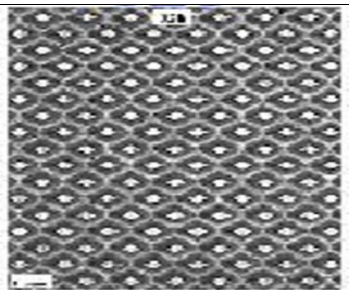
PP3, PE3	24.5%	diamond	133.6	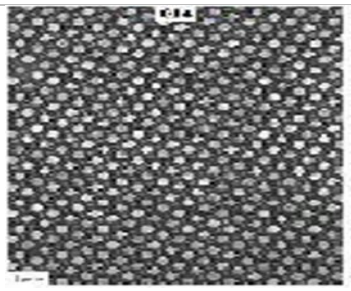

6.2.2 Fabric surface roughness measurement

In this study, two contact methods of surface roughness measurement were used: Kawabata Evaluation System (KES-FB4 Surface Tester, Japan) and Tissue Softness Analyzer measurement. Both of them have been developed to correlate surface roughness with the perception of the human hand [4][5].

6.2.2.1 Kawabata Evaluation System (KES)

The surface roughness measurement of the Kawabata Evaluation System [4] measured the arithmetic mean of the surface heights in the evaluation length. A U-shaped single wire probe with

a diameter of 0.5 mm contacted the fabric surface. The sampling rate was 5 Hz. The fabric was moved 3 cm in the forward direction and then the same length in the backward direction with 1 mm/s velocity. A constant tension load of 19.6 N/m (20 gf/cm) and 0.098 N (10 g) normal load was applied to the sample. The machine direction of the fabric was tested as that was the direction of the fabric tested on human subjects. Three replications were done for each fabric sample and the mean value was used to represent the surface roughness of fabric.

6.2.2.2 Tissue Softness Analyzer (TSA)

The tissue softness analyzer (Emtec, Germany) had a measuring head with lamellas that can vertically move down to touch the fabric and rotate over it under 100mN load force. The rotational contact with the fabric produced vibrations and the vibration sound was recorded by a sensor and this generated a sound spectrum. In the sound spectrum, the highest peak around 750 Hz (named TS750) was generated by the vibration of the fabric. It is related to the surface structure and geometry and was used to indicate the surface smoothness-roughness. A higher peak or TS750 stands for a rougher surface while a lower TS750 means higher smoothness [6]. Two replications were done for each fabric and the mean value was used to indicate the surface roughness of fabric.

6.2.3 In vivo skin physiology and sensation evaluation

6.2.3.1 Friction measurement

The same method for the in vivo friction measurement as in Chapter 5 was used.

6.2.3.2 Skin physiology measurements, and skin sensation evaluation

The same methods for the measurement of TEWL(transepidermal water loss) and skin redness as in Chapter 5 were used. The skin sensation was evaluated from five perspectives: pleasantness sensation, localized sensation, texture sensation, wetness sensation, and stickiness sensation, using the same ordinal scales demonstrated in Chapter 5.

6.2.3.3 Study protocol

Participants

Eleven healthy volunteers were recruited from North Carolina State University (the same participants in Chapter 6). There were 10 females and 1 male, all with ages between 18 and 21. All participants had no prior history of diagnosed dermatological illnesses and no open wounds or skin infections. The content and test procedure were explained to them verbally before they consented to participate. The study was reviewed and approved by the North Carolina State University Institutional Review Board for the Use of Human Subjects in Research (protocol #15425) and the written informed consent was obtained from each participant. Subjects were instructed not to apply body care products like lotions to the forearm skin on the day of testing.

Experiment in dry condition

The experimental procedure for the test in the dry condition was included in Chapter 5 (seen the test protocol for the neutral environment).

Experiment in wet condition

The experiments in the wet condition were conducted on different days from the test in the dry condition for each subject. Subjects were acclimated for 15 minutes in a thermoneutral room (22°C) and read the questionnaire to familiarize themselves with the questions in a waiting room before the start of experiments. After the subject left the waiting room, they entered the climatic chamber where the temperature and humidity were controlled. The temperature was 22°C and the relative humidity was between 45% and 50%, which was the same as the environment of the dry test. The experimental set-up was the same as the test in neutral and warm environments demonstrated in Chapter 5 and the same operator conducted the tests. The only difference during the experimental procedure for the wet condition test was that deionized water was applied to the

tested skin area before each friction test. Before each friction test, the measurement of TEWL and the skin image was taken as demonstrated in Chapter 5. After that, a pipette was used to apply 0.1 ml deionized water as three droplets evenly distributed to the tested skin region. After each friction test, a piece of the napkin was used to gently wipe the skin to absorb the visible water left on the skin, and then the TEWL was measured and skin images were taken again. The four fabric samples were tested in random order.

Water amount measurements in wet condition tests

In the wet condition test, the water stored in the topsheet nonwoven fabric, acquisition layer, and the water left on the skin was measured respectively. The dry weight of each topsheet fabric and acquisition layer was measured before each test, and the weight was measured again after the wet friction test. The difference between the fabric weight before and after the test was recorded as the water amount stored in the topsheet and acquisition layer. Napkins were cut at 8 cm by 6 cm. It was used to absorb the visible excess water on the skin surface after each friction test. A new piece of the napkin was used for each test. The weight of the napkin was measured before the use of it and after it wiped the skin surface. The difference between the weight before and after the test was recorded as the water amount left on the skin surface.

6.2.3.4 Statistical Analysis

All statistical analyses were performed with SPSS (IBM, U.S.A.). All data were tested for normal distribution and homogeneity of variance using the Shapiro-Wilk test and Levene's test respectively. To evaluate the effects of wetness, the paired t-test was used for Δa^* to assess if there was a significant difference between the dry and wet conditions. The distribution of the differences in ΔTEWL, friction, and skin sensation between dry and wet conditions were not normally distributed so the nonparametric Wilcoxon Signed Rank test was used. To evaluate the effects of

fabric and bond area, the paired t-test was used for ΔTEWL while the nonparametric Wilcoxon Signed Rank test was used for the other parameters that did not conform to the normal distribution. The distribution of the differences in measured water amount of topsheet fabric, and that on the skin surface of different fabrics was not normally distributed so the nonparametric Wilcoxon Signed Rank test was used to identify if there was a significant difference between the fiber types and between the bond areas. For the water amount in the acquisition layer, the paired t-test was used for the comparison of PE/PP and PP fabrics and the fabrics with small and big bond areas. A P value <0.05 was recognized as statistically significant.

6.3 Results and Discussion

6.3.1 Effects of Wetness

Figure 6. 1 shows the water distribution of all samples after the friction test in the topsheet fabric, acquisition layer, and on the skin surface. Most of the water went into the acquisition layer. This corresponds to the function of it in an absorbent hygiene product which is transporting the water from the topsheet fabric. However, there still was about 10% of the water (0.01 ml) water left on the skin and 20% in the topsheet fabric. This indicated that the skin-topsheet interface was not dry during and after the rubbing of the fabric on the skin. The water left on the skin surface would hydrate the skin and the water in the topsheet fabric can keep inducing moisture to the interface and keep the microclimate humid if it cannot be transferred to the acquisition layer. In our experiments, it was observed that, on average, about 30% of the water was lost. This was likely due to the evaporation during the entire measurement procedure. The fabrics were hydrophobic and the napkin also allowed some evaporation before weighing. Moreover, some of the water may have been absorbed by the stratum corneum, which is the uppermost layer of the skin [7].

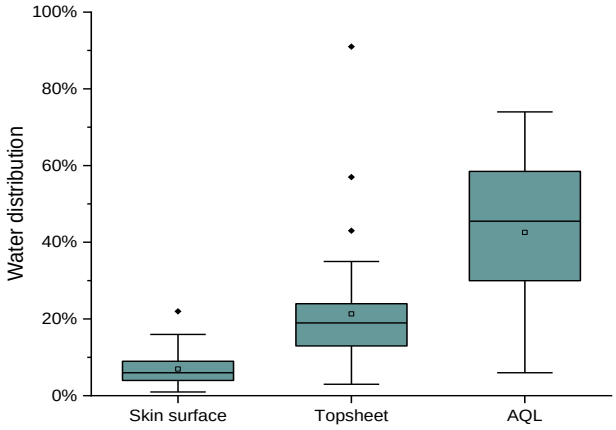

Figure 6.1. Water distribution on the skin surface, in topsheet nonwoven fabric, and the AQL (acquisition) layer. The length of the box is the interquartile range (25% to 75%). The upper whisker and lower whisker are determined by the 5th and 95th percentiles respectively. The line in the box is the median mark. The hollow square is the mean value and the solid dot are outliers.

With the application of water on the skin, the friction was significantly($P<0.001$) increased compared to the friction in the dry condition (Figure 6. 2). This result is consistent with many studies on skin friction under dry and wet conditions [8][9]. This increase of friction was believed to be a consequence of a larger real contact area caused by the moisture-induced softening and smoothing of the skin surface[10].

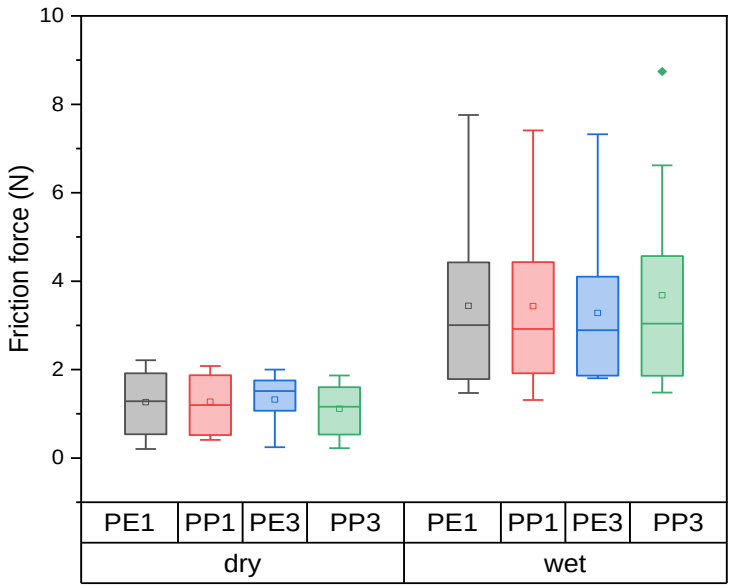

Figure 6.2. Friction of four nonwoven fabrics in dry and wet conditions (PE1 and PP1 are PE/PP bicomponent fabric and PP fabric with a bond area of 8.7%. PE3 and PP3 are the fabrics with a bond area of 24.5%). The length of the box is the interquartile range (25% to 75%). The upper whisker and lower whisker are determined by the 5th and 95th percentiles respectively. The line in the box is the median mark. The hollow square is the mean value and the solid dot are outliers.

Figure 6. 3 shows both the TEWL($P<0.001$) and skin redness($P=0.002$) increased significantly in the wet condition, which indicated a more permeable skin and increased skin redness in the wet condition. The increased friction force in the wet condition is likely related to this increase in skin physiology. Figure 6. 4a displays that the change of TEWL tends to be positively related to the increase of friction force. However, this relationship was not linear. The size of the effect may vary depending on the subjects. There were two subjects that had the highest friction force (blue and green dots in Figure 6. 4a) but a lower TEWL change compared to other subjects who had lower friction force in the wet condition. The skin redness (Δa^*) also showed a tendency of increase with the increase of friction force, but it seemed the increase of redness reached a threshold around 5 of the Δa^* value (Figure 6. 4b). It is uncertain whether there was a threshold of the increase in redness or this tendency was caused by subject variation, as the same

two subjects who had the highest friction presented both less change of TEWL and skin redness. These two subjects may perform differently from other subjects, with a higher resistance to the impact of friction on skin physiological parameters. In addition, the negative delta Δa* value showed the skin did not always turn redder after the rubbing against the fabric, especially in the dry condition. The reduction of skin redness may be caused by reduced blood flow resulting from the applied pressure and shearing to the skin during the friction test. Since the skin images were taken immediately after the friction test, the blood flow may still be reduced when the image was taken. In the wet condition, the skin may have been more abraded with more stratum corneum cells removed[11] which may have made the skin more susceptible to irritation and corresponding skin blood flow increase, thus presenting redder.

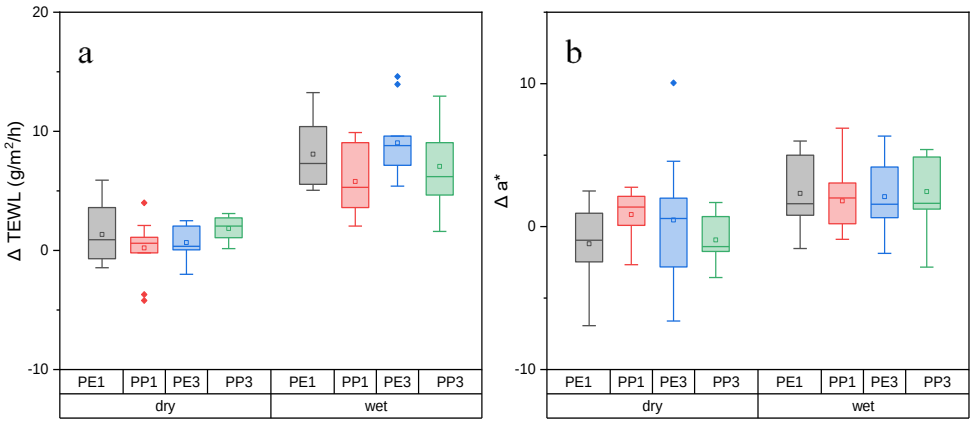

Figure 6.3. Change of TEWL and skin redness(a*) of four nonwoven fabrics in dry and wet conditions (PE1 and PP1 are PE/PP bicomponent fabric and PP fabric with a bond area of 8.7%. PE3 and PP3 are the fabrics with a bond area of 24.5%). The length of the box is the interquartile range (25% to 75%). The upper whisker and lower whisker are determined by the 5th and 95th percentiles respectively. The line in the box is the median mark. The hollow square is the mean value and the solid dot are outliers.

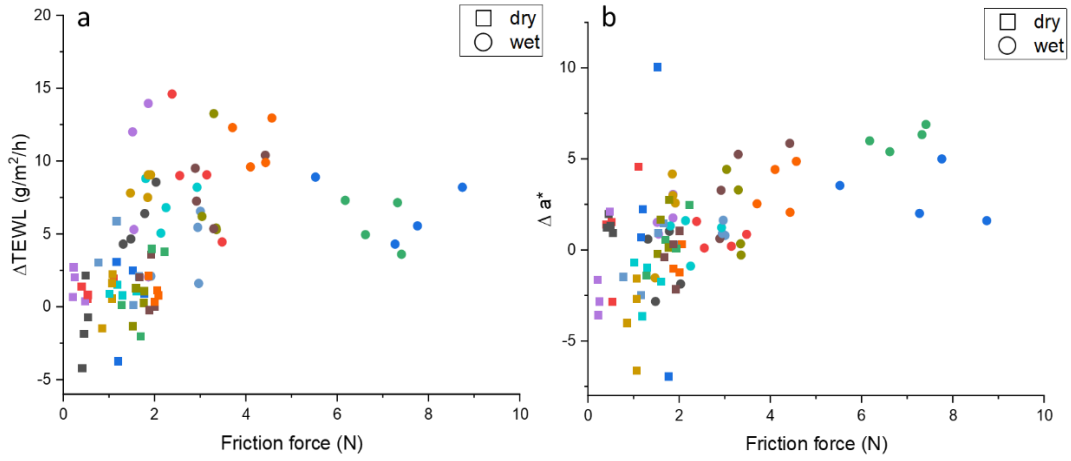

Figure 6.4. a. friction force and the corresponding change of TEWL (transepidermal water loss) in dry and wet conditions after friction test; b. friction force and the corresponding change of a* value (skin redness) in dry and wet conditions after friction test. One symbol color represents one subject.

Figure 6. 5 shows the skin sensation in dry and wet conditions. The wetness showed significant effects on skin sensation in terms of the pleasantness sensation ($P<0.001$), localized sensation ($P=0.021$), texture sensation ($P<0.001$), wetness sensation ($P<0.001$), and stickiness sensation ($P=0.001$). The interaction between the skin and nonwoven topsheet fabric during the wet test was perceived as less pleasant with a tickle to itch feeling and rougher sensation, as well as an increased wetness and stickiness sensation. It has been reported that the unpleasant sensation is related to the increased friction force in the wet condition [12]. The water or moisture between the fabric and skin is likely to increase the adhesion force and thus increase the contact area. The skin also becomes softer in a wet condition so the deformation of skin can increase. The increased contact area as well as the deformation caused increased friction and a larger stimulus may be transferred to skin receptors. leading to the discomfortable tickle, rougher and stickier sensations in the wet condition [13]. The increased wetness sensation may not only be affected by the mechanical inputs but also by a reduction of skin temperature with the water applied and evaporating[14].

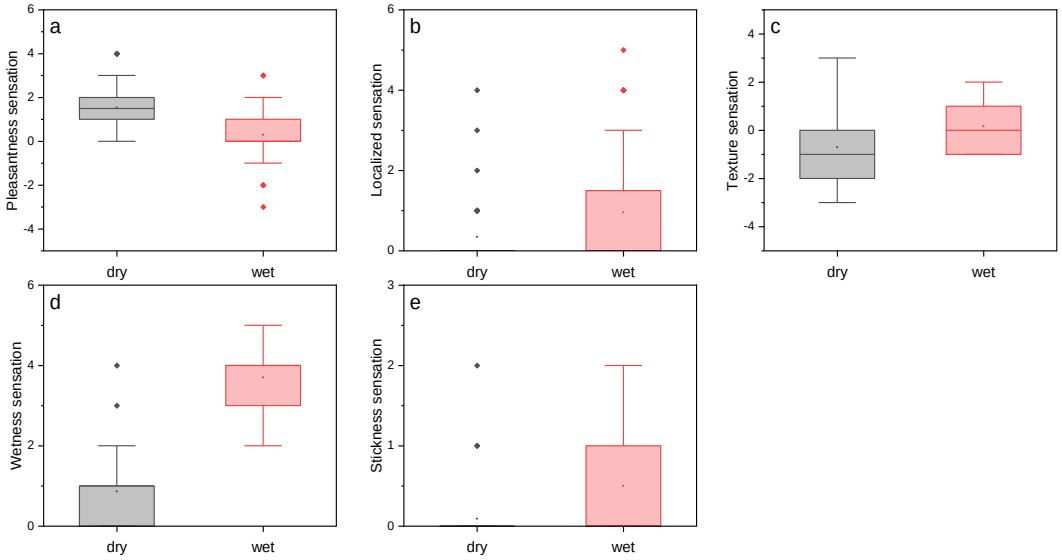

Figure 6.5. Skin sensation in dry and wet conditions: a. pleasantness sensation: 0-neutral, positive side- increase in pleasantness, negative side- increase in unpleasantness. b. localized sensation: 0-neutral touch;1-tickle; 2-itch; 3-tingle; 4-prickle; 5-abrasive. c. texture sensation: negative side-increase in smoothness, positive side-increase in roughness. d.wetness sensation: larger value, wetter sensation. e.stickness sensation: larger value, stickier sensation. The length of the box is the interquartile range (25% to 75%). The upper whisker and lower whisker are determined by the 5th and 95th percentiles respectively. The line in the box is the median mark. The hollow square is the mean value and the solid dot are outliers.

6.3.2 Effects of fabric materials and bond areas

6.3.2.1 Friction and skin physiology

In this section, the data obtained in the warm environment in Chapter 5 was compared to the wet experiments to explore the effects of fabric parameters. There was no significant difference in the water amount distribution across fabrics ($P>0.05$). Both the surface material and bond area did not significantly influence the water distribution ($P>0.05$) as well as the friction force ($P>0.05$) regardless of the test condition (dry-wet) and environment (neutral-warm).

The fabric material and bond area did not show distinguishable effects ($P>0.05$) on the change of skin redness and there was no difference of ΔTEWL ($P>0.05$) observed between fabrics

with different bond areas regardless of the test condition (Figure 6. 6a). However, the PE/PP fabrics presented a higher increase of TEWL (P=0.022) than PP fabrics (Figure 6. 6b) after the friction test in the wet condition. This indicates the contact material possibly influenced the actual water loss from the skin surface. Since the water amount captured on the skin surface and fabrics did not show a significant difference. It is possible that the impact on skin hydration was different when using the two materials but further investigation is needed by evaluating the hydration of the skin.

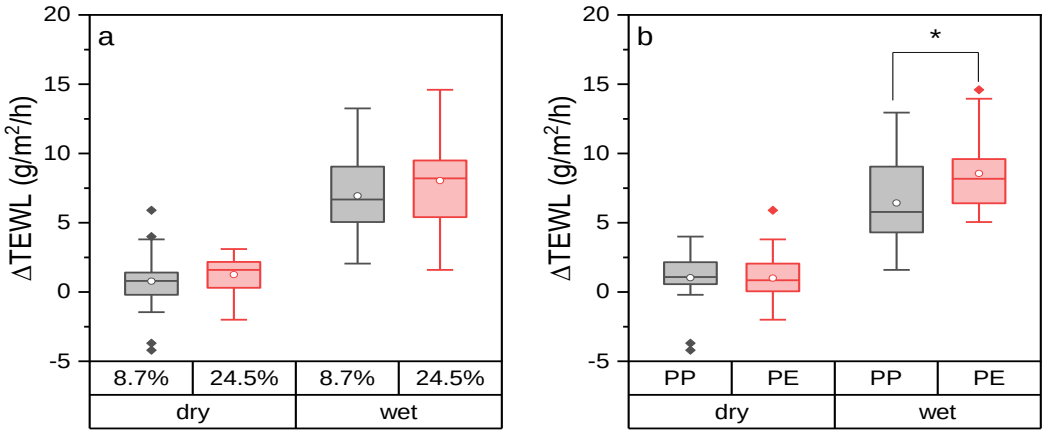

Figure 6.6. The change of transepidermal water loss in dry and wet conditions at the neutral environment: a. between different bond areas of fabrics: small bond area-8.7%; big bond area-24.5%. b: between different materials of fabrics: PP-polypropylene fibers; PE-polyethylene/polypropylene bicomponent fibers. * significant differences($P<0.05$) in ΔTEWL between PP and PE/PP fabrics at the wet condition. The length of the box is the interquartile range (25% to 75%). The upper whisker and lower whisker are determined by the 5th and 95th percentiles respectively. The line in the box is the median mark. The hollow square is the mean value and the solid dot are outliers.

6.3.2.2 Subjective Sensations

When considering the sensation in dry, wet, and warm environments (Figure 6. 7), the fabrics with the smaller bond area were significant as being more pleasant (P=0.030) than the fabrics with the larger bond area but the difference was not statistically significant when considering the environment conditions separately. The texture sensation also showed a significant

difference (P=0.035) between bond areas when combining all the data in dry, wet, and warm environments (Figure 6. 8). The small bond area fabric was sensed smoother. When considering the test conditions separately, the difference of texture sensation was significant in the neutral environment under dry(P=0.045) and wet (P=0.038) conditions but not in the warm environment (P=0.961). Nevertheless, the bond area did not present differences (P>0.05) for localized sensation, wetness, and stickiness. Therefore, the difference of the pleasantness sensation was likely contributed by the texture sensation. The smoother sensation of fabrics with a small bond area is likely caused by a smaller spatial variation in the impulse rates of slowly adapting type 1(SA1) afferents, which is one type of mechanical receptors of skin [15]. Based on the information of bond pattern (Table 6. 1), the area of each bond point was about 0.2 mm^2 for the small bond area fabric and about 0.18 mm^2 for the big bond area fabric so the size of the bond point was similar but the spacing between two bond pints of the small bond area fabric (~1 mm) was larger than that of the big bond area fabric (< 0.5 mm). Figure 6. 9 illustrates the different spacing between bond points for the fabrics with the small bond area and big bond area. The width of the bond point was assumed the same as the bond point had a similar area and the same diamond shape. Goodman and Bensmaia studied the relationship between an embossed dot pattern and perceived roughness. They reported the perceived roughness decreased with an increase of dot width [16]. For the spunbond, thermal calender bonded fabric in our study, the unbonded region is the “dot” while the bond point is compacted. Thus, the fabric with a smaller bond area had a larger distance between two bond points means it had wider “dots”. It is believed that this spatial pattern with a less contact variation caused a smaller variation in the SA1 afferent population response and presented as smoother perception[16]. The surface fiber type, PE or PP, did not show differences (P>0.05) for the evaluated skin sensation regardless of the effects of conditions.

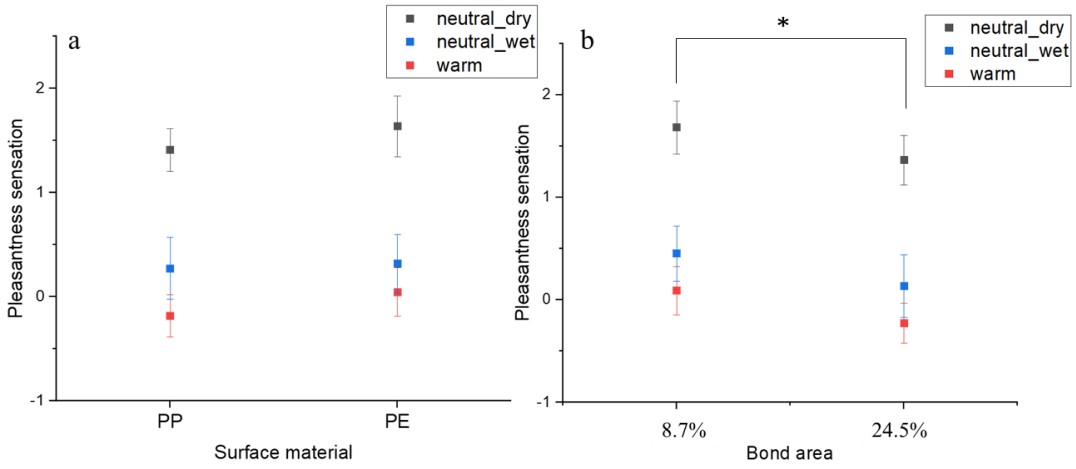

Figure 6.7. Pleasantness sensation in the neutral environment (dry and wet conditions) and warm environment: a. between different materials of fabrics: PP-polypropylene fibers; PE-polyethylene/polypropylene bicomponent fibers b: between different bond areas of fabrics: small bond area-8.7%; big bond area-24.5%. * significant differences($P<0.05$) in pleasantness sensation between small and big bond area fabrics when considering all conditions together. The mean values with standard errors were displayed in the graphs.

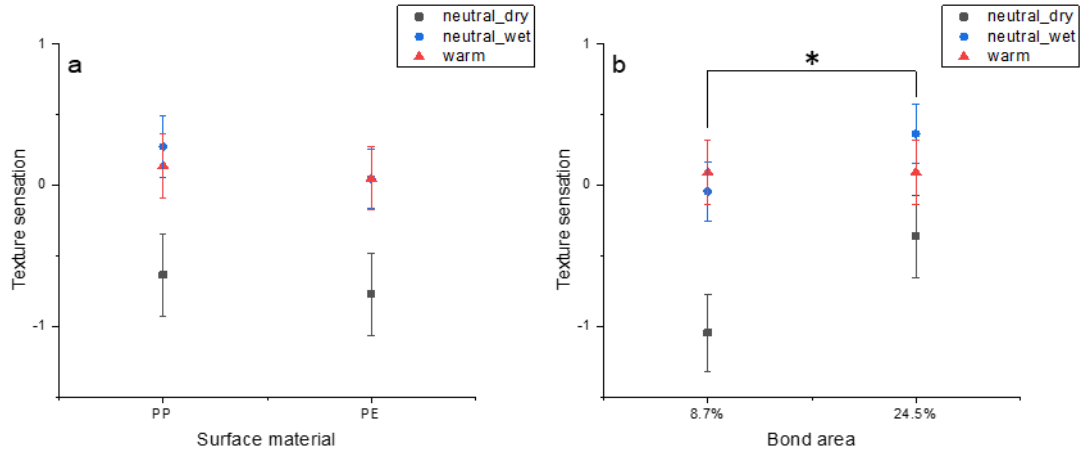

Figure 6.8. Texture sensation in the neutral environment (dry and wet conditions) and warm environment: a. between different materials of fabrics: PP-polypropylene fibers; PE-polyethylene/polypropylene bicomponent fibers b: between different bond areas of fabrics: small bond area-8.7%; big bond area-24.5%. * significant differences($P<0.05$) in texture sensation between small and big bond area fabrics at dry and wet conditions not warm. The mean values with standard errors were displayed in the graphs.

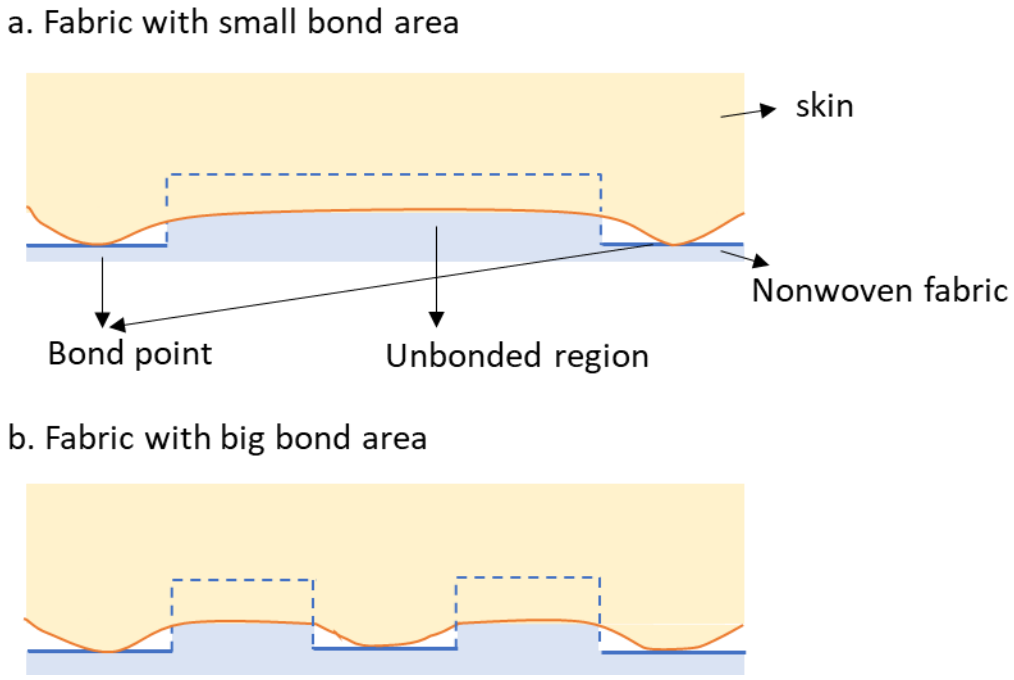

Figure 6.9. Schematic diagram of the skin-fabric contact. a. small bond area fabric. b. big bond area fabric. The dash line illustrates where the fabric surface is before the interaction with the skin.

6.3.3 Texture sensation and surface roughness measurement

The texture sensation likely played an important role in the distinction of the pleasantness sensation for the tested fabrics in these experiments, because the differences in the pleasantness sensation did not correlate with other evaluated sensations. Figure 6. 10 shows the texture sensation in the dry condition as a function of the surface roughness measured by KES and TSA. Figure 6. 10a indicates that the surface roughness measured by KES did not correspond to the texture sensation (smoothness-roughness) perceived by subjects. The smaller bond area fabrics (PP1 and PE1) had a higher surface roughness measured by KES while they were perceived smoother compared to the fabrics with big bond areas (PE3 and PP3). In addition, the PP3 and PP1 had almost the same surface roughness measured by the KES but the texture sensation was very different. This indicates the KES surface roughness measurement did not predict the smoothness-roughness sensation for the topsheet nonwoven fabrics accurately. This may imply the spatial parameters were more dominant than the calculated arithmetic mean height of surface for the perception of the tested nonwoven fabrics. The surface roughness measured by the KES may miss detailed information on spacing because of the calculation. It was calculated as below:

$$SMD = \frac{1}{L}\int_0^L \left|\mathrm{T} - \mathrm{T}'\right| dL$$

Where L is the total evaluation length, T is the local surface height and T' is the mean fabric surface height. If we consider the plane height of the bond area surface as the mean fabric surface height (T') and assume the height of the unbonded region (T) was the same for both fabrics. Then, the term $\int_0^L \left|\mathrm{T} - \mathrm{T}'\right| dL$ would be smaller for the fabric with a big bond area than the fabric with a small bond area because it has a longer total length of the bond points at unit length (Figure 6. 9). In other words, the fabric with a big bond area has a shorter length of unbonded region (T) which means a smaller integral area. Therefore, the numerator would be smaller for the big bond area

fabric than the small bond area fabric while the denominator was the same for both so the SMD was smaller for the big bond area fabric. In this case, the way KES calculates the roughness does not reflect the difference of the spacing between bond points or the width of "dots" and this may be the reason for the inaccurate prediction of roughness perception.

The roughness measured by TSA showed the fabric measured rougher tended to be perceived rougher (Figure 6. 10b). Unlike the average roughness data from the KES measurement, which are only focused on the deviation from mean surface height, the TSA roughness measured the fabric vibration generated during the rotation of lamellas on the fabric surface. The vibration was not only influenced by the local surface height but the frequency of the peaks and valleys on the surface so both the variation of lateral spacing and vertical height contributed to the fabric vibration. Although the TSA roughness presented a positive relationship to the perceived roughness compared to the KES roughness, there is still a discrepancy between the TSA measurement and roughness sensation. The TSA measured a different roughness for the PP and PE/PP fabrics with a difference of ~5 dB but this difference was not reflected in the perceived roughness of fabrics with different fiber types. The possible reason may be that this difference (~5dB) of vibration cannot be perceived by the volar forearm skin.

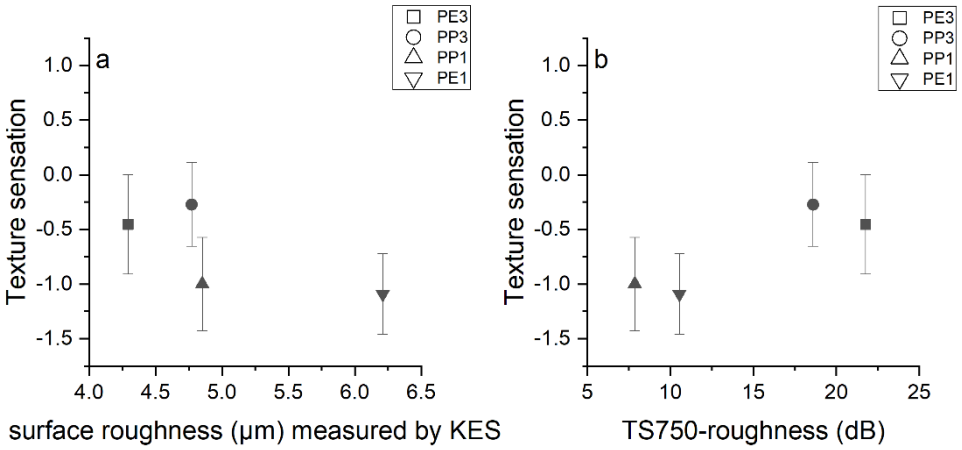

Figure 6.10. Texture sensation and surface roughness measured by Kawabata Evaluation System (graph a) and the roughness measured by Tissue Softness Analyzer (graph b) in dry condition. Texture sensation scale: 0-neutral, positive side-rougher sensation, negative side-smoother sensation. The mean value and standard deviation of surface roughness measured by KES and TSA were given in Table 6. 2.

Table 6.2. Measured surface roughness of tested nonwoven fabrics by KES and TSA.

Fabric	Mean value ± standard deviation of KES roughness (μm)	Mean value ± standard deviation of TSA roughness (dB)
PE1	6.2±0.2	10.6±0.1
PE3	4.3±0.1	21.8±0.3
PP1	4.9±0.4	7.9±0.2
PP3	4.8±0.4	18.6±2.3

6.4 Conclusions

The widely used spunbond, thermal calender bonded nonwoven fabrics made of polypropylene fibers and polyethylene/polypropylene bicomponent fibers were evaluated for their skin comfort performance in dry and wet conditions. The nonwoven fabrics were perceived pleasant and had slight effects on TEWL in the dry condition but the water applied to the skin surface affected the results significantly. The transepidermal water loss (TEWL) and skin redness were increased significantly after the fabric rubbing on the skin in the wet condition. The skin sensation was less pleasant with more tickle sensation, less smooth sensation, increased wet and sticky sensation with significantly increased friction. This indicates the skin can be easier impaired in a wet condition than a dry condition which suggests the importance of wetness reduction for the use of skin-contact nonwoven products to improve skincare. Nevertheless, there was water left on the skin surface and stored in the topsheet during the skin-fabric interaction which is unfavorable for the skin-care but the absorbent core layer used in absorbent hygiene products should be added in future studies to inspect if the water left on the interface would be reduced with the absorbent core layer as only the acquisition layer was used in this study.

In this study, the material and bond area of the fabric presented smaller effects on the skin sensation and physiology compared to wetness. The fabrics made of PP and PE/PP material with small and big bond areas did not cause different friction on the skin. However, the PE/PP fabric presented more impact on the change of TEWL than the PP fabric in the wet condition. The reason was unclear. Further investigation of the effects of fabric fiber types and structure on skin physiology should be done. The hydration and temperature of the skin before and after the interaction with different materials may also be investigated. The fabrics with small bond areas were perceived as more pleasant and smoother than the fabrics with big bond areas. Since there

was no significant difference between friction for the tested fabrics but they performed differently on skin physiology and sensation, the skin-fabric friction measured in vivo cannot always represent the differences in fabric performance related to skin comfort for these tested nonwoven fabrics. A higher surface roughness measured by the Tissue Softness Analyzer (TSA) was related to a higher roughness sensation of the tested fabrics while the Kawabata Evaluation System (KES) gave an inverse prediction for the roughness sensation. The inaccurate prediction of perceived roughness for KES in this study is likely caused by not involving the spatial variation of fabric surface while it can be the reason for the different roughness perception of fabrics with a small and big bond area.

6.5 References

[1] B. Runeman, “Skin interaction with absorbent hygiene products,” *Clin. Dermatol.*, vol. 26, no. 1, pp. 45–51, Jan. 2008.

[2] M. Rinnert, Thorsten Schneider, N. A. Reichardt, and B. Kruse, “Disposable diaper having nonwoven topsheet with particular combination of basis weight and bonding configuration,” US8530722B2, 24-Jun-2013.

[3] J. R. Ajmeri and C. J. Ajmeri, “Nonwoven personal hygiene materials and products,” in *Applications of Nonwovens in Technical Textiles*, Woodhead Publishing, 2010, pp. 85–102.

[4] S. Kawabata and M. Niwa, “Objective Measurement of Fabric Mechanical Property and Quality: Its Application To Textile And Clothing Manufacturing,” *Int. J. Cloth. Sci. Technol.*, vol. 3, no. 1, pp. 7–18, 1991.

[5] Y. Wang *et al.*, “Relationship between human perception of softness and instrument measurements,” *BioResources*, vol. 14, no. 1, pp. 780–795, 2019.

[6] T. de Assis *et al.*, “Comparison of wood and non-wood market pulps for tissue paper application,” *BioResources*, vol. 14, no. 3, pp. 8781–6810, 2019.

[7] M. Egawa and T. Kajikawa, “Changes in the depth profile of water in the stratum corneum treated with water,” *Ski. Res. Technol.*, vol. 15, no. 2, pp. 242–249, May 2009.

[8] G.-M. Rotaru *et al.*, “Friction between human skin and medical textiles for decubitus prevention,” *Tribol. Int.*, vol. 65, pp. 91–96, Sep. 2013.

[9] S. Derler and L. C. Gerhardt, “Tribology of skin: Review and analysis of experimental results for the friction coefficient of human skin,” *Tribol. Lett.*, vol. 45, no. 1, pp. 1–27, Jan. 2012.

[10] L. C. Gerhardt, V. Strässle, A. Lenz, N. D. Spencer, and S. Derler, “Influence of epidermal hydration on the friction of human skin against textiles,” *J. R. Soc. Interface*, vol. 5, no. 28, pp. 1317–1328, Nov. 2008.

[11] R. E. Zimmerer, K. D. Lawson, and C. J. Calvert, “The Effects of Wearing Diapers on Skin,” *Pediatr. Dermatol.*, vol. 3, no. 2, pp. 95–101, Feb. 1986.

[12] A. R. Gwosdow, J. C. Stevens, L. G. Berglund, and J. A. J. Stolwijk, “Skin Friction and Fabric Sensations in Neutral and Warm Environments,” *Text. Res. J.*, vol. 56, no. 9, pp. 574–580, 1986.

[13] K. P. M. Tang, K. H. Chau, C. W. Kan, and J. T. Fan, “Assessing the accumulated stickiness magnitude from fabric-skin friction: Effect of wetness level of various fabrics,” *R. Soc. Open Sci.*, vol. 5, no. 8, Aug. 2018.

[14] D. Filingeri, D. Fournet, S. Hodder, and G. Havenith, “Why wet feels wet? A neurophysiological model of human cutaneous wetness sensitivity,” *J. Neurophysiol.*, vol. 112, no. 6, pp. 1457–1469, Sep. 2014.

[15] T. Yoshioka, B. Gibb, A. K. Dorsch, S. S. Hsiao, and K. O. Johnson, “Neural coding mechanisms underlying perceived roughness of finely textured surfaces,” *J. Neurosci.*, vol. 21, no. 17, pp. 6905–6916, Sep. 2001.

[16] J. M. Goodman and S. J. Bensmaia, “A variation code accounts for the perceived roughness of coarsely textured surfaces,” *Sci. Rep.*, vol. 7, no. 1, pp. 1–10, Apr. 2017.

CHAPTER 7 Summary and Future Work

To improve the experience of skin health and sensation when using absorbent hygiene products, it is necessary to understand skin-fabric interaction. To understand the interaction between the skin and materials in daily life, human skin friction has been commonly studied throughout the literature. There are previous studies on the effects of environmental conditions and contact materials on skin friction. These studies showed a high friction force or a high coefficient of friction could lead to skin damages or lesions and unpleasant sensations. Similarly, the effects of friction between the skin and nonwoven fabric used in absorbent hygiene products on skin comfort should be studied as there is no direct evidence that the friction generated during the contact between skin and fabric can cause skin damages and lead to contact dermatitis. Furthermore, friction is a complex system property that can be affected by various factors. So, it needs to be investigated whether the effects of environmental condition and contact material properties on skin-fabric friction are similar for nonwovens, and the relationship between friction and skin physiology and sensation are also similar. In this study, the nonwoven fabrics used for the topsheet of absorbent hygiene products were characterized. Both in vivo and in vitro approaches were developed to study the skin-fabric friction, skin physiology, and sensation.

The typical topsheet nonwoven fabrics had similar characteristics such as fiber diameters (~13μm to 17μm), thickness (below 1 mm), and basis weight (lower than 22 g/m^2). In general, they were very thin and lightweight fabrics regardless of the manufacturing methods. The in vitro friction measurement using skin simulants showed the coefficient of friction was more related to surface properties while the skin deformation can contribute to stick-slip behavior. In the literature, it has been reported both the coefficient of friction and the stick-slip can relate to tactile sensation. However, the tested fabrics were not differentiated by the coefficient of friction measured in vivo.

The dynamic stick-slip observed in vitro can distinguish the fabrics while the coefficient of friction cannot so it may provide the potential to reflect the tactile sensation.

In the human subject studies, the approach for TEWL and skin color measurement provided a way to quantitatively evaluate the effects of friction on skin physiological properties. It showed the environmental condition had significant effects on skin-fabric interaction. In a neutral (22℃, ~50%RH) and dry condition, the rubbing of the fabric against the skin did not cause considerable effects on skin physiology and sensation. The topsheet fabrics were perceived pleasant with no redder skin observed and a very slight increase of transepidermal water loss (TEWL) (the increase of TEWL after friction: 1.2±2.1 g/m^2/h). The water on the skin surface and a warm (35℃, ~50%RH) environment both caused significantly increased TEWL (the increase of TEWL after friction: wet: 7.5 ±3.1 g/m^2/h; warm:7.8±9.4 g/m^2/h) and significantly reduced pleasantness sensation with an increase of friction force. Thus, the wetness and high temperature were unfavorable for skin barrier function and skin sensation. Besides, a redder skin was observed in the wet condition that can signify the adverse impact on the skin as skin rash usually occurs for contact dermatitis. The relationship between friction and skin physiology, sensation showed a higher friction force led to a larger change of TEWL, skin redness, and skin sensation in the dry condition. However, this relationship did not hold in a warm environment. The smooth topsheet fabrics and rough fabrics could have the same high friction force in the warm environment but the smooth fabrics had a smaller effect on skin physiology and sensation than the rough fabric. Furthermore, the smooth fabric had a higher increase of friction than the rough fabric when the environment changed from neutral to warm. Based on this finding, it was hypothesized that the larger increase in friction of smooth fabrics was attributed to the dominance of adhesion force. This would suggest that the effects of deformation friction might be larger than adhesion friction on skin physiology and

sensation. Thus, the skin deformation should receive more attention and this might be reflected in the dynamic stick-slip behavior observed in the in vitro friction measurement.

Although the friction measured in vivo was indistinguishable for the commercial topsheet nonwoven fabrics, the PE/PP fabrics showed more influence on the TEWL change than the PP fabrics. The spunbond fabric with a small bond area was perceived as more pleasant and smoother than that with a big bond area. The pleasantness sensation was highly correlated to the texture sensation, more than to the other sensations, e.g. localized sensation, wetness sensation. However, the surface roughness of fabrics measured by KES did not indicate the texture sensation of these topsheet nonwoven fabrics in our experiments. This suggests considering the spatial variation of the fabric rather than the arithmetic mean height only.

Both the in vivo and in vitro studies suggest the skin deformation can be important and the dynamic stick-slip observed in the friction measurement with skin simulants can potentially discriminate the fabric performance in terms of skin sensation. Unfortunately, this hypothesis was not verified in the current study because the same samples were not able to be tested in both in vitro and in vivo studies. In the future study, the fabrics that were perceived differently (i.e. the spunbond fabric with small and big bond areas) should be investigated using the skin simulants to see if the stick-slip motion can relate to their tactile sensation. The skin simulants enable investigations that may not be discernible from results obtained on human subjects because the stick-slip behavior was not observed in the human subject experiments. This indicates the current in vivo friction measurement may not be sensitive enough to detect the stick-slip, which might be improved by increasing the sampling frequency and/or reducing the speed of the sliding friction test. Additionally, since the tested commercial topsheet fabrics did not present significant differences in skin physiology and sensation, and the difference of small and big bond area fabrics

presented only when considering all the test data in different conditions, it suggests a big difference in fabrics and/or a larger population is needed for the detection of statistically significant difference between the tactile sensation of fabrics.

The adhesion and deformation friction for smooth and rough fabrics under dry and wet conditions can also be further studied. An observation of the skin-fabric interface would be helpful to better understand the adhesion friction as the adhesion friction results from the shearing of the bonds between the two surfaces during the relative motion. An investigation of the real contact area between the fabric and skin under pressure and the measurement of surface energies of both skin and fabric can help to calculate the adhesion force. It may also be important to observe whether the water between the hydrophobic fabric and the skin can form capillary bridges and increase the shearing force. The skin deformation may be detected by indention measurement on the skin with fabrics of varying surface roughness or the digital image correlation (DIC) technology could be used to analyze the displacement of the skin during a dynamic friction process.

For the measurement of skin physiology, the self-healing capacity of the skin may affect the observation of effects on the skin and there might be thresholds for the alteration of skin physiological properties. A longer time rubbing of fabric on the skin could be done to measure the TEWL and skin redness changes and compare them with the results from the current study. This may tell whether the TEWL and redness would keep increasing or reach a threshold. The TEWL and skin redness can be monitored as a function of time after the friction test to evaluate the recovery dynamics of the skin as well. Additionally, the environmental condition seems to have influenced skin physiological performance, because the increase of skin redness was found in the wet condition but not the warm condition so it may be helpful to evaluate more skin physiological properties in different environments to know the effects on skin health. Other skin physiological

properties such as skin pH and hydration may be measured in the warm environment. The reason for the different effect of PP and PE/PP fabrics on the TEWL was unknown. It could be studied further by measuring the TEWL and skin hydration for the skin interaction with PP and PE fabrics with different amounts of water.

For the measurement of skin sensation, the tested PP and PE/PP fabrics did not present a considerable difference in skin sensation, but the PE/PP fibers used in this study had a ratio of 10 to 90 and the low proportion of PE may reduce the difference from the PP fibers. A higher ratio of PE to PP like 30/70 or 50/50 can be used as the 10% PE may be worn away during the rubbing. The PE/PP fabrics had a lower bonding temperature than PP fabrics because of the lower melting temperature of PE. This lower temperature might reduce fabric strength and stiffness. Besides, the effects of temperature on texture sensation can be further studied as the distinguishable texture sensation of fabrics with small and big bond areas became indistinguishable in the warm environment.